EGE UNIVERSITY
GRADUATE SCHOOL OF NATURAL AND APPLIED SCIENCES

(MSc. THESIS)

REMOVAL OF HEAVY METALS FROM AQUEOUS SOLUTION BY LOW-CROSSLINKED CHELATING RESINS CONTAINING AMIDOXIME GROUPS

Nesrin ÇETİN

Chemical Engineering Department

Science Section Code: 603.03.00
Presentation Date : July 31, 2006

Supervisors :

Prof. Dr. Nalan KABAY

Prof. Dr. Mithat YÜKSEL

Bornova – İZMİR
July, 2006

ÖZET

AMİDOXİME GRUPLARI İÇEREN DÜŞÜK ÇAPRAZ BAĞLI ŞELATLAYICI REÇİNELERLE SULU ÇÖZELTİLERDEN AĞIR METALLERİN GİDERİLMESİ

ÇETİN, Nesrin

Yüksek Lisans Tezi,
Kimya Mühendisliği Bölümü

Tez Yöneticileri:

Prof. Dr. Nalan KABAY
Prof. Dr. Mithat YÜKSEL

Temmuz 2006, 129 sayfa

Ağır metallerin atık sular içerisindeki varlığı, hem çevre ve insan sağlığını hem de ekonomiyi olumsuz yönde etkilemektedir. Şelatlayıcı reçineler, ağır metallere karşı daha üstün seçimlilik gösterdiği için doğal ve lağım sulardaki toksik metallerin uzaklaştırılmasında kullanılabilirler.

Bu çalışmada, büyük gözenek yapısına sahip, metilen fosfonik gruplar içeren RCSP(II) reçinesi; ticari, sülfonik gruplar içeren güçlü katyon değiştirici Purolite C-160H reçinesi ve amidoxime grupları içeren düşük derecede çapraz bağlı şelatlayıcı RNH-CH120 reçinesi

kullanılmıştır. Bu reçinelerin sulu çözeltilerden ağır metal iyonlarının uzaklaştırılmasında uygulanabilirliği, kesikli ve sürekli yöntemlerle incelenmiştir. Kesikli çalışmalarda sulu çözeltilerden Cu(II) iyonlarının uzaklaştırılmasında pH ve reçine miktarının etkisi araştırılmıştır. Sürekli çalışmalarda ise Cu(II) iyonlarının uzaklaştırılmasında iki farklı türde reçine kullanılarak, bu reçinelerin performansları karşılaştırılmıştır.

Şelatlayıcı reçinelerin metal iyon seçimliliği, 10^{-4} M Cu(II), Cr(III) ve Cd(II) iyonları içeren çözeltiler kullanılarak bu iyonların tutulma miktarlarının pH'a bağlı değerleri ölçülerek araştırılmıştır. Metal analizleri atomik absorpsiyon spektrofotometresiyle yapılmıştır. Cr(III) iyonlarının RCSP(II) reçinesi ile %100 giderimle pH 2'de platoya eriştiği, Cu(II) iyonları için ise bu değerin pH 3'de platoya eriştiği görülmüştür. Ticari Purolite C-160H reçinesi, Cu(II) iyonlarına Cr(III) iyonlarından daha yüksek bir seçimlilik göstermiştir. RNH-CH120 reçinesinin Cr(III) iyonlarını pH 6' da %80, Cu(II) iyonlarını pH 6'da %100, Cd(II) iyonlarını ise pH 7'de %100 oranda uzaklaştırdığı görülmüştür.

Purolite C-160H ve RNH-CH120 reçineleriyle 100 mg Cu(II)/L (pH 3.5) çözeltisinden Cu(II) iyonlarının uzaklaştırılması için optimum reçine miktarları bulunmuştur. Elde edilen sonuçlar kinetik çalışmalar için kullanılmıştır.

Kinetik çalışmalar Purolite C-160H ve RNH-CH120 reçineleri kullanılarak yürütülmüştür. Elde edilen kinetik veriler, bazı kinetik modellerde kullanılarak hız belirleme basamağı bulunmaya çalışılmıştır. Her iki reçinenin kinetik çalışmalarında reaksiyon hızının partikül difüzyonla kontrol edildiği saptanmıştır.

Sürekli çalışmalarda, iki farklı türde reçinenin Cu(II) iyonlarını uzaklaştırmadaki reçine performansları karşılaştırılmıştır. Purolite C-160H reçinesinin salıverme kapasitesinin 100 mg Cu(II)/L çözeltisinde RNH-CH120 reçinesine göre daha fazla olduğu görülmüştür. Aynı zamanda RNH-CH120 reçinesinin Purolite C-160H reçinesine göre difüzyon mekanizmasının daha yavaş ve metal iyonu bağlama kapasitesinin daha az olduğu gözlemlenmiştir. Reçineler üzerindeki Cu(II) iyonları 1 M HCl çözeltisi ile sıyrılabilmiştir.

Sürekli çalışmaların ikinci bölümünde, RNH-CH120 reçinesi kullanılarak Cu(II) iyonlarının uzaklaştırılmasında konsantrasyonun ve besleme akış hızının etkileri araştırılmıştır. Kolon performansları, aynı akış hızında ve farklı Cu(II) konsantrasyonları (10-30-50 mg Cu(II)/L) kullanılarak karşılaştırılmış ve 50 mg Cu(II)/L çözeltisinin salıverme kapasitesinin diğerlerine göre daha yüksek olduğu gözlemlenmiştir. Fakat sıyırma verimlerinin yaklaşık olarak aynı olduğu görülmüştür. Aynı zamanda besleme akış hızı düşürüldüğünde salıverme kapasitesinin arttığını tespit edilmiştir.

Kullanılmış ve orijinal Purolite C-160H ve RNH-CH120 reçineleri, IR spektrofotometri cihazı kullanılarak analiz edilmiştir. Yaklaşık 1480-1500 cm^{-1}' de RNH-CH120 reçinesinde karboksilat ($-COO^-$) gruplarının varlığı gözlemlenmiştir. Bu sonuç reçinedeki amidoksim gruplarının asitli ortamda hidrolize uğradığını ortaya koymuştur. Purolite C-160H reçinesinde ise kullanımdan sonra kimyasal yapısında hiçbir değişiklik olmadığı görülmüştür.

ABSTRACT

REMOVAL OF HEAVY METALS FROM AQUEOUS SOLUTIONS BY LOW CROSSLINKED CHELATING RESINS CONTAINING AMIDOXIME GROUPS

ÇETİN, Nesrin

MSc Thesis
In Chemical Engineering Department

Supervisors:

Prof. Dr. Nalan KABAY
Prof. Dr. Mithat YÜKSEL

July, 2006

Heavy metals in industrial wastewaters generate detrimental effect on environment, human health and economy. The chelating resins can be used for extraction of toxic metals in the natural and waste waters, exhibiting greater selectivity for heavy metals.

In this study, the macroporous chelating resins; RCSP(II) containing methylene phosphonic groups (DVB: 10 mol%),

commercially available Purolite C-160H containing sulphonic groups (DVB: 10 mol%), RNH-CH120 containing amidoxime groups (DVB: 5 mol %) were used for metal removal from aqueous solutions by batch and column methods. In batch studies performed in the laboratory, the effect of pH and resin amount on Cu(II) removal from aqueous solutions were investigated. In column studies, the resin performances of two different kinds of resins on removal of Cu(II) were compared.

Metal ion selectivity of chelating resins was studied by measuring pH dependency of distribution ratios of various metal ions (Cu(II), Cd(II), Cr(III)) by these resins using solutions containing 10^{-4} M metal ions. Metal analysis was carried out by atomic absorption spectrophotometer. The percent removal of Cr(III) and Cu(II) reached a plateau with about 100% of removal at pH 2 and at pH 3 by RCSP(II) resin respectively. Commercial Purolite C-160H resin showed a higher selectivity to Cu(II) ions than Cr(III) ions. The percent removals reached a plateau with about 80% of removal at pH 6, 100% of removal at pH 6, 100% of removal at pH 7 on the RNH-CH120 resin, for Cr(III),Cu(II) and Cd(II) ions, respectively.

The optimum resin amounts of Purolite C-160H and RNH-CH120 resins were determined for removal of Cu(II) from 100 mg Cu(II)/L (pH:3.5) solution. The obtained results were used for the kinetic studies.

Kinetic studies were performed by using Purolite C-160H and RNH-CH120 resins. The kinetic data were applied on some mathematical kinetic models and the rate controlling steps were found. In the kinetic studies of both resins, it was found that the reaction rate was controlled by particle diffusion.

In column studies, the resin performances of two different kinds of resins on removal of Cu(II) were compared. The breakthrough capacity of Purolite C-160H was greater than RNH-CH120 with 100 mg Cu(II)/L (pH:3.5) stock solution. It was also observed that the diffusion mechanism of RNH-CH120 resin was slower and its functional groups were less than Purolite C-160H resin. The copper on the resins was quantitatively eluted with 1 M HCl.

In the second part of column studies, the effects of concentration and feed flow rate were investigated for the removal of Cu(II) by RNH-CH120 resin. The column performances were compared with different Cu(II) concentrations (at 10-30-50 mg Cu(II)/L) at the same flow rate, it was observed that the breakthrough capacity of 50 mg Cu(II)/L solution was higher than the others. But the elution efficiencies were nearly the similar. It was observed that if feed flow rate was decreased breakthrough capacity increased.

The used and original RNH-CH120 and Purolite C-160H resins were analyzed using IR spectrophotometer. It was observed that at nearly 1550 cm^{-1} some $-COO^{-}$ (carboxylate) groups appeared on RNH-CH120 resin after sorption-elution steps. This result shows that amidoxime groups hydrolyzed to carboxylate groups in the acidic medium. In case of Purolite C-160H resin, there was no change after column use.

ACKNOWLEDGEMENTS

I would like to thank my supervisors Prof. Dr. Nalan KABAY and Prof. Dr. Mithat YÜKSEL for their valuable suggestions, guidance and support throughout the whole study.

This project was partly supported by Ege University Research Foundation (Project Number: MÜH-2004-024). I am grateful for the financial support.

I would like to thank Prof.Dr. Ümran YÜKSEL and Prof.Dr. Mehmet SAĞLAM for their contributions on preparations of my thesis.

I have to thank Ass. Prof. Müşerref Arda and Research Assistant İdil Yılmaz for their kind helps in the laboratory.

In addition, I thank Chemist M. Akçay for measurements by AAS. Also I want to thank graduate students Ö. Solak, S. Sarp, Ö.Arar, S. Samatya for their kind helps in Avicenne Project Laboratory.

Finally, I want to thank my family for their support throughout my life.

CONTENTS

CONTENTS (continued)

Page

CONTENTS (continued)

Page

CONTENTS (continued)

Page

INDEX OF FIGURES

INDEX OF FIGURES (continued)

Figure **Page**

INDEX OF FIGURES (continued)

INDEX OF FIGURES (continued)

Figure **Page**

INDEX OF FIGURES (continued)

Figure **Page**

INDEX OF TABLES

INDEX OF TABLES (continued)

ABBREVIATIONS AND SYMBOLS

Symbols	Explanation
Ce	Equilibrium concentration, M
Co	Initial concentration, M
C	Total concentration of both exchanging species
C_r	Total concentration of both exchanging species in the ion exchanger, M
$\overline{C}_A$	Concentration of species in the resin phase, M
C_{Ao}	Concentration of species A in bulk solution, M
C_{so}	Concentration of solid reactant at the bead's unreacted core, M
k	Rate constant of ion Exchange
D	Diffusion coefficient in solution phase, $m^2\,s^{-1}$
D_o	Inter-diffusion coefficient in the film
$\overline{D}$	Inter-diffusion coefficient in the ion exchange resin
D_r	Diffusion coefficient in solid phase, $m^2\,s^{-1}$
$D_{e,r}$	Diffusion coefficient in solid phase, $m^2\,s^{-1}$

ABBREVIATIONS AND SYMBOLS (continued)

Symbols	Explanation
δ	Liquid film thickness, m
a	Stoichiometric coefficient
K_D	Distribution coefficient, mL/g
K	Equilibrium constant
K_{li}	Rate constant for film diffusion
K_{MA}	Mass transfer coefficient of species A through the liquid film, m s^{-1}
K_s	Reaction constant based on surface, m s^{-1}
X	Fractional attainment of equilibrium
r_o	Particle radius, m
J_i	Flux, mol/s m^2
F	Total surface area of the ion exchanger, m^2
V_b	Breakthrough volume
V_{eq}	Equilibrium volume
t_b	Breakthrough time
t_{eq}	Equilibrium time

ABBREVIATIONS AND SYMBOLS (continued)

Abbreviations

B.C	Breakthrough capacity
EPA	Environmental Protection Agency
T.C	Total capacity
WHO	World Health Organization
MCLG	Maximum Contaminant Level Goals

1.0 INTRODUCTION

1.1 Heavy Metals

Industrial wastewaters often contain considerable amounts of heavy metals that would endanger public health and the environment if they are discharged without adequate treatment. An effort to minimize production of hazardous waste and to remediate existing, accumulated waste has become one of the most important environmental challenges that the world faces today.

According to recent surveys, the most common contaminants reported in groundwater are heavy metals. Heavy metals such as Pb, Hg, Cr, Ni, Cd, Cu, Co and Zn are usually associated with toxicity (1).

Chromium is a steel-gray, lustrous, hard metallic element naturally found in rocks, soil, animals, and in volcanic dust and gases. (WHO, Chromium is present in the environment in several different forms. The most common forms are chromium (0), chromium (III), and chromium (VI). No taste or odor is associated with chromium compounds. Chromium enters the air, water, and soil mostly in the chromium (III) and chromium (VI) forms. In air, chromium compounds are present mostly as fine dust particles which eventually settle over land and water. Chromium can strongly attach to soil and only a small amount can dissolve in water and move deeper in the soil to underground water (2).

Chromium (III) occurs naturally in the environment and is an essential nutrient. Chromium (VI) and chromium (0) are generally produced by industrial processes. The metal chromium, which is the chromium (0) form, is used for making steel. Chromium (VI) and chromium (III) are used for chrome plating, dyes and pigments, leather tanning, and wood preserving (2).

In Europe, ferrochromium is produced mainly in Finland, France, Italy, Norway, Sweden and former Yugoslavia. Potassium chromate is produced mainly in Germany, Italy, Switzerland and the United Kingdom. Sodium chromate and dichromate are now among the most important chromium products, and are used chiefly for manufacturing chromic acid, chromium pigments, in leather tanning and for corrosion control (3,4). Chromium levels in soil vary according to area and the degree of contamination from anthropogenic chromium sources. Tests on soils have shown chromium concentrations ranging from 1 to 1000 mg/kg, with an average concentration ranging from 14 to about 70 mg/kg. Chromium (VI) in soil can be rapidly reduced to chromium (III) by organic matter. As chromium is almost ubiquitous in nature, chromium in the air may originate from wind erosion of shales, clay and many other kinds of soil. In countries where chromite is mined, production processes may constitute a major source of airborne chromium. In Europe, endpoint production of chromium compounds is probably the most important source of chromium in air (5).

The MCLG for chromium has been set at 0.1 parts per million (ppm) because EPA believes this level of protection would not cause any of the potential health problems (6).

Production of the most water soluble forms of chromium, the chromate and dichromates, was in the range of 250,000 tons in 1992. Though chromium occurs in nature mostly as chrome iron ore and is widely found in soils and plants, it is rare in natural waters. The two largest sources of chromium emission in the atmosphere are from the chemical manufacturing industry and combustion of natural gas, oil, and coal.

From 1987 to 1993, according to the Toxics Release Inventory, chromium compound releases to land and water totaled nearly 200 million pounds. These releases were primarily from industrial organic chemical industries. The largest releases occurred in Texas and North Carolina. The largest direct releases to water occurred in Georgia and Pennsylvania (2).

EPA has found chromium to potentially cause the following health effects when people are exposed to it at levels above the MCL. Low-level exposure can irritate the skin and cause ulceration. Long-term exposure can cause kidney and liver damage, and damage too circulatory and nerve tissue. Chromium often accumulates in aquatic life, adding to the danger of eating fish that may have been exposed to high levels of chromium (7).

Copper is a very common substance that occurs naturally in the environment and spreads through the environment through natural phenomena. Humans widely use copper. For instance it is applied in the industries and in agriculture. The EPA requires that levels of copper in drinking water should be less than 1.3 mg of copper per one liter of drinking water (1.3 mg/L) (7).

Copper can be found in many kinds of food, drinking water and air. Because of that we absorb eminent quantities of copper each day by eating, drinking and breathing. The absorption of copper is necessary, because copper is a trace element that is essential for human health. Although humans can handle proportionally large concentrations of copper, too much copper can still cause eminent health problems. Most copper compounds will settle and be bound to either water sediment or soil particles. Soluble copper compounds form the largest threat to human health. Usually water-soluble copper compounds occur in the environment after release through application in agriculture (7).

Copper concentrations in air are usually quite low, so that exposure to copper through breathing is negligible. But people that live near smelters that process copper ore into metal do experience this kind of exposure. People that live in houses that still have copper plumbing are exposed to higher levels of copper than most people, because copper is released into their drinking water through corrosion of pipes (7).

Occupational exposure to copper often occurs. In the work place environment copper contagion can lead to a flu-like condition known as metal fever. This condition will pass after two days and is caused by over sensitivity (7).

Long-term exposure to copper can cause irritation of the nose, mouth and eyes and it causes headaches, stomachaches, dizziness, vomiting and diarrhoea. Intentionally high uptakes of copper may cause liver and kidney damage and even death. Whether copper is carcinogenic has not been determined yet. There are scientific articles that indicate a link between long-term exposure to high concentrations of copper and a decline in intelligence with young adolescents.

Whether this should be of concern is a topic for further investigation (8).

Industrial exposure to copper fumes, dusts, or mists may result in metal fume fever with atrophic changes in nasal mucous membranes. Chronic copper poisoning results in Wilson’s Disease, characterized by a hepatic cirrhosis, brain damage, demyelination, renal disease, and copper deposition in the cornea (8).

The world's copper production is still rising. This basically means that more and more copper ends up in the environment. Rivers are depositing sludge on their banks that is contaminated with copper, due to the disposal of copper-containing wastewater. Copper enters the air, mainly through release during the combustion of fossil fuels. Copper in air will remain there for an eminent period of time, before it settles when it starts to rain. It will than end up mainly in soils. As a result soils may also contain large quantities of copper after copper from the air has settled (7).

Copper can be released into the environment by both natural sources and human activities. Examples of natural sources are wind-blown dust, decaying vegetation, forest fires and sea spray. A few examples of human activities that contribute to copper release have already been named. Other examples are mining, metal production, wood production and phosphate fertilizer production. Because copper is released both naturally and through human activity it is very widespread in the environment. Copper is often found near mines, industrial settings, landfills and waste disposals. When copper ends up in soil it strongly attaches to organic matter and minerals. As a result it does not travel very far after release and it hardly ever enters groundwater. In surface water copper can travel great distances, either suspended on sludge particles or as free ions (7).

Copper does not break down in the environment and because of that it can accumulate in plants and animals when it is found in soils. On copper-rich soils only a limited number of plants has a chance of survival. That is why there is not much plant diversity near copper-disposing factories. Due to the effects upon plants copper is a serious threat to the productions of farmlands. Copper can seriously influence the proceedings of certain farmlands, depending upon the acidity of the soil and the presence of organic matter. Despite of this, copper-containing manures are still applied (8).

Copper can interrupt the activity in soils, as it negatively influences the activity of microorganisms and earthworms. The decomposition of organic matter may seriously slow down because of this. When the soils of farmland are polluted with copper, animals will absorb concentrations that are damaging to their health. Mainly sheep suffer a great deal from copper poisoning, because the effects of copper are manifesting at fairly low concentrations (9).

Cadmium can mainly be found in the earth's crust. It always occurs in combination with zinc. Cadmium also consists in the industries as an inevitable by-product of zinc, lead and copper extraction. After being applied it enters the environment mainly through the ground, because it is found in manure and pesticides. Human uptake of cadmium takes place mainly through food; Foodstuffs that are rich in cadmium can greatly increase the cadmium concentration in human bodies. Examples are liver, mushrooms, shellfish, mussels, cocoa powder and dried seaweed (10).

An exposure to significantly higher cadmium levels occurs when people smoke. Tobacco smoke transports cadmium into the lungs. Blood will transport it through the rest of the body where it can increase effects by potentiating cadmium that is already present from cadmium rich food. Other high exposures can occur with people who live near hazardous waste sites or factories that release cadmium into the air and people that work in the metal refinery industry. When people breathe in cadmium it can severely damage the lungs. This may even cause death (10).

Other health effects that can be caused by cadmium are:

- Diarrhoea, stomach pains and severe vomiting

- Bone fracture

- Reproductive failure and possibly even infertility

- Damage to the central nervous system

- Damage to the immune system

- Psychological disorders

- Possibly DNA damage or cancer development

The average daily intake for humans is estimated as 0.15µg from air and 1µg from water. Smoking a packet of 20 cigarettes can lead to the inhalation of around 2-4µg of cadmium, but levels may vary widely (6).

Naturally a very large amount of cadmium is released into the environment, about 25,000 tons a year. About half of this cadmium is released into rivers through weathering of rocks and some cadmium is released into air through forest fires and volcanoes. The rest of the cadmium is released through human activities, such as manufacturing.

Cadmium waste streams from the industries mainly end up in soils. The causes of these waste streams are for instance zinc production, phosphate ore implication and bio industrial manure. Cadmium waste streams may also enter the air through (household) waste combustion and burning of fossil fuels. Because of regulations only little cadmium now enters the water through disposal of wastewater from households or industries (6).

Another important source of cadmium emission is the production of artificial phosphate fertilizers. Part of the cadmium ends up in the soil after the fertilizer is applied on farmland and the rest of the cadmium ends up in surface waters when waste from fertilizer productions is dumped by production companies. Cadmium can be transported over great distances when it is absorbed by sludge. This cadmium-rich sludge can pollute surface waters as well as soils.

In aquatic ecosystems cadmium can biologically accumulate in mussels, oysters, shrimps, lobsters and fish. The susceptibility to cadmium can vary great1y between aquatic organisms. Salt water organisms are known to be more resistant to cadmium poisoning than freshwater organisms (6).

Mercury is a global pollutant with complex and unusual chemical and physical properties. The major natural source of mercury is the degassing of the Earth's crust, emissions from volcanoes and evaporation from natural bodies of water (11).

World-wide mining of the metal leads to indirect discharges into the atmosphere. The usage of mercury is widespread in industrial processes and in various products (e.g. batteries, lamps and thermometers). It is also widely used in dentistry as an amalgam for fillings and by the pharmaceutical industry. Concern over mercury in the environment arises from the extremely toxic forms in which mercury can occur (11).

Mercury is mostly present in the atmosphere in a relatively unreactive form as a gaseous element. The long atmospheric lifetime (of the order of 1 year) of its gaseous form means the emission, transport and deposition of mercury is a global issue(11).

Natural biological processes can cause methylated forms of mercury to form which bioaccumulate over a million-fold and concentrate in living organisms, especially fish. These forms of mercury: monomethylmercury and dimethylmercury are highly toxic, causing neurotoxicological disorders. The main pathway for mercury to humans is through the food chain and not by inhalation (12).

The main sources of mercury emissions in the UK are from the manufacture of chlorine in mercury cells, non-ferrous metal production, coal combustion and crematoria. UK emissions of mercury are uncertain and it is estimated that the range is from 13 to 36 tonnes per year (DERA). Emissions are estimated to have declined by around ¾'s between 1970 and 1998 (NAEI), mainly due to improved controls on mercury cells and their replacement, and the fall in coal use (12).

Mercury is a toxic substance which has no known function in human biochemistry or physiology and does not occur naturally in living organisms. Inorganic mercury poisoning is associated with tremors, gingivitis and/or minor psychological changes, together with spontaneous abortion and congenital malformation (12).

Monomethylmercury causes damage to the brain and the central nervous system, while foetal and postnatal exposure have given rise to abortion, congenital malformation and development changes in young children (9).

1.2 Removal of Heavy Metals from Water and Wastewater

Different treatment techniques have been developed to remove either or both dissolved and suspended heavy metal ions from waters and wastewaters. Therefore, inexpensive materials for removing and entrapping heavy metal wastes from contaminated water are required. Treatment of aqueous wastes containing soluble heavy metals requires concentration of the metals into a smaller volume followed by recovery or secure disposal (13).

A number of traditional treatment techniques include precipitation-neutralization, ultra-filtration, reverse osmosis, electrodeposition, solvent extraction, foam flotation, cementation, filtration and evaporation. Adsorption on solid matrices is also reported to be a potential method for heavy metal removal (13). Nonspecific sorbents, such as activated carbon, metal oxides, and ion-exchange resins have been used. Specific sorbents consisting of a metal chelating ligand which interacts with the heavy metal ions specifically, and a carrier matrix which may be an inorganic material (e.g., activated carbon, alumina, silica or glass) or polymer microspheres (e.g., polystyrene or polymethymethacrylate) have also been reported (14).

Major anthropogenic sources of heavy metals in the environment include metal extraction, metal fabrication, surface finishing, metallurgical, tannery, chemical manufacturing, mining, paints and pigments, as well as the manufacture of batteries. Pollution by chromium is of considerable concern as the metal has found widespread use in electroplating, leather tanning, metal finishing, nuclear power plant, textile industries and chromate preparation.

Previous researchers reported reasonable methods, from the economical and technological point of view, to remove heavy metals in general from superficial waters, with the aim of the preservation of the entire ecosystem from the damages due to their accumulation (15).

Among the various treatment techniques available, the most commonly used ones are:

- chemical coagulation
- solvent extraction
- reduction and precipitation
- membrane separation
- ion exchange
- adsorption

These methods suffer from some drawback such as high capital and operational costs or the treatment and disposal of the residual metal sludge. Among these methods, ion exchange is a highly popular one and has been widely practiced in industrial wastewater treatment process. The main advantages of ion exchange over chemical precipitation are recovery of metal value, selectivity, less sludge volume produced and the meeting of strict discharge specifications. In ion exchange systems, polymeric resins are usually employed (16). Ion exchange using synthetic resins is the method of choice in many water treatment processes for removing inorganic contaminants in water and wastewater (17).

1.3 Ion exchange

1.3.1 Ion exchange phenomenon

An ion exchange reaction may be defined as the reversible interchange of ions between a solid phase (the ion exchanger) and a solution phase, the ion exchanger being insoluble in the medium in which the exchange is carried out. If an ion exchanger M^-A^+, carrying cations A^+ as the exchanging ions, is placed in an aqueous solution phase containing B^+ cations, an ion exchange reaction takes place which may be represented by the following equation (19):

$$\overline{M^-A^+} + B^+ \longleftrightarrow \overline{M^-B^+} + A^+$$

Solid Solution Solid Solution

The equilibrium represented by the above equation is an example of cation exchange, where M^- is the insoluble fixed anionic complement of the ion exchanger M^-A^+, often called simply the fixed anion. The cations A^+ and B^+ are referred to as counter-ions, whilst ions in the solution which bear the same charge as the fixed anion of the exchanger are called co-ions. In much the same way, anions can be exchanged provided that an anion-receptive medium is employed. An analogous representation of an anion exchange reaction may be written as follows (27):

$$\overline{M^+C^-} + D^- \longleftrightarrow \overline{M^+D^-} + C^-$$

Solid Solution Solid Solution

Ion exchange is most useful for dilute wastewaters (less than 100 mg/L metals). It is effective at higher metal concentrations but the economics favor other technologies must be discussed. Effluent metal concentrations in the single digit part per billon (ppb) levels are achievable using ion exchange (19).

Ion exchange process used in;

- *Water treatment:* Softening and deionization, condensate treatment, process water treatment, drinking water treatment, effluent treatment, wastewaters treatment, brewing water treatment. The treatment of a variety of industrial wastes to recover valuable waste materials, such as the ionic forms of the gold, silver, platinum, chromium, and uranium.

- *Hydrometallurgy:* Recovery and concentration of precious metals, extraction and concentration of uranium and nickel from dilute leaching solutions, separation of rare earth metals and of heavy metals, purification of plutonium.

- *Food industry:* Sugar and sweetening agents; wine-making; fruit juices; citric acid and amino acid separation, protein recovery, sorbitol deionization.

- *Dairy industry:* Milk whey demineralization, purification of lactose, removal of calcium and sodium from milk, preparation of pure casein.

- *Medicine:* Reduction in serum cholesterol, bipolar resins for blood preservation.

- *Biochemistry and biotechnology:* Immobilized enzymes, immobilized microorganisms, virus and protein sorption, preparation of biologically active substances.

- *Analytical chemistry:* Ion exchange chromatography, ion chromatography.

- *Electronic Industry:* The production of ultra pure water for the electronic and pharmaceutical industries.

- *Photography:* Silver separation from photographic baths, recovery of color developers, removal of hexacyanoferrate.

- *Pollution control:* Detoxification, removal of toxic gases, stabilization of metallic pollutant in industrial wastes, treatment of waste gases and waste waters (20).

1.3.2 History of Ion Exchange

The widespread interest in ion exchange and its general utility during the past decade are direct results of the development and commercial availability of stable and high capacity ion-exchange resins (21).

From a chronological and historical point of view, the following developments and dates are of considerable interest (21):

1850-1854: Discovery of ion exchange by Thompson and Way in England.

1905: Development of commercial use of ion exchange developed by Gans in Germany.

1935: Synthesis of synthetic ion-exchange resins by Adams and Holmes.

1939: Introducing patents of Adams and Holmes to U.S. industry.

1940: Development of first commercial phenol formaldehyde-based cation and anion exchange resins.

1946: Development of anion exchange resins for ulcer therapy.

1948: Development of styrene-based ion-exchange resins and first unifunctional carboxylic cation exchange and first strong base anion exchange resins.

1950: Development of resins for sodium reduction.

1952: Construction of first commercial ion-exchange uranium recovery plant.

1955: Construction of first commercial uranium resin-in-pulp plant and first atomic-powered submarine with an ion exchange deionizing Monobed.

1956: Development of first large-scale commercial ion-exchange rare earth separation plant.

1957: Processing of first commercial liquid ion-exchange operation.

1.3.3 Ion Exchange Resins

Ion exchangers are insoluble materials carrying reversibly exchangeable ions. These ions can be stoichiometrically exchanged for other ions of the same sign when the ion exchanger is in contact with an electrolyte solution. They are polymers carrying fixed functional groups (22).

The fixed groups are either permanently ionized so that they always possess a formal charge, or are capable of ionization or acceptance of protons to from the charged site. The resin interacts with mobile ions from an external solution. Ions of opposite charge to that on the resin, and which are exchanged by the resin, are known as counter-ions, while ions of the same charge as that of the exchange sites are known as co-ions. The polymeric network of the resin is known as the matrix (23).

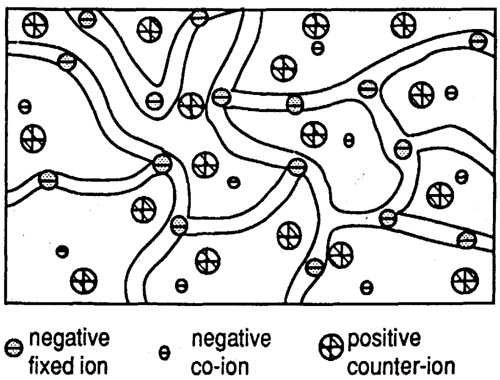

Figure 1.1 A cation exchange resin structure

Basic requirements of ion exchange resins are:

1. Resin must be highly polymeric and sufficiently crosslinked.

2. Resin must be of high exchange capacity.

3. Resin must be as stable as possibly chemically and physically.

4. Resin must be sufficiently hydrophilic.

5. Resin must be of granulation tuned to envisaged application.

6. Resin in swollen state should be denser than water (23).

1.3.3.1 Production of Ion Exchange Resins

Today, synthetic organic resins have become most efficient and most widely used ion exchangers. A great variety of such resins with different properties are available and have been described in the literature. The largest manufacturer companies and trade names of their resins are tabulated in Table 1.1.

The preparation of high-performance ion exchangers is not a simple matter. The synthesis of ion exchange resins must yield a tree-dimensional, crosslinked matrix of hydrocarbon chains carrying fixed ionic groups. This can be achieved by various methods.

The availability of polymerization ion exchangers based on styrene and divinylbenzene as well as acrylics and divinylbenzene as matrices brought a tremendous expansion of ion exchange tecniques.

These resins are in bead form could be readily manufactured in any mesh size desired, and are very stable over the total pH range. The particle size range is between 0.3- 1.2 mm in diameter. For special application, fine and ultra fine resins are of interest. These resins have fixed pores built into the matrix before they are converted to the ion exchanger if the pores of ion exchange resins could be formed with identical shapes and diameters such resin could be called as isoporous. But the primary distinction made in synthetic polymeric ion exchangers is that between gel type or macroporous type as shown in Figure 1.2. (20).

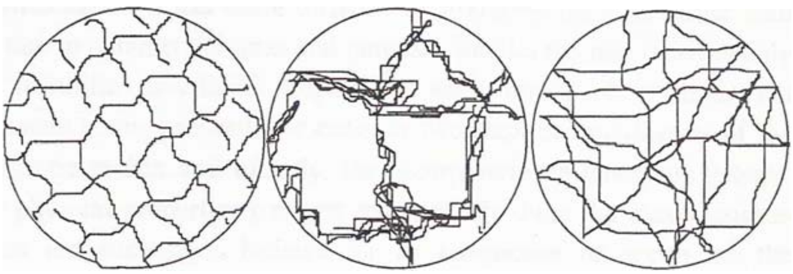

(a) (b) (c)

Figure 1.2 Structural models of gel type (a), macroporous (b) and isoporous (c) ion-exchangers (20).

Table 1.1 Trade names and manufacturers of ion-exchangers (N.Kabay, 1996) (20)

Trade Name	**Manufacturer**
Amberlite	Rohm&Haas Co., USA
Purolite	Purolite Ltd., England
Dowex	Dow Chemical Co., USA
Duolite	Chemical Process Co., USA
Lewatit	Bayer, Germany
Permutit	Permutit Co.,USA and Permutit A.G.,Germany
Resex, Resanex	Jos. Crosfield & Sons Ltd., England
W ofatit WEB	Germany
Zeo- Karb	The Permutits Co., Ltd., England
Zerolite	United Water Softeners, England
MIS$O ALM	Nippon Soda, Japan
CR20,CRP200 (Diaion)	Mitsubishi, Japan
Chelex	Bio-Rad, USA
Diphonix, Actinide	EiChrom, USA

For preparation and manufacture of ion exchange resins, there are in principle two factors to be considered, for both polymerization and polycondensation ion exchangers. These are:

1. The construction of the matrix as a basic polymer and its crosslinking by suitable crosslinking agents.

2. The incorporation of ionogenic groups into the matrix for the

exchange of ions (20).

1.3.3.2 Synthesis of ion exchange resins

The majority of ion exchange resins are made by the copolymerization of styrene and divinylbenzene (DVB). The styrene molecules provide the basic matrix of the resin, while the DVB is used to crosslink the polymers to allow for the general insolubility and toughness of the resin. The degree of crosslinking in the resin's three-dimensional array is important because it determines the internal pore structure, which will have a large effect on the internal movement of exchanging ions (24).

Typically a styrene and DVB mixture containing a polymerization initiator is dispersed as spherical liquid droplets in water. The styrene and DVB, both liquids at the start, are put into a chemical reactor with roughly the same amount of water. The suspension is continuously stirred and heated. A surfactant is also present to keep everything dispersed. The styrene/DVB begin to form large globules of material, and as the speed of agitation increases, the globules break up into smaller droplets until reaching the size of about a milimeter. At this point, the polymerization reaction is initiated by the addition of benzoyl peroxide, which causes styrene/DVB molecules to form the resultant small plastic beads. The divinylbenzene is a crosslinking agent that gives the beads their physical strength, and without which the styrene would be water-soluble. Higher DVB content gives the bead additional strength, but the additional crosslinking can hinder kinetics by making the bead too resistant to the shrinking and swelling necessary during normal operation (25).

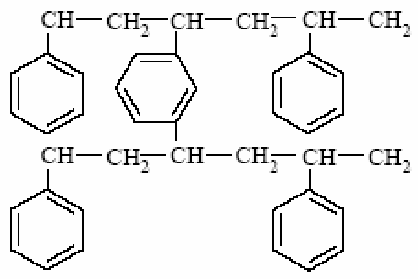

Figure 1.3 Styrene-divinylbenzene copolymer

There are three parameters defining the chemical structure of an ion-exchange resin (26):

1. The nature of the exchange grouping,

2. The degree of cross-linking, usually defined by the percentage of cross-linking agent used in the preparation of the cross-linked matrix,

3. The number of exchange groups per unit amount of exchanger.

Active groups are attached to provide chemical functionality to the bead. Each active group has a fixed electrical charge, which is balanced by an equivalent number of oppositely charged ions, which are free to exchange with other ions of the same charge. Strong acid cation resins are formed by treating the beads with concentrated sulphuric acid (process called sulphonation) to form permanent, negatively charged sulphonic-acid groups throughout the beads. Important here is the fact that the exchange sites thus formed are located throughout the bead. The ion exchange process is not a surface phenomenon; more than 99% of the capacity of anion exchange material is found in the interior of the bead (25).

Strong base anion resins are activated in two steps process that consists of chloromethylation followed by amination. The two steps process begins with the same styrene/DVB material as is used for cation resins. The only difference is that the amount of DVB used is less to allow for a more porous bead. The first reaction step is the attachment of a chloromethyl group to each of the benzene rings in the bead structure (25).

This intermediate chloromethylated plastic material needs to be reacted with an amine in a process called amination. The type of amine used determines the functionality of the resin (25).

1.3.3.3 Properties and characterization of ion exchange resins

1.3.3.3.1 Chemical specification of ion exchange resins

Matrix:

The common choice is between "styrene-divinylbenzene" or "acrylic-divinylbenzene" copolymer. In the case of the cation exchange resins selection is easily made since the acrylic products are weakly acidic whilst the styrenic resins are strongly acidic. Therefore for cation exchange the choice of copolymer is primarily decided by the process application and operating pH. The situation is very different with anion exchange resins since the two types of matrix pertain to products of both weak and strong functionality. Here anion exchange resins are concerned the choice between an acrylic resin and its styrenic equivalent is often made on considerations of operating exchange capacity, physical strength, and fouling resistance to complex high molecular weight organic anions (27).

Structure:

The polymer structure of the resin influences the mechanical strength, swelling characteristics, ion exchange equilibria, and exchange kinetics properties of all resins (27).

Capacity :

The total capacity of an ion exchange resin is defined as the total number of chemical equivalents available for exchange per some unit weight or unit volume of resin. The capacity may be expressed in terms of milliequivalents per dry gram of resin or in terms of milliequivalents per dry gram of resin or in terms of millequivalents per milliliter of wet resin (25).

The more highly crosslinked a resin, the more difficult it becomes to introduce additional functional groups. Sulfonation is carried out after the crosslinking has been completed and the sulfonic acid groups are introduced inside the resin particle as well as over its surface. Likewise, the quaternary ammonium groups are introduced after the polymerization has been completed and they too are introduced both inside the particle as well as on its surface. Fewer functional groups can be introduced inside the particles when they are highly crosslinked and hence the total capacity on a dry basis drops slightly (25).

This situation is reversed when a wet volume basis is used to measure the capacity on a resin. Although fewer functional groups are introduced into a highly crosslinked resin, these groups are spaced closer together on a volume basis because the volume of water is reduced by the additional crosslinking. Thus the capacity on a wet volume basis increases as cross-linking increases.

Crosslinking:

Crosslinking provides the fundamental chemical bonding between adjacent polymer chains thus giving the resin its inherent physical strength. The degree of crosslinking also governs the extent of swelling of the dry exchange resin upon absorbing water. The more weakly crosslinked the resin the greater the swelling and water uptake (27).

Swelling:

Ion exchangers are able to sorb solvents in which they are placed. Ion exchange resins swell in polar solvents (water, alcohol, etc.), but only to a limited degree. The swelling is limited by the crosslinked matrix ability to be stretched (22).

Ionic form:

Most ionic forms may be prepared by passing a large excess of an appropriate acid, alkali, or salt solution through a column of resin over 20-30 minutes. The ease of resin conversion generally increases with decreasing particle size, decreasing crosslinking, and decreasing charge of the ion being displaced (27).

Water content:

Water content or swelling water as it is sometimes called can be looked upon as a measure of the “water of hydration” of an ion exchange resin. Water enters a dry resin thereby hydrating the fixed ions and counter-ions and at the same time causing the resin to swell against the restraining action of crosslinks. Eventually an osmotic equilibrium is reached whereby the internal swelling pressure within the resin opposes any further water uptake. The swelling of a resin as measured by its water content is inversely related to the degree of crosslinking and is a most important structural characteristic (27).

pH range:

The pH range is very much dependent upon the strength of the functional group, but the following guidelines could be applied (27):

1. Strong acid cation: any pH

2. Weak acid cation: > 4

3. Strong base anion: any pH

4. Weak base anion (tertiary): < 9

Chemical stability:

At the macroscopic level, the chemical stability of modern resins at normal ambient temperatures is excellent, being insoluble in all common organic solvents and electrolyte solutions (27).

Two principle exceptions are resin breakdowns caused by sustained exposure to ionizing nuclear radiation and powerful chemical oxidizing agents such as nitric, chromic (VI) acid, chlorate (V) ions, halogens, and peroxy compound (27).

Thermal stability:

Over a temperature range, the stability characteristics of resins in common use may be summarized as follows (27):

Cation exchange resins: Cation exchange resins are generally quite stable, especially if they are in their salt forms.

Anion exchange resins: Strong base and weak base materials are also most stable in their salt forms compared with their hydroxide and free base forms, respectively. The effect of increased temperature is to accelerate the loss of exchange capacity, in which respect acrylic anion exchangers whether weak or strong base are significantly more unstable than their styrenic counterparts.

1.3.3.3.2 Physical specifications of ion exchange resins

Physical appearance:

Gel resins: usually shiny beads, clear to transmitted light.

Macroporous resins: usually dull beads of opaque or translucent appearance.

Resin particle size:

The particle size and size distribution of resins may be determined by a variety of techniques such as mechanical sieving, microscopic examination. The bead size range of conventional products is 300 μm to 1200 μm with a true mean value of approximately 700 μm (27).

Resin Density:

The true density of any resin in its dry or swollen form will, of course, depend upon resin type, structure, degree of crosslinking, and ionic form (27).

Measurement of density for swollen exchanger is easily determined in water using pycnometric or simple density bottle methods; whilst a non-swelling agent, for example octane, may be used for determinations on dried resins (27).

1.3.3.4 Types of Ion Exchange Resins

According to their material, ion exchangers are divided into two groups:

1. Inorganic ion exchangers: Most inorganic materials are crystalline alumosilicates with cation exchange properties. Characteristic representatives of this group of materials are the *zeolites* which are the best known of these, and included the minerals: analcite ($Na[Si_2AlO_6]_2.6H_2O$), chabazite ($Ca,Na[Si_2AlO_6]_2.6H_2O$), harmotome

($K,Ba[Si_5Al_2O_{10}].5H_2O$), heulandite ($Ca[Si_3AlO_8].5H_2O$), natrolite ($Na_2[Si_3Al_2O_{10}].2H_2O$) (23).

2. Organic ion exchangers: The majority of organic resins have a matrix of an irregular, three-dimensional network of macromolecular hydrocarbon chains. In most cases this consists of a copolymer of styrene and divinylbenzene (DVB), with the latter providing the crosslinking. The properties of the resins are determined all else by the ion-exchange groups present on the matrix. In general, these may be divided into three groups: cation exchangers (strong acid or weak acid groups); anion exchangers (strong base or weak base groups); specific ion exchangers (selective chelating groups) as mentioned before (23).

According to their physical structures, ion exchange resins are divided into five groups:

1. Gel Resins: The organic ion exchangers first developed were so-called gel resins. They have an essentially homogeneous distribution of water throughout the resin matrix (23).

Gel resins are homogenous crosslinked polymers and are the most common resins available. Gel resins usually have higher operating efficiencies and cost less. There are no permanent pore structures for the gel type resins. These pores are generally considered to be quite small and are referred as gelular pores or molecular pores. The pore structures are determined by the distance between the polymer chains and crosslinks which vary with the crosslink level of the polymer, the polarity of the solvent and the operating conditions. The gel type resins are generally translucent (25).

2. Macroporous resins: Macroporous resins are made with large pores that permit access to interior exchange sites. Macroporous resins are manufactured by a process that leaves a network of pathways throughout the bead. This sponge like structure allows the active portion of the bead to contain a high level of DVB crosslinking without affecting the exchange kinetics. Unfortunately, it also means that the resin has a lower capacity because the beads contain less exchange sites (25).

Macroporous copolymers, being highly crosslinked, are generally tougher than their gel equivalents and are more resistant to physical breakdown through mechanical forces, osmotic volume changes, and chemical degradation of crosslinking through the action of oxidizing agents (27).

3. Isoporous resins: It is claimed that some of the disadvantages of macroporous resins can be overcome by the synthesis of isoporous resins, in which the matrix has a substantially uniform network, free of highly crosslinked regions (23).

4. Microporous resins: Microporous is the term used to describe polymer particles manufactured with a low level of cross-linker. Improved rates of exchange can be obtained by using smaller particles, which make a larger surface area available. Powdered ion exchangers are employed in what has been termed precoat filters. However, because they are very fine particles (even though they are present in a coagulated form) they cause a high pressure loss in operation. Because of the high pressure loss, they can not be employed in a column system (23).

5. Magnetic resins: The difficulties of handling small, rapidly reacting resin beads can be surmounted by incorporating a magnetic filler such as the iron oxide γ-Fe_2O_3 within the particles. The magnetized resin beads then flocculate strongly to give agglomerates, which have settling rates comparable to those of normal sized beads. The flocs, which are held together by magnetic forces, are readily broken up by agitation so that the fast exchange rates associated with the small size of the resin particles can be achieved. Magnetic resins therefore combine some of the handling characteristics of conventional resin beads with the reaction rates of small particles (23).

The ionizable group attached to resin structure determines the functional capability of the exchanger. According to their functional groups, ion exchangers are divided into three groups:

Cation exchange resins:

Strongly Acid Type: The most important cation exchange resins are those of the *sulfonic acid type* (-SO_3H), which are used in acid, neutral, or alkaline solution . The resins are widely used for the uptake and chromatographic separation of ampholytic substances, e.g., amino acids (24).

Weakly Acid Type: These cation exchange resins possess *carboxylic acid groups* (-COOH) as the functional species. Being of weak electrolyte character, the carboxylic acid groups dissociate to varying extents depending on the pH level. They are essentially undissociated at pH 3 and below, dissociation increases with increase in pH until by pH 10 until they are fully dissociated. Carboxylic acid resins are very stable thermally. This type of resin used for separation of basic amino acids and the separation of strong organic bases from weak ones (28).

Anion exchange resins:

<u>Strongly Basic Type:</u> In analytical chemistry, resins of the strong basic resin type are much more useful than weakly basic resins. Anion-exchange resins of the strong base type are usually based on *quaternary ammonium groups* ($-N^+R_3OH^-$), connected to the aromatic rings of styrene-DVB copolymers via a methylene group. In general, strong base resins are very much less stable than strong acid resins. This type of resins used for the uptake and chromatographic separation of complex metal ions (23).

<u>Weakly Basic Type:</u> Weak base resins can possess *tertiary* ($-NR_2$), *secondary* (-NHR) or *primary* ($-NH_2$) *amino groups*, or mixtures of the same. The matrix can be as for strong base resins, although there are other matrices employed specifically for weak base resins. In acid medium a weakly basic resin in the free-base form is a valuable tool for the removal of acids from solutions of various non-electrolytes. These resins are prefered when solutes which are unstable at high pH are present in solution (28).

Chelating ion exchangers:

Organic ion exchangers have been used for many years in laboratory and industry plants. These materials consist of a network or matrix carrying functional groups, which are responsible for their ion exchange properties. Those functional groups may be immobilized in a polymeric matrix by chemical reaction or may be introduced by physical adsorption, in this case they are denominated impregnated resins (1). Resins containing selective functional groups were developed for application in hydrometallurgy processes, where conventional ionic exchangers were less selective. The sorption of metal ions in chelating resins leads to the complex formation. This is the main difference between the action of simple ionic exchangers and chelating resins (13). The chelating resin employed in the ion exchange processes in general is non-selective and has affinity for alkaline earth, alkali and heavy metals (14).

Improvement of the resin selectivity for heavy metal involves introducing specialty functional groups onto the polymer matrix of the ion exchange resin (30).

The interest in polymer complexing agents has largely grown in the last two decades because of the specific use of such polymers. These materials have been used for selective separation of metal ions from aqueous solutions (31).

Colella et al. (29) reported the application of a divinylbenzene crosslinked poly(acrylamidoxime) resin for the concentration of trace metals from aqueous solutions. The pH dependence of metal resin chelation was determined for several metals. The resin exhibited no affinity for the alkali or alkaline earth metals tested.

Vernon (32) obtained chelating resins containing hydroxamic acid groups derived from acrylonitrile–ethylacrylate–divinylbenzene copolymers. These resins were successfully applied to remove trace metals (copper, iron, lead, manganese, bismuth, titanium, zirconium, thorium, vanadium and molybdenum) from uranium solutions.

Egawa et al. (30,31) synthesized chelating resins with amidoxime groups derived from divinylbenzene crosslinked acrylonitrile copolymers with an effective pore structure (macropores) for recovering uranium from sea water. Spherical particles of macroreticular chelating resins containing specific chelating groups can be prepared through suspension copolymerization (1). These macroreticular resins are more efficient than gel type ones in relation to the selective removal and recovery of heavy metal ions because of their superior physical stability (18). In suspension polymerization, a mixture of organic phase, constituted of vinyl monomers, crosslinking agent, porogenic agent and free radical initiator, is stirred in an aqueous phase containing suspension stabilizers. The stabilizers serve to prevent coalescence and agglomeration of the monomer droplets and polymer beads, respectively (33).

The mechanism of the morphological structure formation of the resins is deeply influenced by the polymerization conditions such as: type and amount porogenic agent or diluent, dilution degree of the monomers, crosslinking degree, reaction temperature, etc (15). The swelling properties of the resins depend on the porous structure produced (16).

The main influencing factor of the resin morphological structure is the monomer diluent (solvating or non-solvating) used in copolymer syntheses. These agents are inert substances that when removed from the resin structure after polymerization liberates the pores.

The thermodynamic affinity of the diluent for the polymer structure determines the porous structure and swelling properties of the produced resins. When the diluent is a solvating one, in the stage of the phase separation, the polymer chains and polymer nuclei become less entangled and consequently the microspheres, more solvated, less compact, producing a higher number of small pores. As the solvating power of diluent is reduced, it occurs the contraction of the polymer chains, the nuclei and their agglomerates are formed in a more compact way, increasing thus the space among the agglomerates of microspheres (macropores) and the microspheres size (1,15,17).

The reduction of the solvating power of the diluent produces beads with a more heterogeneous polymer structure. The light passage these beads provokes intense light reflection that is the cause of the opaque appearance of these beads (1,15,17)

The proportion of crosslinking agent is an important variable in the resins synthesis, besides of being responsible for their insolubilization it determines the resins swelling capacity.

A macroporous resin is made up of a pore phase and a continuous gel phase. These resins have the necessary structural feature of inter connecting pores for rate enhancement and for greater accessibility of the active exchanging or chelating sites within the polymer particle. In the macroporous resins, the pores are invariant with time in opposition to the microporosity that arises from the swelling of the gel phase by a solvating liquid (34).

The other characteristic of macroporous resins is their high mechanical resistance. The friction between the polymer beads during the exchange process and the expansion and contraction of the polymeric matrix caused by solvents with inverse polarities, do not destroy or modify the beads pore structure (35).

Extraction of metal ions using chelating resins has several advantages over conventional methods (35):

(a) Selective determination of metal ions will be possible by using a chelating resin having a ligand possessing high selectivity to the targeted metal ion.

(b) It is free from difficult phase separation, which is caused by the mutual solubility between water and organic solvent layers.

(c) The chelating resin method is an economical method since it uses only a small amount of ligand and extraction solvent and this also increases the sensitivity of the system.

(d) Trace metal ions at as low as ppb can be determined because the targeted ion is enriched on the solid phase.

(e) The concentration of metal ion can be visibly estimated from the color intensity of the solid phase if the metal complex formed possesses adsorption in the visible wavelength region.

(f) Use of carcinogenic organic solvents is avoided and thus the technique is ecofriendly to nature.

Compared with sulfonic acid resins the chelating resins show superior selectivity in their sorption of various metallic cations. The published data show that the affinities for alkali metals are low, whereas most multivalent cations are held very strongly by the chelating resins (28).

These are weak acid cation exchangers consisting of iminodiacetate, aminomethyl and phosphonic functional groups in sodium form. These groups impart to the resin properties similar to those of ethylenediaminetetra-acetic acid (EDTA), in that the resin can form strong complexes with heavy metal ions. These resins have optimum porosity and surface area that give excellent operating capacities (28).

Certain resins can exchange both cations and anions, and are termed as *amphoteric ion* exchangers (23).

1.3.3.5 The Kinetics of ion exchange

Studies of ion exchange reactions on organic exchangers have identified the possible rate controlling steps to be (27):

1. Coupled diffusion or transport of counter-ions in the "external" solution phase.

2. Coupled diffusion or transport of counter-ions within the ion exchange resin.

3. Chemical reaction at the sites of the functional groups within the exchanger.

An understanding of the kinetics of ion exchange reactions has application in two broad areas. Firstly, it helps to understand the nature of the various fundamental ionic transport mechanisms, which control or contribute to the overall exchange rate. Secondly, derived numerical parameters such as rate constants, mass transfer coefficients, or diffusion coefficients found from a rate investigation are of value when making projections concerning the dynamic behaviour of columns and process design (27).

Figure 1.6 shows the radial concentration profiles of the exchanging species. The right sides of the diagrams show the profiles of species A (initially in the ion exchanger) and the left sides those of species B (initially in the solution). The various curves are for different contact times, t (Helfferich, 1962).

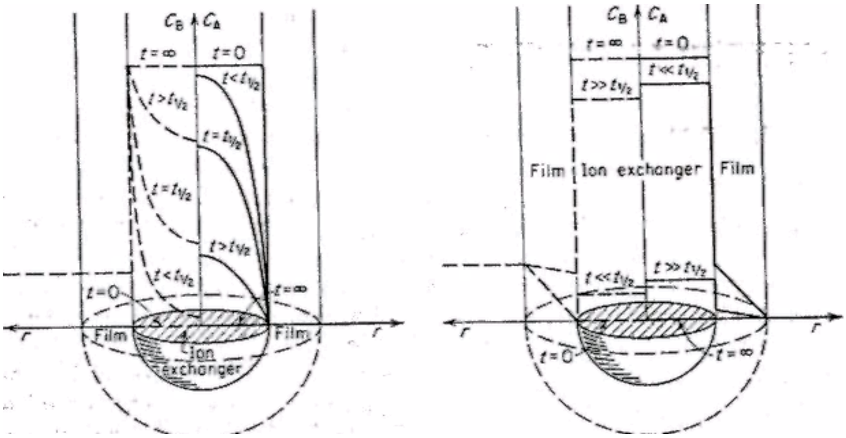

Figure 1.4 Radial concentration profiles for ideal particle diffusion control (schematic)

Two main rate–determining steps in kinetics of ion exchange could be given as:

$$\frac{X\,\bar{D}\,\delta}{CD_0 r_0}(5+2\alpha_B^A) \qquad << 1 \quad \text{particle diffusion control} \qquad (1.1)$$

$$\frac{X\bar{D}\delta}{CD_0 r_0}(5+2\alpha_B^A) \quad >> 1 \text{ film diffusion control} \tag{1.2}$$

X: concentration of fixed groups

C: solution concentration

$\bar{D}$: inter-diffusion coefficient in the ion exchange resin

D_0: inter-diffusion coefficient in the film

r_0: bead radius

δ: film thickness

α_B^A: separation factor

Rate laws can be derived by applying the diffusion equations to ion exchange systems. In general case, the differential equations and boundary conditions are nonlinear due to complications arising from diffusion-induced electric forces, selectivity, specific interactions and changes in swelling (36).

The following diffusion kinetic treatments are applicable for idealized ion exchange, i.e., they are only strictly true for isotropic exchange in a system which is in equilibrium expect for isotropic distribution. It is also assumed that all exchanger beads are spherical and have uniform size (24).

Diffusion processes are usually described in terms of Fick's first law:

$$J_i = -D \text{ grad } C_i \tag{1.3}$$

where J_i is the flux (in moles per unit time and unit cross section) of the diffusing species i, C_i is its concentration (in moles per unit volume), and D is the diffusion coefficient (24).

- ***Particle Diffusion***

In the case of particle diffusion control, concentration gradients will exist in the ion exchange bead. A quasi-homogenous model is assumed to derive the rate laws. The theoretical treatment of the diffusion within the solid phase is considered as occurring through a homogenous spherical electrolyte gel. The flux of the isotope A (J_A) in the ion exchanger is given by;

$$J_A = -\overline{D} \text{ grad } \overline{C_A} \tag{1.4}$$

where $\overline{D}$ is self diffusion coefficient of species and $\overline{C_A}$ is the concentration of species in the resin phase (24).

The time dependence of the concentration is interrelated with the flux by material balance (Fick's second law, termed the condition of continuity)

$$\frac{\partial \overline{C_A}}{\partial t} = -\text{div } J_A \tag{1.5}$$

where t is time.

The combination of Eqn. (4) and Eqn. (5) for systems with spherical geometry and with a constant diffusion coefficient gives

$$\frac{\partial \overline{C_A}}{\partial t} = \overline{D}\left(\frac{\partial^2 \overline{C_A}}{\partial r^2} + \frac{2}{r}\frac{\partial \overline{C_A}}{\partial r}\right) \tag{1.6}$$

where r is radial space coordinate (distance from the bead center) (24).

This equation must be solved under the appropriate initial condition, all ions A are in the ion exchanger at a uniform concentration $\overline{C_A}^{o}$, and no A is in the solution:

$$r > r_o,\ t = 0 \qquad \overline{C_A}(r) = 0$$

$$0 < r \le r_o,\ t = 0 \qquad \overline{C}_A(r) = \overline{C_A^{o}} = \text{const.} \tag{1.7}$$

The first and simpler condition applies when the concentration of A in the solution remains negligible throughout the process. This is true when a solution of constant composition is continuously passed through a thin layer of beads or in the case of batch operation if, the solution volume is so large (24).

$$\overline{C}\overline{V} << CV \tag{1.8}$$

where $\overline{V}$ and V are total volume of ion exchange material and solution respectively. This condition is called the "infinite solution volume". The infinite solution volume condition thus is,

$$r = r_o,\ t > 0 \qquad \overline{C_A}(t) = 0 \qquad (1.9)$$

Under this initial and infinite solution volume condition, the equation may be solved and integrated to give:

$$X = 1 - \frac{6}{\pi^2}\sum_{n=1}^{\infty}\frac{1}{n^2}\exp\left(-\frac{\overline{D}t\pi^2 n^2}{r_o^2}\right) \qquad (1.10)$$

where X is the fractional attainment of equilibrium.

A simplified expressions of this equation is given by the Vermeulen's approximation (37).

$$X = \left(1 - \exp\left(-\frac{\overline{D}\pi^2}{r_o^2}t\right)\right)^{1/2} \qquad (1.11)$$

The half time $t_{1/2}$ of ion exchange is readily calculated from Eqn. (1.11). The substitution X = 0.5 gives;

$$t_{1/2} = 0.03\frac{r_o^2}{\overline{D}} \qquad (1.12)$$

Secondly, the "finite solution volume" condition which does not meet the condition (1.8). The solution obtained by Peterson is;

$$X = \frac{w+1}{w}\left[1 - \frac{1}{\alpha-\beta}\left[\alpha \exp(\alpha^2\tau)(1+\operatorname{erf}\,\alpha\;\tau^{1/2}) - \beta \exp(\beta^2\tau)(1+\operatorname{erf}\,\beta\;\tau^{1/2}\right]\right] \quad (1.13)$$

where α and β are the roots of the equation $X^2 + 3wX - 3w = 0$.

▪ **Film Diffusion**

The rate laws for film-diffusion controlled isotopic exchange are derived under the following assumptions:

1. Interdiffusion in the film is treated as quasi-stationary, i.e.; it is assumed that diffusion across the film is fast as compared with the concentration changes at the film boundaries.

2. The film is treated as a planar layer (one-dimensional diffusion).

This is admissible if the film thickness is much smaller than the bead radius. Under this condition, the momentary flux (J_A) constant throughout the film and from Eqn. (1.3) is given by

$$J_A = D\frac{\Delta C_A}{\delta} \quad (1.14)$$

where ΔC_A is concentration difference between the boundaries of the film and δ is the film thickness (24).

Time dependence is obtain from material balance;

$$-\frac{dQ_A}{dt} = FJ_A \qquad (1.15)$$

where F is the total surface area of the ion exchanger.

The equilibrium condition at the interface

$$\frac{\overline{C_A}}{C'_A} = \frac{\overline{C}}{C} \qquad (1.16)$$

Combination of Eqn. (1.15) and Eqn. (1.16) gives after substitution;

$$-\frac{dC'_A}{dt} = \frac{3C}{r_o\overline{C}} J_A \qquad (1.17)$$

Eqn. (1.17) and Eqn. (1.18) are solved under the appropriate initial and boundary conditions. The simple initial condition corresponding to uniform initial concentration $\overline{C_A}^o$ in the ion exchanger and no A in the solution is;

$$r = r_o,\ t = 0 \qquad C'_A = \frac{\overline{C_A}^o C}{\overline{C}}$$

$$r \geq r_o,\ t = 0 \qquad C_A(r, t) = 0 \qquad (1.18)$$

The boundary condition in the case of "infinite solution volume" condition

$$r \geq r_o + \delta,\ t \geq 0 \qquad C_A(r, t) = 0 \qquad (1.19)$$

The mathematical solution under the conditions (17) to (18) is,

$$X = 1 - \exp\left(-\frac{3DCt}{r_o \delta \overline{C}} \right) \qquad (1.20)$$

with a half time of ion exchange :

$$t_{1/2} = 0.023 \frac{r_o \delta \overline{C}}{DC} \qquad (1.21)$$

The rate thus is proportional to the diffusion coefficient in the film and to the concentration of the solution and is inversely proportional to the bead radius, the film thickness, and the counter-ion concentration in the ion exchanger (24).

In the case of "finite solution volume", the condition (1.19) replaces by;

$$r \geq r_o + \delta, \quad t > 0 \qquad C_A(r,t) = \frac{\overline{V}}{V}\left(\overline{C_A}^{\,o} - \overline{C_A}(t)\right) \qquad (1.22)$$

The solution to this case is given by:

$$X = 1 - \exp\left(-\frac{3D(\overline{V}\overline{C} + VC)}{r_o \delta \overline{C} V} t \right) \qquad (1.23)$$

▪ **Chemical Reaction Kinetics**

Chemical reaction between the fixed ion exchange sites is one of the general ion exchange mechanisms. In certain cases, chemical reaction kinetics can control the ion exchange. This is seen to be the case in some chelating and solvent impregnated type ion exchange resins (36).

For non-catalytic reactions of solid particles with surrounding liquid, two basic models are considered; “continuous” or “homogenous” reaction model and heterogeneous “unreacted shrinking core” or “shell progressive” model (38).

In the case of homogenous reaction the ion exchange reaction assumed to occur uniformly throughout the resin particle. This model fits well if the resin contains enough porosity to allow the fluid to pass through freely. So that the concentration of the reacting ions is uniform throughout the resin. In the case of heterogeneous reaction, the porosity of the polymer is small and thus practically impervious to the fluid reactant, the reaction may be explained by the “Shell Progressive”, “Unreacted Shrinking Core” or “Ash Layer Models” (38). Slicing a partly reacted bead and examining its cross-section, the unreacted core is found to be sharply distinguished form the layer of product as shown in Figure 1.5.

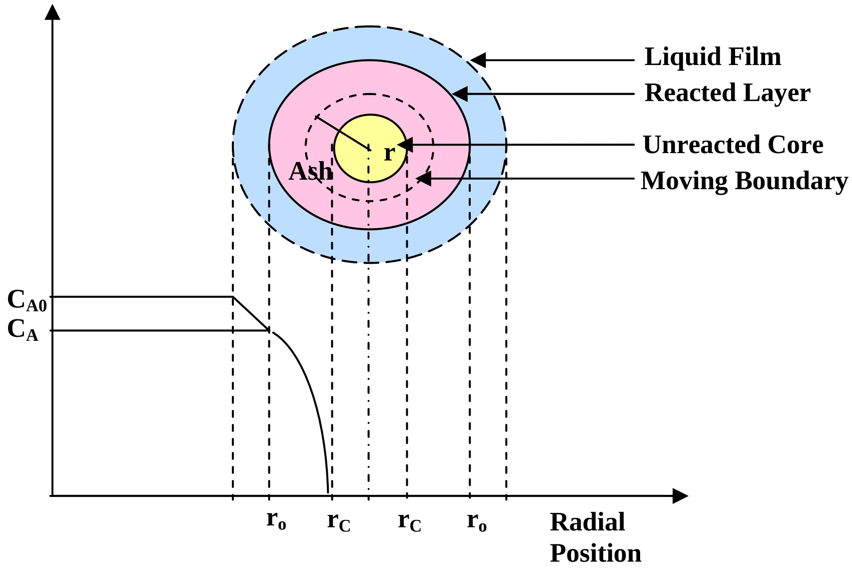

Figure 1.5 Concentration profile of a partially reacted ion exchange bead, C_{A0}; Concentration of species a in bulk solution and C_{As} ; Concentration of species A on the outer surface of the resin

The rate at which counter ions A react with the unreacted core is controlled by the three consecutive processes:

1. Interface mass transfer of the reacting species A from the bulk solution to the outer surface of the solid bead,

2. Interparticle diffusion of the reacting species from the outer surface through the reacted portion of the solid bead to the zone of reaction and,

3. Chemical reaction of the reacting species with the ion exchange surface of the zone.

The kinetic concept of a "shell progressive" mechanism can be described in terms of the concentration profile of a liquid reactant containing a counter ion A advancing into a spherical bead of a partially substituted ion exchanger. As the reaction progresses in the bead, the material balance of counterion A follows Fick's diffusion equation with spherical coordinates. In this case, the relationship between reaction time and degree of conversion gives the following expressions (39).

When the fluid film is controlling

$$t = \frac{a r_o C_{so}}{3 C_{Ao} K_{mA}} X \tag{1.24}$$

When the diffusion through the reacted layer control

$$t = \frac{a r_o^2 C_{so}}{6 D_{e,r} C_{Ao}} \left[3 - 3(1 - X)^{2/3} - 2X\right] \tag{1.25}$$

When the chemical reaction control

$$t = \frac{r_o}{k_s C_{Ao}} \left[1 - (1 - X)^{1/3}\right] \tag{1.26}$$

1.3.3.6 Selectivity of ion exchange resins

The ability of the ion exchanger to distinguish between various counter ion species is called selectivity (24).

Ion exchange resins generally have greater selectivities for ions with, increasing valance or charge. Among ions with the same charge, higher affinities are seen for ions with a higher atomic number (25).

Some factors which can cause ion exchange selectivity (22):

1. Charge of counter ion: as a rule, the ion exchanger prefers the counter ion of higher valence. The preference increases with dilution of the solution and it strongest for higher capacity resins

2. The ion exchanger prefers the counter ion having the smaller solvated equivalent volume

Two effects listed are true if:

1. There are not any specific interactions between counter ions and fixed groups. Functional groups are completely dissociated

2. There are not any specific interactions between counter ions and matrix

3. There is not complex formation in the inner solution

1.3.3.7 Ion exchange operational techniques

Ion exchange operations include batch and column operations (21).

1.3.3.7.1 Batch operation

The comparison of various ion-exchange resins with respect to their relative equilibrium and kinetic behaviour can be performed by batch techniques, i.e., by following the change in composition of an electrolyte solution in contact with an ion-exchange resin. The kinetic behaviour may be approximated by observing the change in composition of the solution as a function of time (21).

In batch contact, a method with only slight usefulness, maximum removal (neutralization, etc.) is limited by the equilibrium relationship between resin and solutes. When viscous solutions are being processed or when the equilibria are irreversible (neutralization, etc.), batch contact may offer some advantages (21).

1.3.3.7.2 Column operation

Ion-exchange materials are frequently tested for performance in a given application by small-scale column tests (21).

Generally, ion exchange operations are dictated when extreme removal of solute is required. Obviously many contacts with solute-free resin are required. Obviously many contacts with solute-free resin are required. Column operation conveniently suffices for complete removal. In equilibrium operation, the solution continuously contacts with resin and consequently there is a high driving force for the removal of solute from solution. In order to achieve maximum removal, the resin in the column must be most highly regenerated (21).

Figure 1.6 shows a typical breakthrough curve obtained at the end of a column operation.

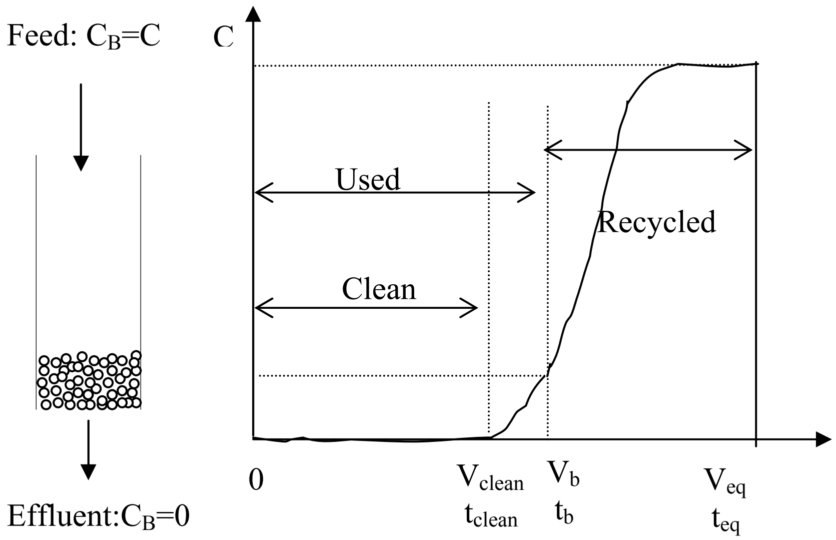

Figure 1.6 Breakthrough curve of column operation

1.3.3.7.3 Ion exchange capacity

Capacity and related data are primarily used for two purposes: lon characterizing of ion-exchange materials and for use in the numerical calculation of ion-exchange operations (24).

Ion exchange capacity could be defined as concentration of fixed functional groups per specified amount of ion exchanger (22).

Ion exchange capacities can be classified as (21):

1. Anion exchange capacity
2. Cation exchange capacity
3. Breakthrough capacity
4. Saturation column capacity

Taking into consideration the breakthrough curve given in Figure 1.6 and types of capacities given above, the following equations could be formulated:

$$\textbf{Total Capacity} = \int_0^{V_{eq}} (C_0 - C)dV$$

Breakthrough Capacity = $\int_{0}^{Vb} (C_0 - C)dV$

Degree of the Column Utilization = $\dfrac{\int_{0}^{V_b} (C_0 - C)dV}{\int_{0}^{V_{eq}} (C_0 - C)dV}$

2.0 EXPERIMENTAL

2.1 Materials

2.1.1 Ion exchange resins

The macroporous methylene phosphonic type chelating resin RCSP(II); strong acid, macroporous cationic exchange resin Purolite C-160H (product of Purolite International Ltd.); low-crosslinked chelating resin containing amidoxime groups RNH-CH120 were used. The properties of these resins are given in Tables 2.1-2.3.

2.1.2 Chemicals

- $Cr(NO_3)_3 .9 H_2O$
- $Cu(NO_3)_2 .3H_2O$
- $Cd(NO_3)_2.9 H_2O$
- HNO_3: 95-97 %, d:1.84 g/L, J.T: Baker
- HCl : 37 %, d:1.19 g/L, Merck
- NaOH: 99 %, (solid-pulp), J.T: Baker
- pH=4 and pH=7 buffer, Metrohm

The structure of RCSP(II) macroeticular styrene-divinylbenzene copolymer-based metylene phosphonic acid resin is shown in Figure 2.1 (36).

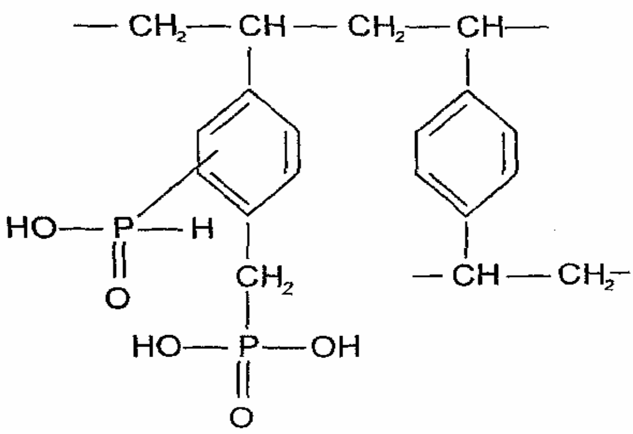

Figure 2.1 The structure of RCSP(II)

Table 2.1 Chemical and physical characteristics of RCSP(II) resin:

Matrix	Methylene phosphonic groups
Particle Size	32- 60 mesh
Crosslinking Degree	%10 DVB
Cation exchange capacity	7.0 meq/ g
P content	4.79 mmol/ g

The structure of commercial strong acid cation exchange resin Purolite C-160H resin is shown in Figure 2.2. Chemical and physical properties of Purolite C-160H are given in Table 2.2.

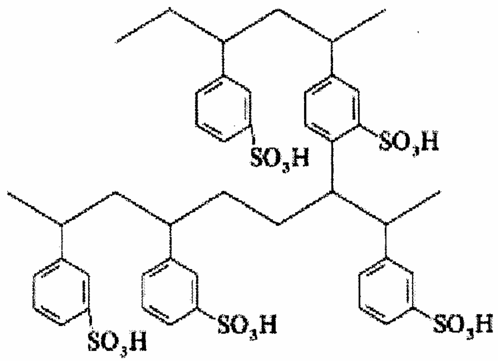

Figure 2.2 The structure of Purolite C-160H

Table 2.2 Chemical and physical characteristics of Purolite C-160H

Matrix	High crosslinked, Styrene DVB
Particle Size	0.5- 0.25 mm.
Crosslinking Degree	%10 DVB
Functional Groups	$-SO^{3-}\ H^{+}$
Standard Ionic Form	H^{+}
Particle size range, mm	0.3-1.2
% Moisture	54- 57
Max. Operating temp.(^{0}C)	120
Total exchange capacity of resin	1.7 meq/ ml
Volume change %	H^{+} to Na^{+} -3 to -6

The structure of amidoxime containing resin (RNH-CH120) is given in Figure 2.3. Chemical and physical properties of RNH-CH120 are given in Table 2.3.

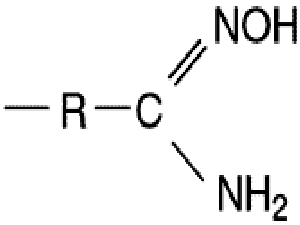

amidoxime group

Figure 2.3 The structure of RNH-CH120

Table 2.3 Chemical and physical characteristics of RNH-CH120:

Matrix	Macroreticular crosslinked
Symbol	Chloroform 120
Crosslinking Degree	% 5 DVB
Moisture holding capacity in %3 NaCl solution	2.7 cm^3/ g before modification with alkaline
Moisture holding capacity in %3 NaCl solution	4.6 cm^3/ g after modification with alkaline
Specific Surface Area	29.7 m^2/ g
Pore volume	0.304 cm^3/ g
Pore diameter	168 A^0
Anion exchange capacity	3.8 meq/ g
Cation exchange capacity	1.6 meq/ g

2.1.3 Equipments

- **Glass Column:** ID= 0.7 cm

- **Vacuum oven:** Gallen Kamp

- **Shaker:** Memmert

- **Peristaltic Pump:** Eyela Yokyo Rikakikai Co.Ltd., Micro Tube Pump (MP-3); Ismatec, ISM 597A-03516

- **Fraction Collector:** Advantec SF-2120, SF-2100W

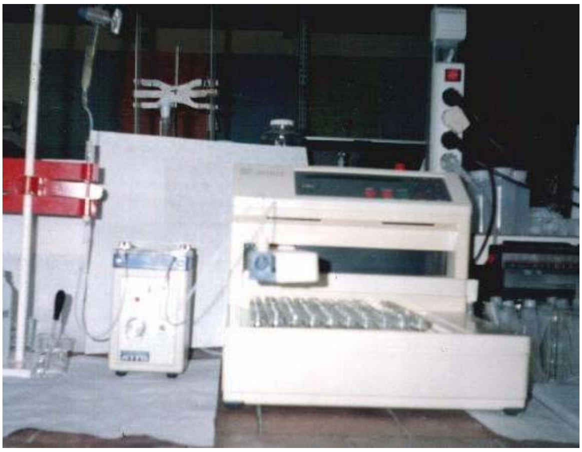

Figure 2.4 Column operation experimental set-up

• **AAS:** Varian 10 Plus model Atomic Absorption Spectrophotometer (Fig. 2.4)

• **Shimadzu Infrared Spectrophotometer**

• **pH meter:** Metrohm 694

• **Magnetic Stirrer:** Ikamag

Figure 2.5 Atomic Absorption Spectrophotometer

2.2 Batch-mode Sorption Studies

2.2.1 Effect of pH on Removal of Cr(III), Cu(II), Cd(II) by Cation Exchange Resins and Chelating Resins:

The removal of metal ions Cr(III), Cd(II), Cu(II) from aqueous solution was investigated at various pH values by using RCSP(II), Purolite C-160H, RNH-CH120 resins by batch mode studies.

For these tests, 0.04 g dry resin of RCSP(II) (32-60 mesh), Purolite C-160H (0.355-0.500 mm), RNH-CH120 (32-60 mesh) were contacted with 25 mL of 10^{-4} M metal solutions (Cr(III), Cd(II), Cu(II) at various pH values (pH 0.5, 1.0, 1.5, 2.0, 2.5, 3.0, 3.5, 4.0, 4.5, 5.0) at 30 ^{o}C for 24 h with continuous shaking in the shaker. pH of the solutions were adjusted by means of NaOH and HCl solutions.

2.2.2 Determination of optimum resin amount on removal of Cu(II):

Optimum resin amounts for removal of Cu(II) were determined using Purolite C-160H (0.355-0.500 mm) and RNH-CH120 (32-60 mesh) resins. Various amounts of dry resins (0.025, 0.050, 0.10, 0.15, 0.20 and 0.25 g) were contacted with 25 mL of 100, 50 and 10 mg Cu(II)/L solutions at pH 3.55, at 30^{o}C for 24 h with continuous shaking in the shaker.

2.2.3 Kinetic Studies:

The kinetic studies were performed with the optimum amount of resins (Purolite C-160H, RNH-CH120) that were 0.5 g-dry resin/500 ml and 3.0 g-dry resin/500 ml with Purolite C-160H, RNH-CH120 resins, respectively and were done by batch mode studies.

The kinetic studies were investigated in a flask replaced in a water bath. The resin beads within the flask were contacted with the solution through a mechanical stirring at a certain rpm. The resin samples were introduced to the reaction flask at time zero and then a specific amount of sample was collected with a syringe at various time intervals where the contact times were 0, 5, 10, 15, 20, 30, 45, 60, 90, 120, 150, 180, 240, 300, 360, 420, 480, 540, 1440 min at 25 ^{o}C. The samples were analyzed by atomic absorption spectrophotometer for metal ion concentration.

2.3 Column-mode sorption–elution studies

In order to get some information about column performances of chelating resins on removal of copper from solution, chelating resins Purolite C-160H (0.355-0.500 mm) and RNH-CH120 (32-60 mesh) were used for column-mode sorption and elution tests.

In these studies, a glass column with an internal diameter of 0.7 cm was employed. The resin beads were immersed into deionized water for 24 h before being packed into the column.

The column was packed with 1.0 mL wet-settled volume of resin. 100 mg Cu(II)/L solution at pH 3.5 was delivered by down-flow to the column at room temperature using a peristaltic pump (Ismatec, ISM 597A-03516 Model) at SV 15 h^{-1}. Each successive 3 mL (3 BV) fractions of the effluent were collected using a fraction collector (Advantec SF 2120 Model). Breakthrough curves were obtained by analysis of these successive fractions. Resin packed into the column was washed with deionized water after sorption step. The copper loaded resin was eluted with 1 M HCl at SV 5 h^{-1}. The column elution profiles were obtained by analysis of each successive 2 mL (2 BV) fractions of eluates.

2.3.1 Effect of Cu(II) Concentration on Removal of Cu(II) by RNH-CH120:

In column studies, the effect of Cu(II) concentration on removal of Cu(II) by RNH-CH120 (32-60 mesh) resin was investigated. The solutions with 10, 30 and 50 mg Cu(II)/L were prepared at pH 3.5 and were delivered by down-flow to the column packed with RNH-CH120 resin at room temperature using a peristaltic pump (Ismatec, ISM 597A-03516 Model) at SV 15 h^{-1}. Each successive 3 mL (3 BV) fractions of the effluents were collected using a fraction collector (Advantec SF 2120 Model). Breakthrough curves were obtained by analysis of each successive fraction. The Cu(II) loaded resin was eluted with 1 M HCl at SV 5 h^{-1}. The column elution profiles were obtained by analysis of each successive 2 mL (2 BV) fractions of eluates.

2.3.2 Effect of Feed Flow Rate on Removal of Cu(II) by RNH-CH120:

In column studies, the effect of feed flow rate on removal of Cu(II) by RNH-CH120 (32-60 mesh) resin was studied. The solutions of 10 mg Cu(II)/L at pH 3.5 were delivered using a peristaltic pump at SV 5, 10 and 15 h^{-1}. The Cu (II) loaded resin was eluted with 1 M HCl at SV 5 h^{-1}.

3.0 RESULTS AND DISCUSSION

3.1 Batch-Mode Removal of Heavy Metal Ions:

3.1.1 Effect of pH on Removal of Cr(III), Cu(II) Ions by RCSP(II):

Effect of pH on removal of Cr(III), Cu(II) from their solutions (25 mL,10^{-4} M) for the pH range of 0.5-5 was studied using RCSP(II) resin. The data obtained are given in Table 5.1 in Appendix part. The respective metal removal vs. pH_{eq} plots are given in Figures 3.1- 3.3.

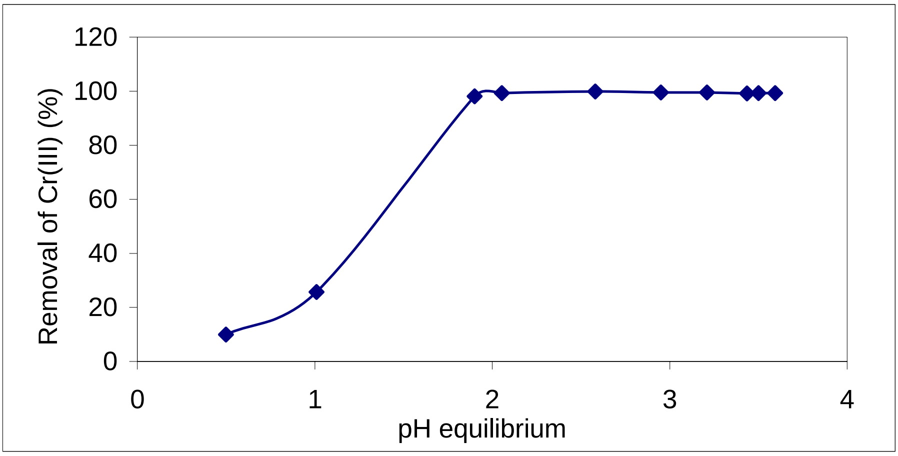

Figure 3.1 Effect of pH on Removal of Cr(III) by RCSP(II)

As shown in Figure 3.1, the percent removal of Cr(III) increases until pH 2. Then, percent removal reached a plateau at pH 2.

The ion exchange reaction between the metal ion and H^+ ions on RCSP(II) resin could be written as follows (36):

$$n(RPO_3H_2) + M^{n+} \rightleftharpoons (RPO_3H^-)_nM + nH^+$$

Distribution ratios K_D is calculated using the following equation:

$$K_D = \frac{\text{amount of metal ion on the resin at equilibrium (mmol / g)}}{\text{amount of metal ion in solution at equilibrium (mmol / ml)}}$$

According to this reaction, the following equation between the distribution ratio and pH can be derived (36).

log K_D = constant + n pH

This equation represents the relationship between log K_D and pH_{eq} for metal removal. **n** is defined as the charge of metal ion if ion exchange is the only mechanism which is responsible for metal removal.

The relationship between log K_D and pH_{eq} for Cr(III) removal by RCSP(II) is shown in Figure 3.2.

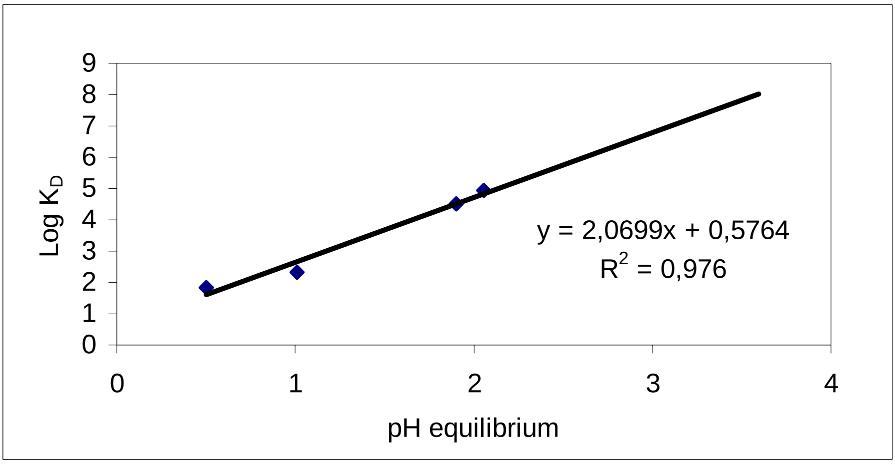

Figure 3.2 Relationship between log K_D and pH_{eq} for Cr(III)

Here the n value which is nearly 2 is less than the charge of Cr(III). This might be due to the existence of other ionic species of Cr(III) with a different charges in the solution. As shown in Figure 3.3 the percentage removal of Cu(II) by RCSP(II) reached a plateau at pH 3.

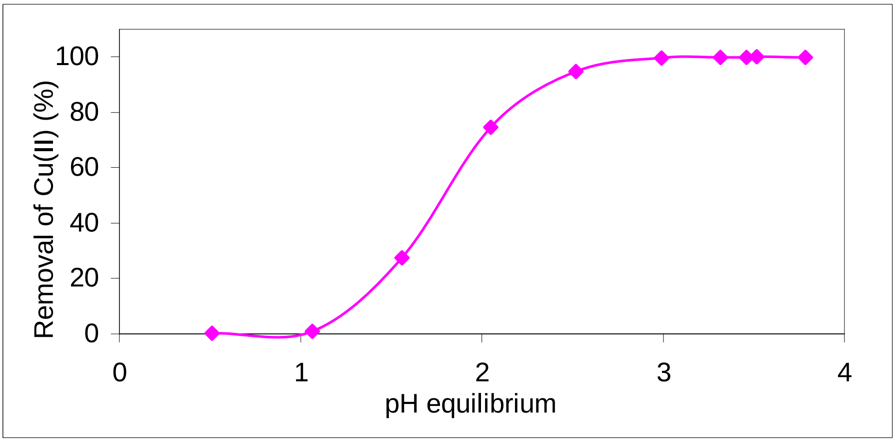

Figure 3.3 Effect of pH on Removal of Cu(II) by RCSP(II)

The relationship between log K_D and pH_{eq} for Cu(II) is shown in Fig 3.4. Here the n value was found to be 2.1 which is almost the charge of Cu(II).

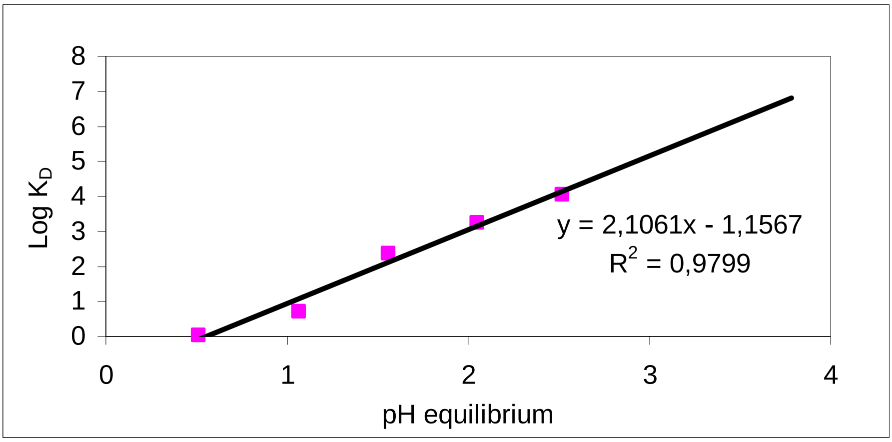

Figure 3.4 Relationship between log K_D and pH_{eq} for Cu(II)

The comparative figures for heavy metal removal by RCSP(II) are given in Figures 3.5 and 3.6.

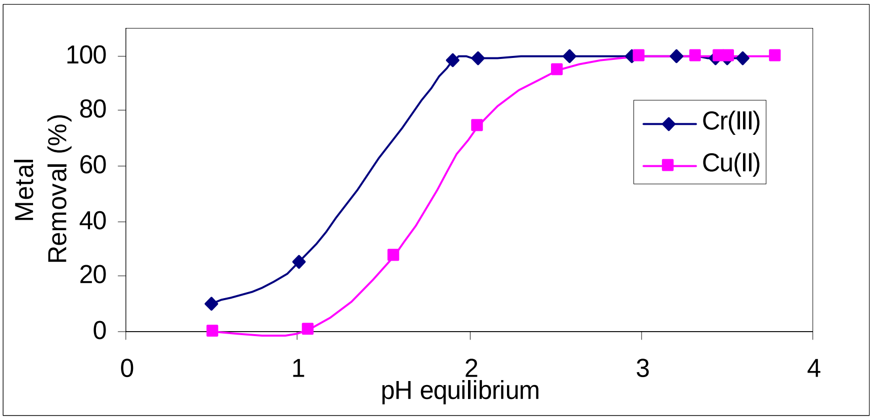

Figure 3.5 Effect of pH on Removal of Cr(III) and Cu(II) by RCSP(II)

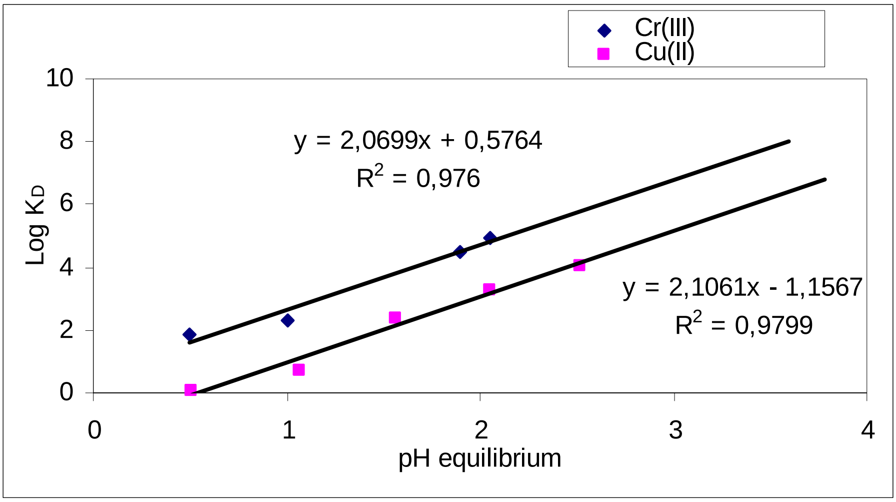

Figure 3.6 Relationship between log K_D and pH_{eq} for Cr(III) and Cu(II)

3.1.2 Effect of pH on Removal of Cr(III), Cu(II) Ions by Purolite C-160H:

Effect of pH on removal of Cr(III), Cu(II) from their solutions at the same conditions was studied using Purolite C-160H. As shown in Figure 3.7 the percentage removal of Cr(III) was almost constant at a pH range between 2-3 and the pH dependency was less compared to RCSP(II) resin.

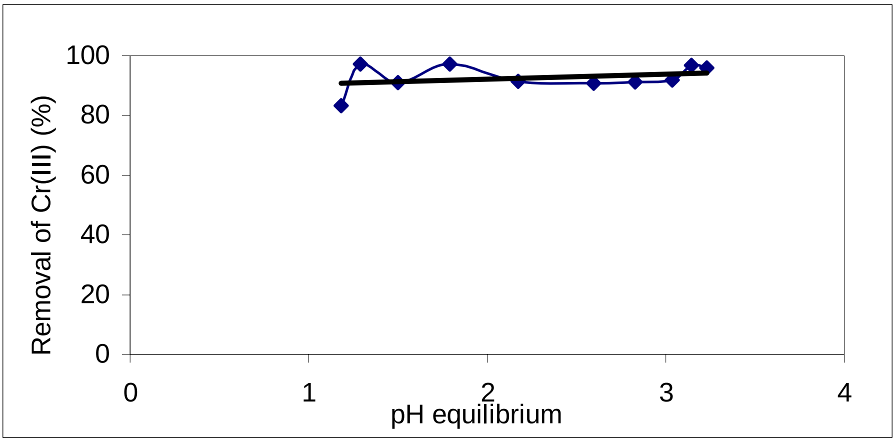

Figure 3.7 Effect of pH on Removal of Cr(III) by Purolite C-160H

The percent removal of Cu(II) reached a plateau with 100% of Cu(II) removal at pH 1.5 on Purolite C-160H resin as shown in Figure 3.8. The data of Purolite C-160H for removal of Cr(III) and Cu(II) are given in Table 5.2 in Appendix part.

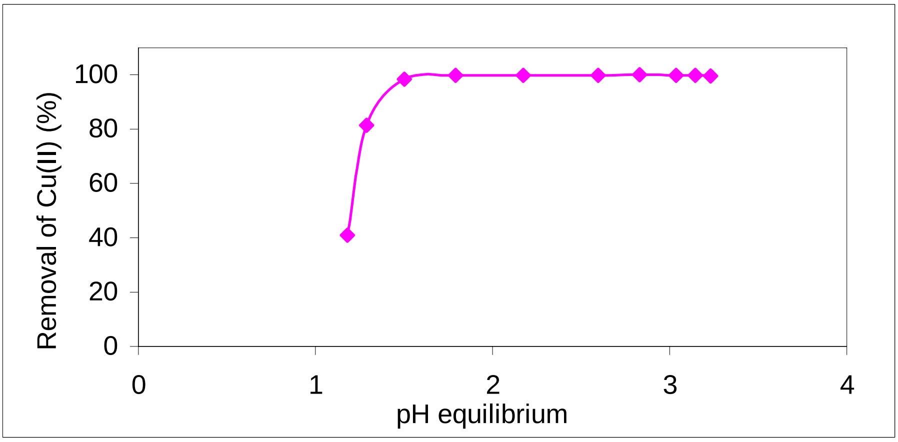

Figure 3.8 Effect of pH on Removal of Cu(II) by Purolite C-160H

The comparative figures for heavy metal removal by Purolite C-160H are given in Figure 3.9.

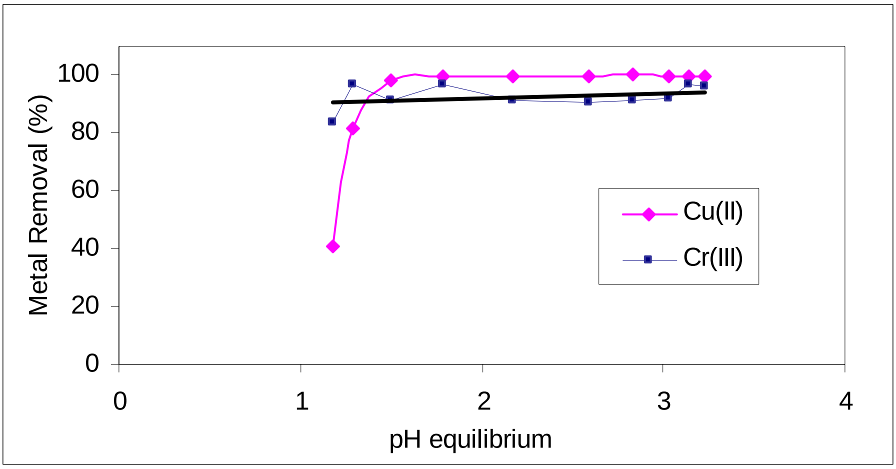

Figure 3.9 Effect of pH on Removal of Cu(II) and Cr(III) by Purolite C-160H

3.1.3 Effect of pH on Removal of Cr(III), Cd(II), Cu(II) Ions by RNH-CH120:

Effect of pH on removal of Cr(III), Cd(II), Cu(II) from their solutions at the same conditions was studied using RNH-CH120. The data for effect of pH on removal of Cr(III), Cd(II), Cu(II) by RNH-CH120 are given in Table 5.3 in Appendix part. As shown in Figure 3.10, the percentage removal of Cr(III) remained constant between pH range of 1-4 by RNH-CH120. The percent removal of Cr(III) reached a plateau with about 80% of Cr(III) removal at about pH 6.

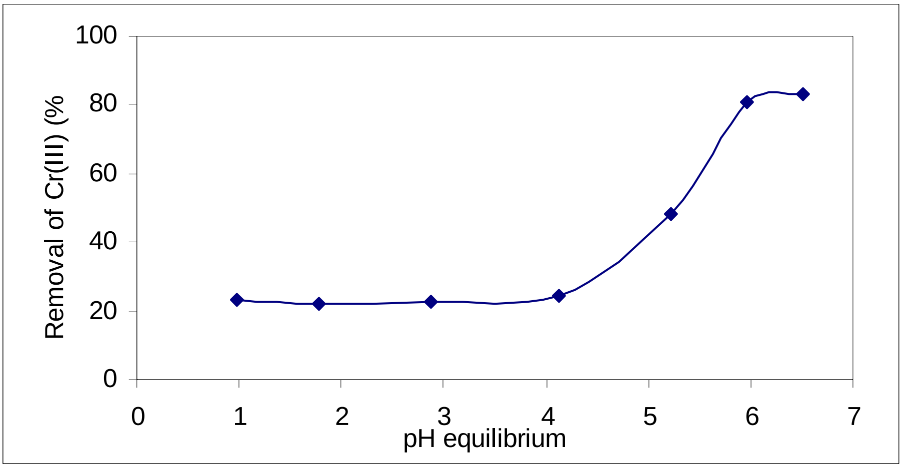

Figure 3.10 Effect of pH on Removal of Cr(III) by RNH-CH120

The respective log K_D vs. pH_{eq} plot is given in Figure 3.11. Here also it was not possible to see n value as 3+ (charge of Cr(III)). This was considered to be due to the different ionic species of Cr(III) as a function of pH and also its binding onto the resin by chelation.

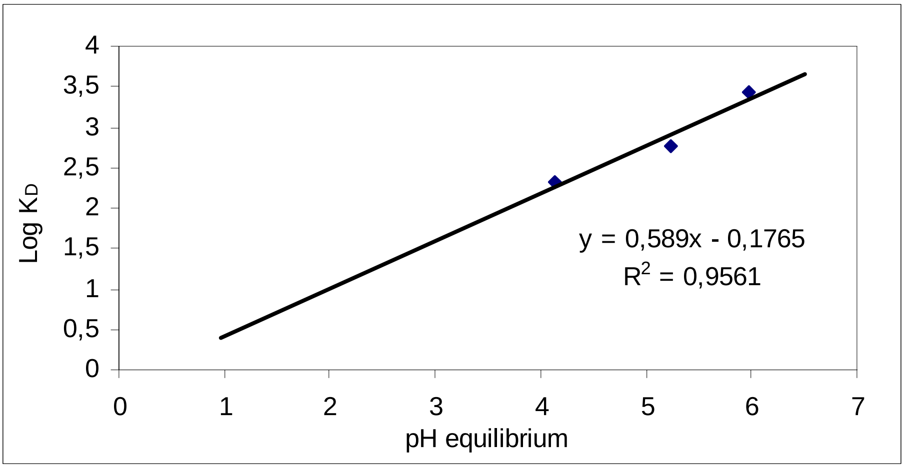

Figure 3.11 Relationship between log K_D and pH_{eq} for Cr(III)

As shown in Figure 3.12, there was not any removal of Cd(II) by

RNH-CH120 resin between pH range of 0.5-~4.5. The percent removal of Cd(II) increased until pH 7 and reached to almost 100% removal at pH 7.

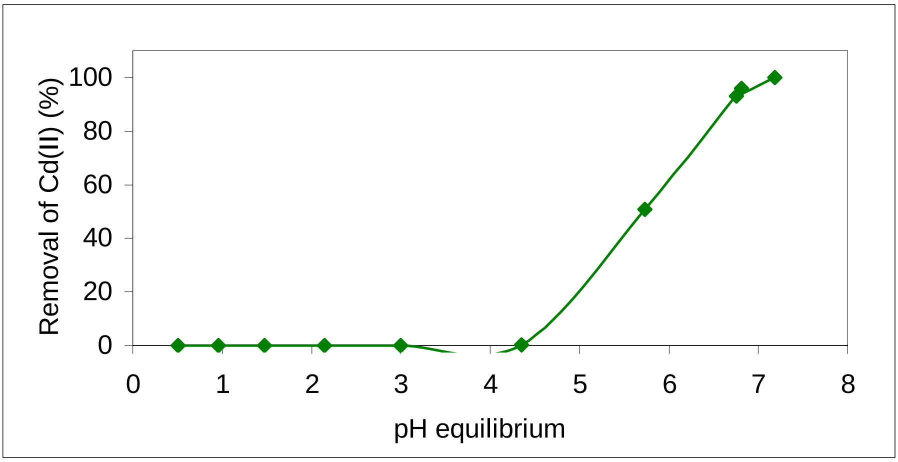

Figure 3.12 Effect of pH on Removal of Cd(II) by RNH-CH120

The relationship between log K_D and pH_{eq} for Cd(II) is shown in Figure 3.13. Here n value which is nearly 2 is the same with the charge of Cd(II).

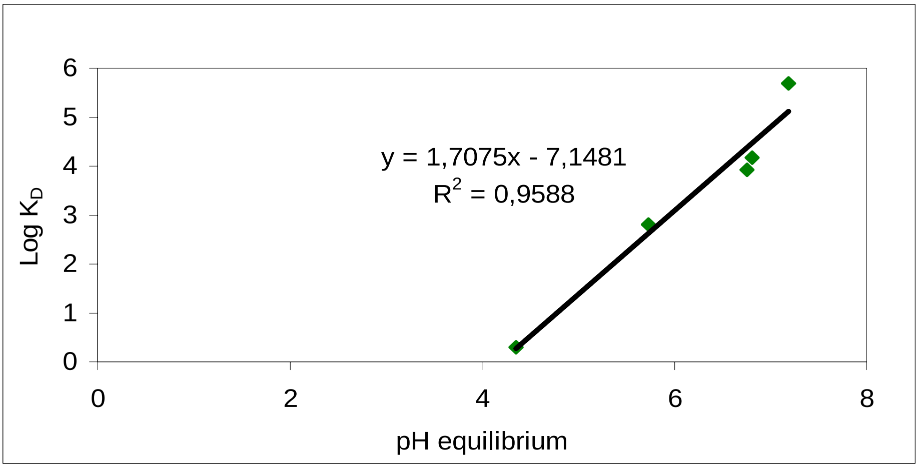

Figure 3.13 Relationship between log K_D and pH_{eq} for Cd(II)

As shown in Figure 3.14 the removal of Cu(II) by RNH-CH120 increased from pH 0.5 to 3. Between pH range of 3-4 the removal of Cu(II) remained constant. The percent removal of Cu(II) reached a plateau with about 100% of removal at pH 6 on RNH-CH120 resin.

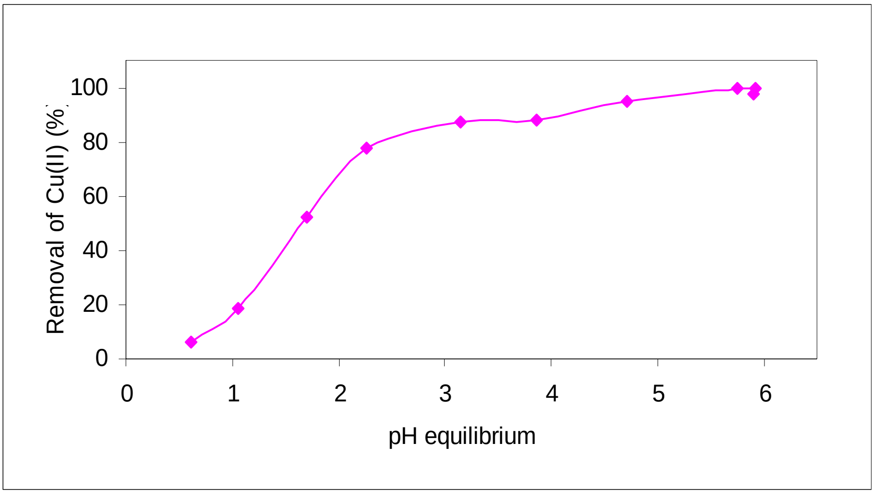

Figure 3.14 Effect of pH on Removal of Cu(II) by RNH-CH120

The relationship between log K_D and pH_{eq} for Cu(II) is shown in Figure 3.15.

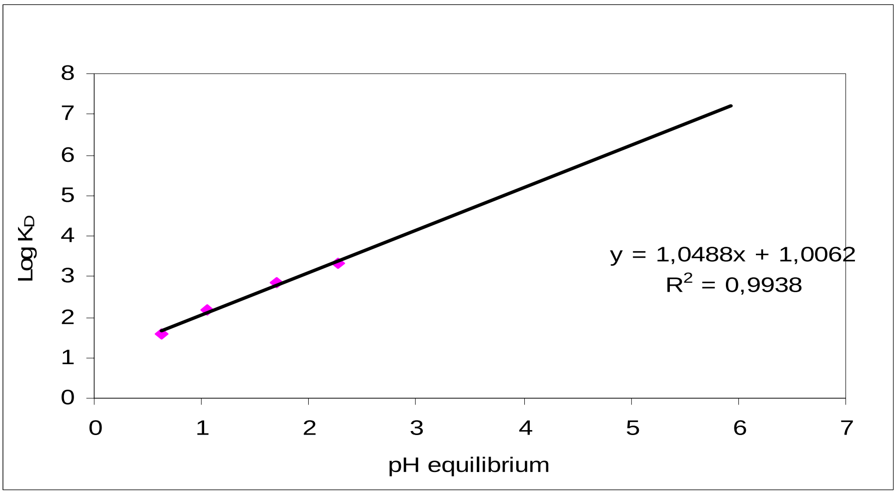

Figure 3.15 Relationship between log K_D and pH_{eq} for Cu(II)

The comparative figures for heavy metal removal by RNH-CH120 are given in Figures 3.16 and 3.17.

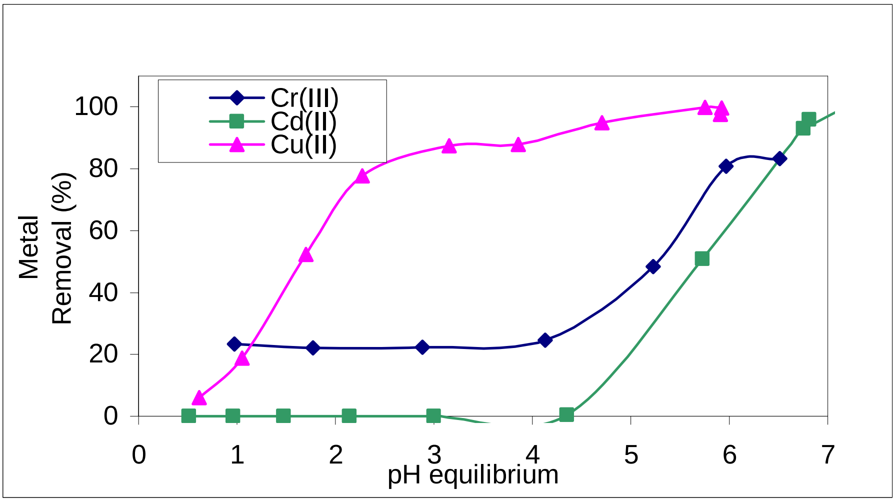

Figure 3.16 Effect of pH on Removal of Cr(III), Cd(II) and Cu(II) by RNH-CH120

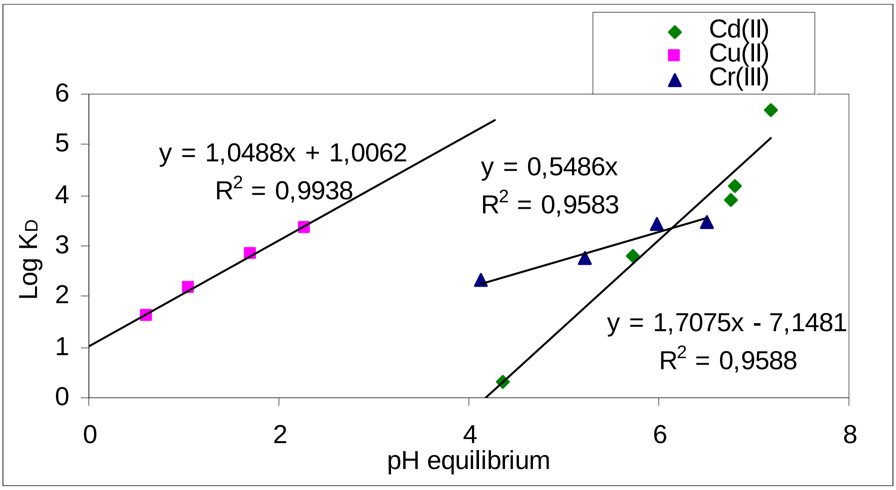

Figure 3.17 Relationship between log K_D and pH_{eq} for Cr(III),Cd(II) and Cu(II) by RNH-CH120

As seen in Figure 3.17, RNH-CH120 resin behaved differently for each metal ion. It seems that it was possible for the resin to remove Cu(II) at lower pH. But this was not the case of Cr(III) and Cd(II) ions.

3.1.4 Effect of resin amount on removal of Cu(II) by Purolite C-160H and RNH-CH120 resins:

Optimum resin amount for removal of Cu(II) was determined using Purolite C-160H and RNH-CH120 resins. Various amounts of resins were employed in batch-mode sorption tests. For this, 0.025, 0.050, 0.1, 0.15, 0.2 and 0.25 g of resins of Purolite C-160H (0.355-0.500 mm) and RNH-CH120 were contacted with 25 mL of 100, 50 and 10 mg Cu(II)/L solutions at pH 3.5 at 30^{o}C for 24 h with continuous shaking.

Table 3.1 and Figure 3.18 show that Cu(II) removal increases with increasing resin amounts from 0.1 to 0.6 g by RNH-CH120. But Cu(II) removal reached a plateau for the resin amounts between 0.6-1.0 g. According to these results, optimum resin amount is found to be 0.6 g-resin/100 mL for RNH-CH120.

Table 3.1 Effect of resin amount on removal of Cu(II) from 100 mg Cu(II)/ L solution by RNH-CH120

Resin Amount	**Copper Removal**	
(g-resin/100ml)	**(%)**	**mg Cu(II) removed**
0.1	21.20	0.488
0.2	48.91	1.125
0.4	85.00	1.955
0.6	98.19	2.258
0.8	99.38	2.286
1.0	99.68	2.293

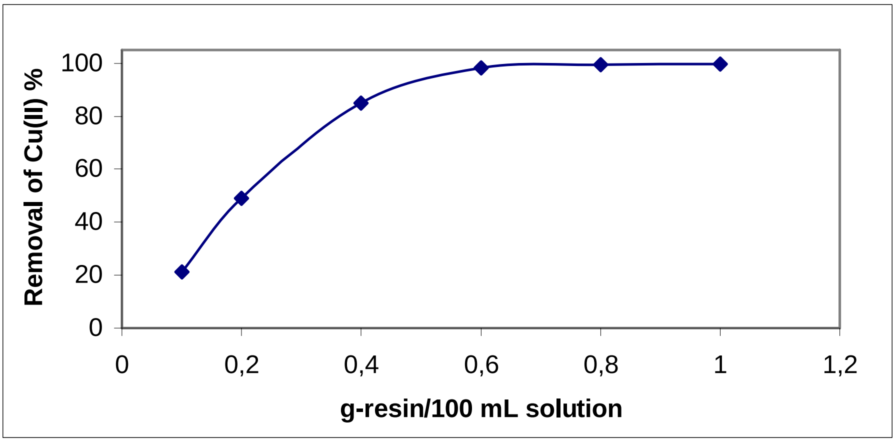

Figure 3.18 Effect of resin amount on removal of Cu(II) from 100 mg Cu(II)/L solution by RNH-CH120

Table 3.2 and Figure 3.19 show that copper removal increases with increasing resin amounts from 0.04 to 0.60 g/100 mL-solution by RNH-CH120. But Cu(II) removal reached a plateau for the resin amounts between 0.60-1.0 g/100 mL-solution. According to these results, optimum resin amount is found to be 0.60 g-resin/100 mL for RNH-CH120.

Table 3.2 Effect of resin amount on removal of Cu(II) from 50 mg Cu(II)/ L by RNH-CH120

Resin Amount	**Copper Removal**	
(g-resin/100ml)	**(%)**	**mg Cu(II) removed**
0.04	40.25	0.48
0.20	78.11	0.90
0.40	88.12	1.01
0.60	93.19	1.04
0.80	92.74	1.05
1.00	96.19	1.07

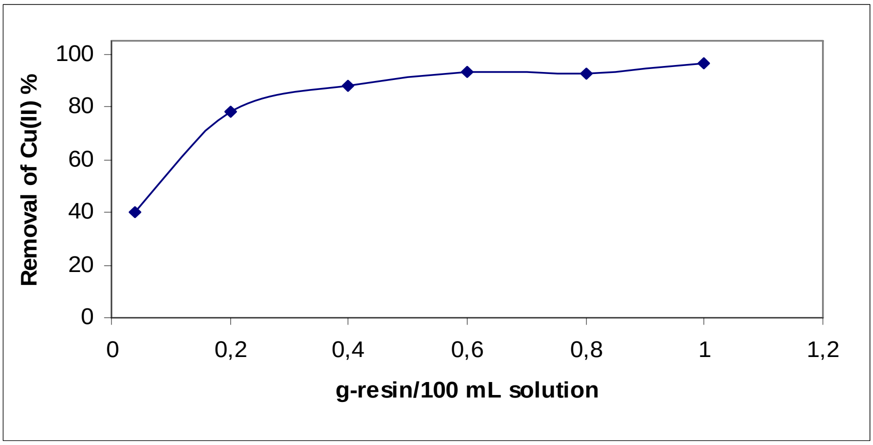

Figure 3.19 Effect of resin amount on removal of Cu(II) from 50 mg Cu(II)/ L solution by RNH-CH120

Finally, the optimum amount of resin has been found for 10 mg Cu(II)/L solution.

As shown in Table 3.3 and Figure 3.20, copper removal increased with an increase in resin amount and almost leveled off in a range of a resin amount of 0.02-0.40 g with approximately 98 % of copper removal by RNH-CH120. According to these results, optimum resin amount is found to be 0.4 g-resin/100 mL for RNH-CH120.

Table 3.3 Effect of resin amount on removal of Cu(II) from 10 mg Cu(II)/ L by RNH-CH120

Resin Amount	**Copper Removal**	
(g-resin/100ml)	**(%)**	**mg Cu(II) removed**
0.02	55.95	0.137
0.04	56.05	0.138
0.10	67.63	0.166
0.20	85.77	0.211
0.40	97.76	0.240
0.60	97.87	0.240
0.80	98.88	0.244

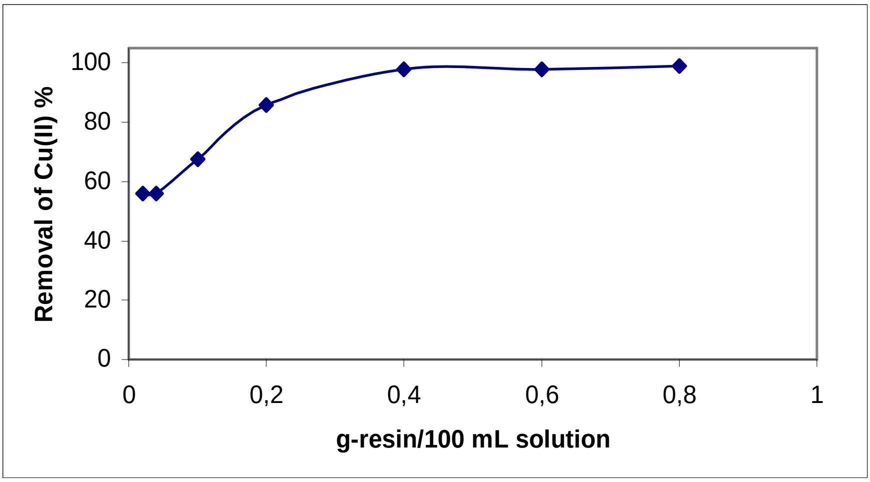

Figure 3.20 Effect of resin amount on removal of Cu(II) from 10 mg Cu(II)/ L solution by RNH-CH120

Optimum resin amount for removal of Cu(II) was determined using Purolite C-160H resin. For this, a solution containing 100 mg Cu(II)/L was used. As shown in Table 3.4 and Figure 3.21, Cu(II) removal increased with an increase in resin amount and almost leveled off in a range of a resin amount of 0.1-0.8 g/100 mL with more than 98 % of Cu(II) removal by Purolite C-160H. According to these results, optimum resin amount is found to be 0.1 g-resin/100 mL-solution for Purolite C-160H. According to this result, one can say that the sorption capacity of Purolite C-160H resin for Cu(II) was greater than that of RNH-CH120 when 100 mg Cu(II)/L solution is used. Smaller amount of Purolite C-160H (0.1 g/100 mL) removed Cu(II) from the solution with the similar percentage obtained with RNH-CH120 with larger amount (0.4 g /100 mL).

Table 3.4 Effect of resin amount on removal of Cu(II) from 100 mg Cu(II)/ L by Purolite C-160H

Resin Amount	**Copper Removal**	
(g-resin/ 100ml)	**(%)**	**mg Cu(II) removed**
0.01	36.52	0.84
0.02	46.20	1.06
0.04	58.15	1.34
0.10	98.28	2.26
0.20	99.55	2.29
0.40	99.59	2.29
0.80	99.60	2.29

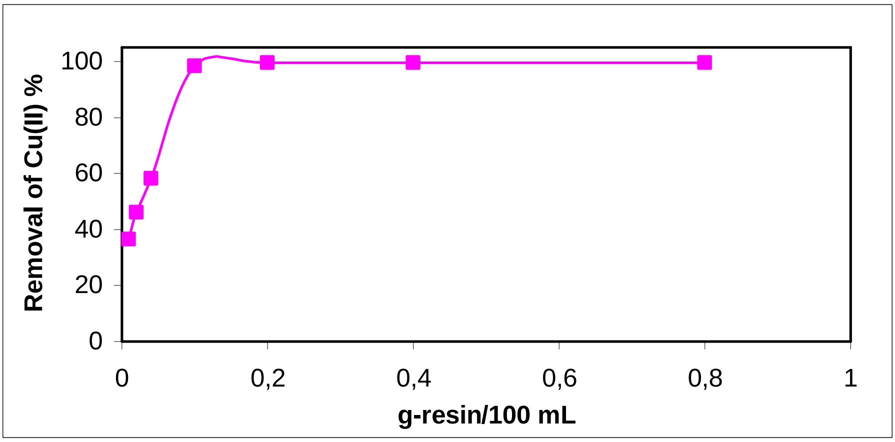

Figure 3.21 Effect of resin amount on removal of Cu(II) from 100 mg Cu(II)/ L by Purolite C-160H

The comparative figures of optimum resin amounts of RNH-CH120 and Purolite C-160H for Cu(II) removal are given in Figure 3.22.

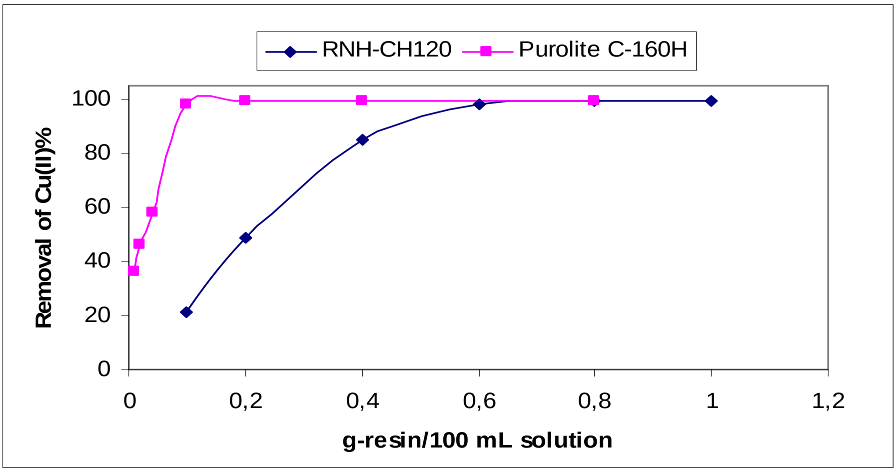

Figure 3.22 Comparison of optimum resin amounts of RNH-CH120 and Purolite C-160H for Cu(II) removal

3.1.5 Kinetic tests

The kinetic performances of RNH-CH120 and Purolite C-160H resins were investigated using 3.0 g dry resin of RNH-CH120 and 0.5 g dry resin of Purolite C-160H with 500 ml solution containing 100 mg Cu(II)/L. Figure 3.23 illustrates the relative concentration decrease of Cu(II) for each resin versus time. Equilibrium conditions were assumed to have been achieved once the metal concentration in solution attained a steady value. This is usually the value obtained at the contact time of 24 hours.

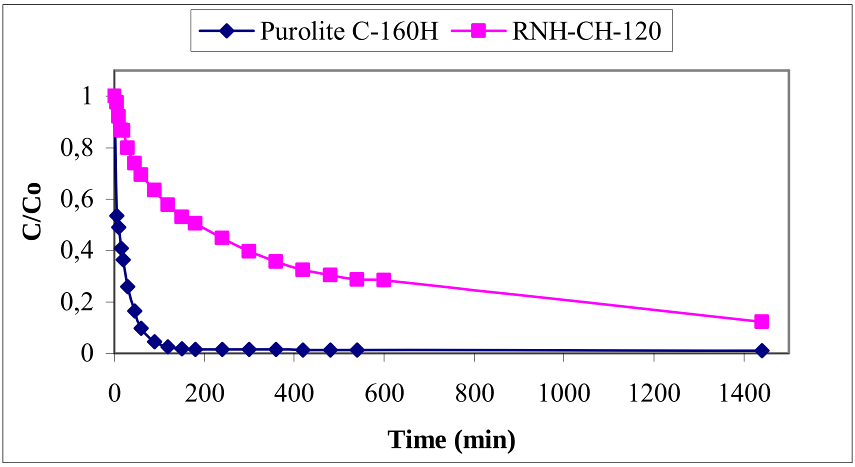

Figure 3.23 Comparison of kinetic performances of RNH-CH120 and Purolite C-160H for Cu(II) removal

The equilibrium half-time for Cu(II) removal was 9 min with Purolite C-160H and the corresponding value for RNH-CH120 was 185 min. It was obtained that removal of Cu(II) by RNH-CH120 was much slower than that of Purolite C-160H resin. The slower kinetic behavior of chelating resins than that of ordinary ion exchange resins are reported in the literature. This was confirmed here as well.

The kinetic data obtained were evaluated using the mathematical models given as infinite solution volume and unreacted core models to determine the rate-controlling steps.

A. Infinite Solution Volume Models (ISV) (37)

A1. Particle Diffusion

Manipulating Vermeulen's approximation given by Eqn. (1.11), a simple expression can be obtained:

$$-\ln(1-X^2) = 2kt \tag{3.1}$$

where $k = \dfrac{D_r \pi^2}{r_o^2}$

If the particle diffusion is the rate controlling mechanism, a plot $-\ln(1-X^2)$ versus time should result in a straight line. The value of diffusion coefficient can be found from the slope.

A2. Film Diffusion

If the film diffusion is the rate controlling mechanism, derivation of Eqn. (1.20) results in;

$$\ln(1-X) = k_{li} t \tag{3.2}$$

where $k_{li} = \dfrac{3DC}{r_o \delta \overline{C}}$

B. Unreacted Core Models (UCM) (37)

B1. Film Diffusion

When the fluid is the rate controlling layer, Eqn. (1.24) can be modified to represent the fractional attainment of equilibrium as a function of time.

$$X = \frac{3C_{Ao}K_{MA}}{ar_o C_{so}} t \tag{3.3}$$

In the case of the film diffusion is in control of the ion exchange mechanism, the extent of the resin conversion X, plotted against t should produce a straight line and its slope is given by the expression 3 $C_{Ao}K_{MA}/ar_oC_{so}$.

B2. Reacted Layer Diffusion

If reacted layer diffusion controls the ion exchange process, Eqn. (1.25) can be used to find the mass transfer coefficient

$$\left[3 - 3(1-X)^{2/3} - 2X\right] = \frac{6D_{e,r}C_{Ao}}{ar_o^2 C_{so}} t \tag{3.4}$$

A straight line should be obtained by plotting $\left[3 - 3(1-X)^{2/3} - 2X\right]$ against time, t if reacted layer diffusion controls. The slope is given by the expression $6\overline{D}_e C_{Ao} / ar_o^2 C_{so}$.

B3. Chemical Reaction

By manipulating the Eqn. (1.26) the following equation can be obtained to represent the controlling mechanism, in the case of the slowest step is the chemical reaction,

$$\left[1-(1-X)^{1/3}\right]=\frac{k_s C_{Ao}}{r_o} \tag{3.5}$$

Then, a plot of $\left[1-(1-\mathrm{X})^{1/3}\right]$ versus time should produce a straight line. The slope is given by $C_{Ao}\, k_s / r_o$.

The summary of the models used to find the rate control mechanism is given in Table 3.5.

Table 3.5 Diffusional and reaction models

Method	Equation	Rate Controlling Step
ISV	**-ln (1-X)**=kt, where $k=Dr\pi^2/r_o^2$	Film Diffusion
	-ln (1-X^2) =k_{li}t, where $k=3DC/r_o\delta Cr$	Particle Diffusion
UCM	**X**=$(3C_{Ao}K_{MA}/ar_oC_{So})t$	Liquid Film
	3-3(1-X)$^{2/3}$-2X = $(6D_{CR}C_{Ao}/ ar_o^2 C_{So})t$	Reacted Layer
	1-(1-X)$^{1/3}$= $(k_sC_{Ao}/ r_o)t$	Chemical Reaction

The various functions plotted to determine the kinetic behavior of RNH-CH120 and Purolite C-160H are shown Figures 3.24 – 3.28.

In the case of kinetic studies of Purolite C-160H reaches equilibrium after about 60 minutes, the data obtained at contact time in later minutes were neglected. In case of RNH-CH120, the data obtained at contact time later than 120 minutes were neglected, considering better fitting is obtained between 0-120 min of contact time.

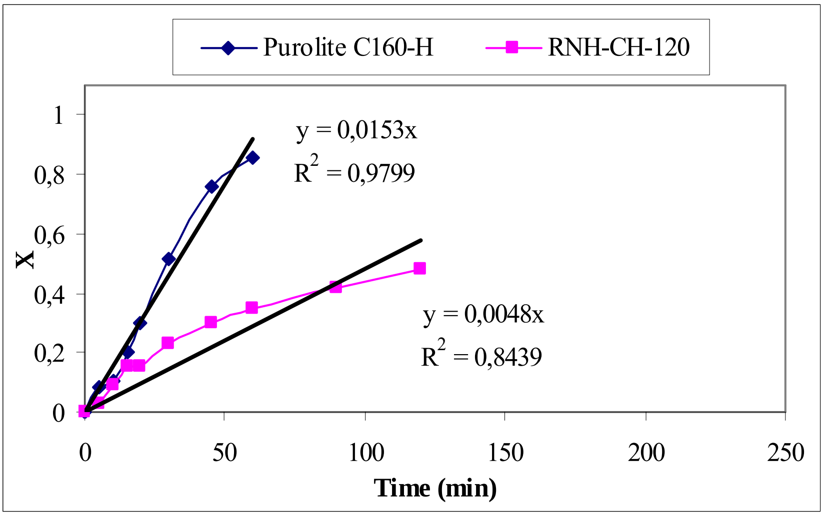

Figure 3.24 Kinetic behaviors of RNH-CH120 and Purolite C-160H based on Unreacted Core Models

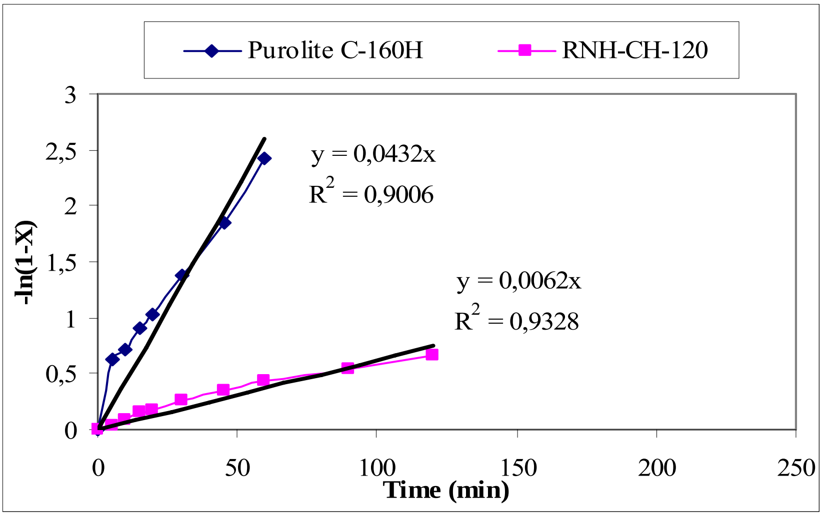

Figure 3.25 Kinetic behaviors of RNH-CH120 and Purolite C-160H based on Infinite Solution Models

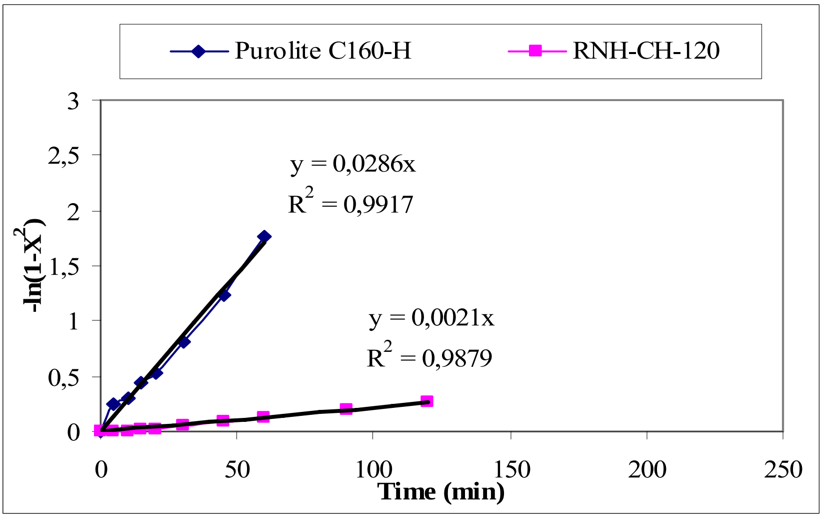

Figure 3.26 Kinetic behaviors of RNH-CH120 and Purolite C-160H based on Infinite Solution Models

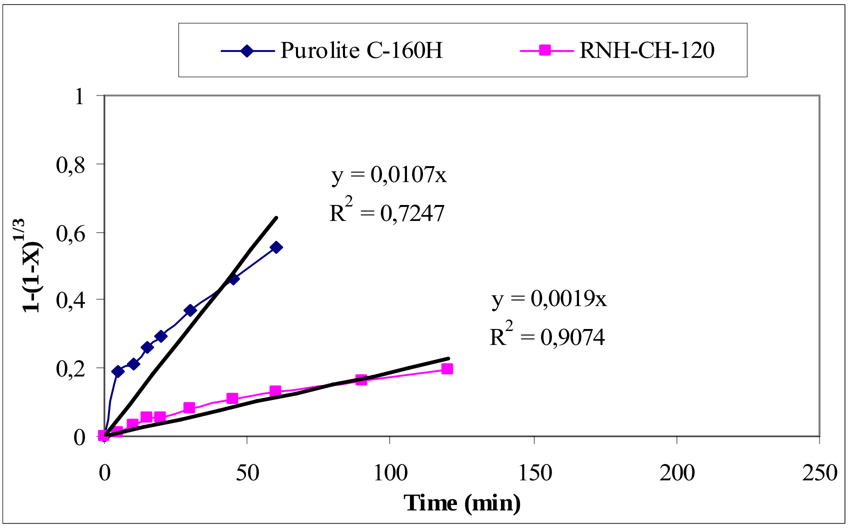

Figure 3.27 Kinetic behaviors of RNH-CH120 and Purolite C-160H based on Unreacted Core Models

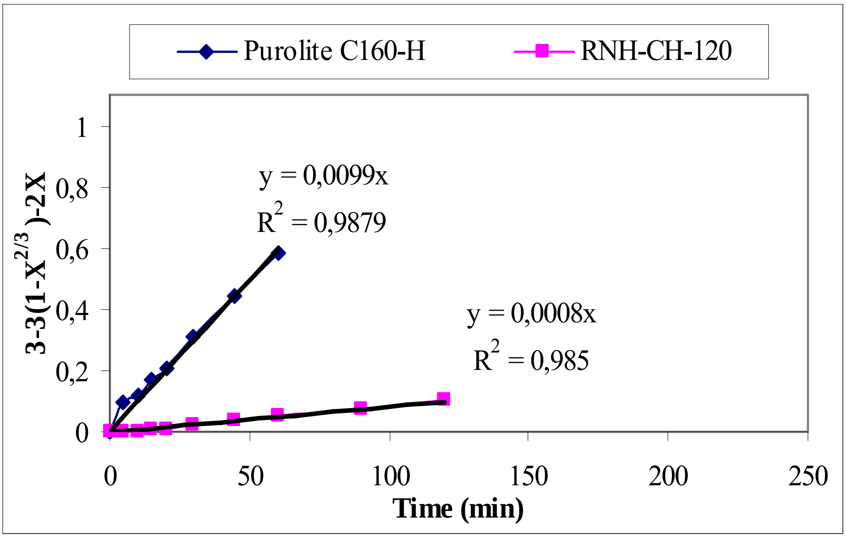

Figure 3.28 Kinetic behaviors of RNH-CH120 and Purolite C-160H based on Unreacted Core Models

According to these graphs, the rate of Cu(II) removal by RNH-CH120 and Purolite C-160H resins was controlled by particle diffusion.

Table 3.6 gives the slope values and the linear correlation coefficients. As seen in the Table 3.6, the correlation coefficients of the model function -ln $(1 - X^2)$ for RNH-CH120 and Purolite C-160H were largest. This shows that the particle diffusion control is the rate determining step according to Infinite Solution Volume Model. Also, the correlation coefficients for reacted layer mechanism were largest for both resins according to unreacted core model.

Table 3.6 Evaluation of kinetic models for RNH-CH120 and Purolite C-160H

Model	RNH-CH120		PUROLITE C-160H	
	slope	$\mathbf{r^2}$	**slope**	$\mathbf{r^2}$
$-\ln(1-X)$	0.0062	0.9328	0.0432	0.9006
$-\ln(1-X^2)$	0.0021	**0.9879**	0.0286	**0.9917**
X	0.0048	0.8439	0.0153	0.9799
$3-3(1-X)^{2/3}-2X$	0.0008	**0.985**	0.0099	**0.9879**
$1-(1-X)^{1/3}$	0.0019	0.9074	0.0107	0.7247

3.2 Column–Mode Removal of Cu(II) from Aqueous Solutions:

In order to get some information about column performances of chelating resins on removal of Cu(II) from aqueous solutions, chelating resins RNH-CH120 and Purolite C-160H were used for column-mode sorption of Cu(II).

To compare the column performances of RNH-CH120 and Purolite C-160H, same conditions such as solution concentration (100 mg Cu(II)/ L at pH 3.5), feed flow rate (SV 15 h^{-1}), column diameter (ID: 0.7 cm) were employed.

Breakthrough curves of Cu(II) for both resins are given in Figures 3.29 and 3.30.

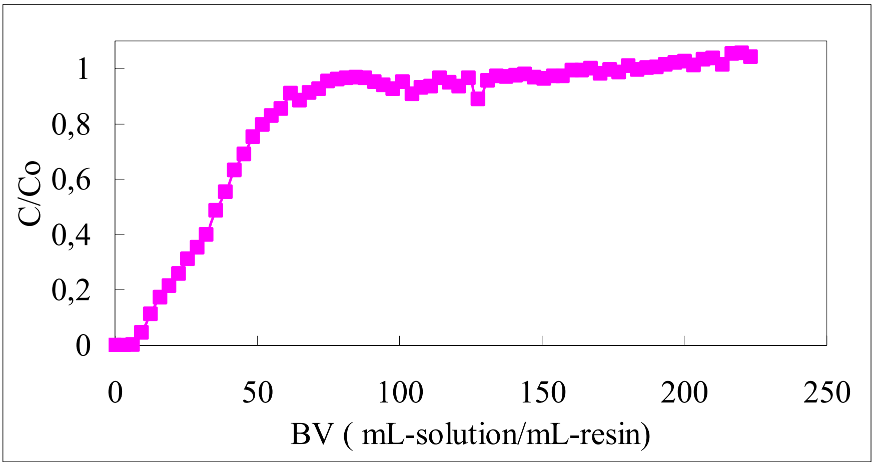

Figure 3.29 Breakthrough curve of Cu(II) by RNH-CH120

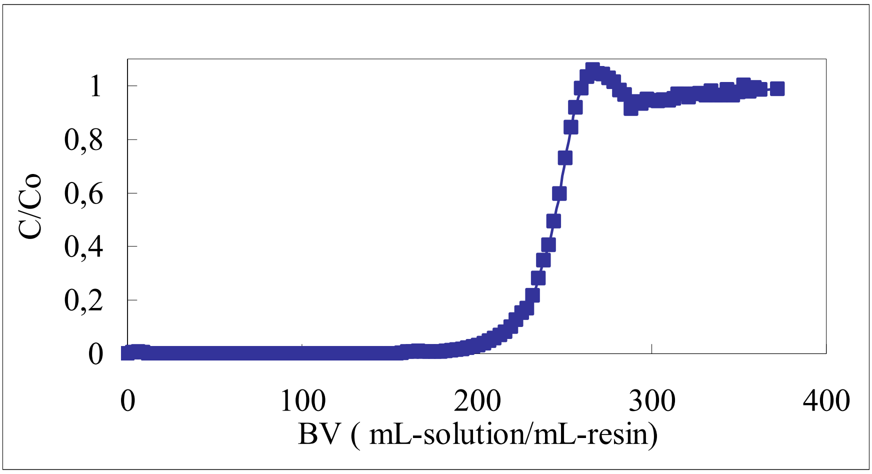

Figure 3.30 Breakthrough curve of Cu(II) by Purolite C-160H

In the column-mode sorption studies, breakthrough capacity, total capacity, degree of column utilization of resins were calculated. Breakthrough capacity was calculated by accepting the breakthrough point as a concentration which is just before than 1 mg Cu/L. As shown in Figure 3.31 and Table 3.7, Purolite C-160H has a larger breakthrough capacity than RNH-CH120. Breakthrough capacities of Purolite C-160H and RNH-CH120 are 17.84 mg Cu(II)/ g-dry resin and 3.90 mg Cu(II)/g-dry resin, respectively. These result was considered to be due to the larger ion exchange capacity and faster kinetics of Purolite C-160H than those of RNH-CH120.

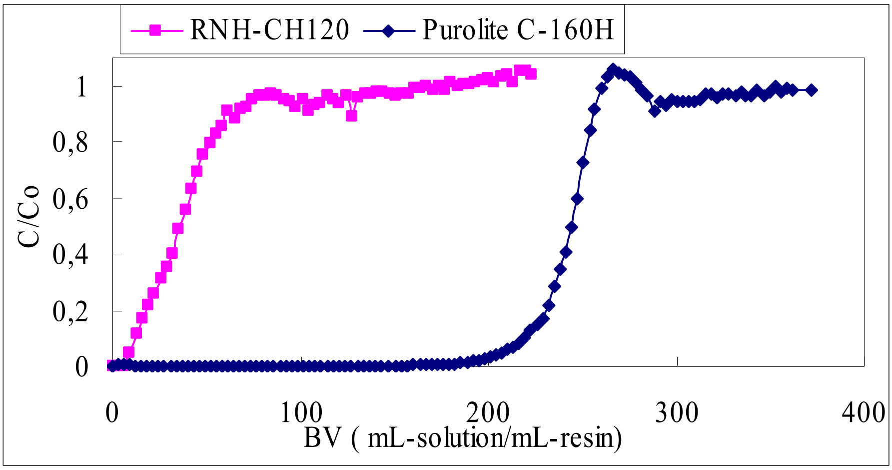

Figure 3.31 Comparative breakthrough curves of Cu(II) obtained by RNH-CH120 and Purolite C-160H resins

Table 3.7 Column-mode sorption–elution performances of RNH-CH120 and Purolite C-160H

Resin	***RNH-CH120***	***Purolite C-160H***
Break. Point (BV)	6.26	182.30
Breakthrough Capacity (mg Cu/mL-resin)	3.90	17.84
Total BV	170.46	262.99
Total Capacity (mg Cu/mL-resin)	3.92	24.09
Column Utilization (%)	99.68	74.06
Elution Efficiency (%)	99.12	97.64

The Cu(II) sorbed by both resins were almost completely removed from the resin by 1 M HCl solution at SV 5 h^{-1}. Elution profiles of Cu(II) using RNH-CH120 and Purolite C-160H obtained are given in Figures 3.32-3.34. The maximum Cu(II) concentration in the eluate reached to 948.8 mg Cu/L and 2350 mg Cu/L using RNH-CH120 and Purolite C-160H, respectively. Comparative elution profiles are given in Figure 3.34.

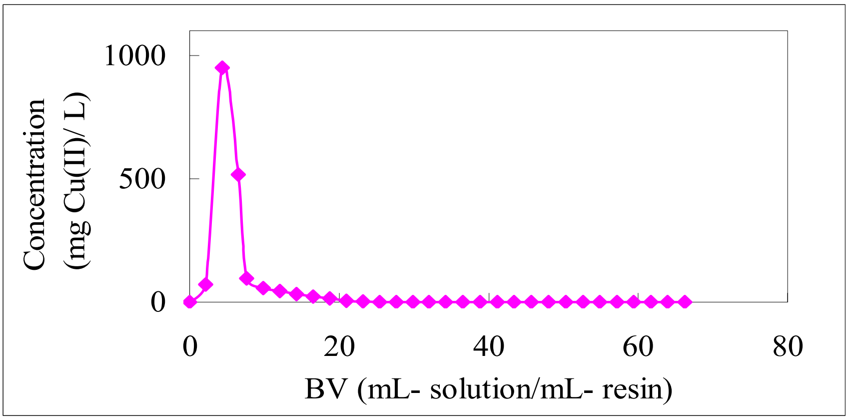

Figure 3.32 Elution curve of Cu(II) by RNH-CH120

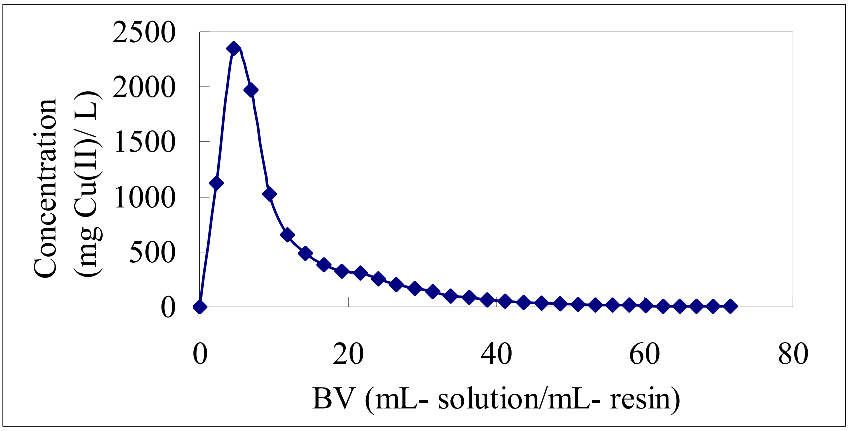

Figure 3.33 Elution curve of Cu(II) by Purolite C-160H

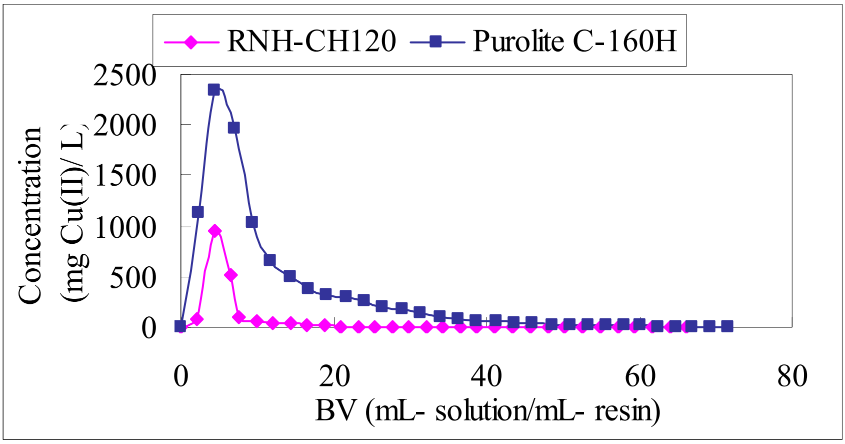

Figure 3.34 Comparative elution curves of Cu(II) obtained on RNH-CH120 and Purolite C-160H

3.2.1 Effect of Cu(II) concentration on removal of Cu(II) by RNH-CH120:

In the second part of the column-mode sorption studies, the effect of Cu(II) concentration on the removal of Cu(II) by RNH-CH120 was investigated. For this purpose, solutions with concentrations of 10, 30 and 50 mg Cu(II)/L at pH 3.5 were prepared. Each column study was carried out at the same conditions such as feed flow rate (SV 15 h^{-1}), column diameter (ID: 0.7 cm) and 1.0 ml RNH-CH120. Breakthrough capacity, total capacity, degree of column utilization of resins were calculated. Breakthrough capacity was calculated by accepting the breakthrough point as a concentration which is just before than 1 mg Cu/L. When the concentration of Cu(II) in the solution increased from 10 to 50 mg Cu(II)/L, the breakthrough appeared more quickly. Breakthrough capacity shifted to left slightly as the concentration of Cu(II) was increased.

Breakthrough curves of Cu(II) obtained with different concentrations are given in Figures 3.35.

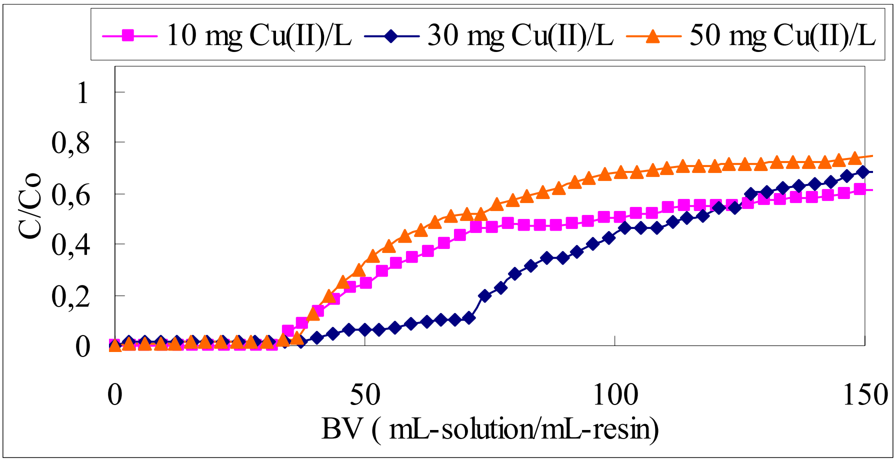

Figure 3.35 Breakthrough curve of Cu(II) by RNH-CH120 as a function of Cu(II) solution

As shown in Figure 3.35, breakthrough point shift was not so great with the change in concentration. On the other hand, breakthrough capacity increased with the increase in initial Cu(II) concentration.

Breakthrough points and capacity values for each concentration are summarized in Table 3.8. Figure 3.36 shows the elution profiles of copper obtained at SV 5 h^{-1}. As seen in Figure 3.36, Cu(II) was quantitatively eluted from the resin using 1 M HCl solution.

Table 3.8 Data of column-mode sorption–elution study of RNH-CH120 using different Cu(II) concentrations

	RNH-CH120		
	10 mg Cu(II) (pH 3.5)	***30 mg Cu(II) (pH 3.5)***	***50 mg Cu(II) (pH 3.5)***
Break. Point (BV)	38	37	30
Breakthrough Capacity (mg Cu/mL-resin)	0.37	1.10	1.46
Total BV	313	272	311
Total Capacity (mg Cu/mL-resin)	1.29	3.79	4.94
Column Utilization (%)	28.4	29.0	29.6
Elution Efficiency (%)	100.0	100.0	99.6

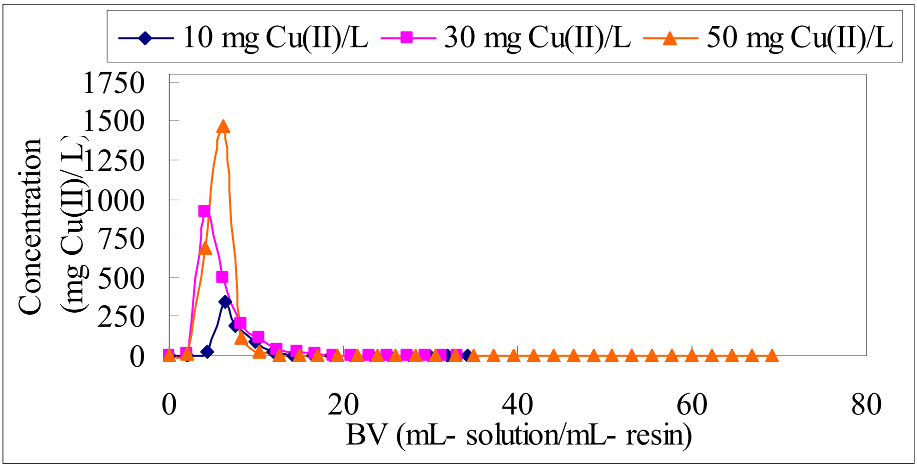

Figure 3.36 Elution curves of Cu(II) by RNH-CH120

3.2.2 Effect of feed flow rate on removal of Cu(II) by RNH-CH120:

Column studies were performed to investigate the effect of feed flow rate on breakthrough profiles of RNH-CH120 by using 10 mg Cu(II)/L at the different flow rates (SV 5, 10, 15 h^{-1}). As shown in Table 3.9, the breakthrough point of RNH-CH120 shifted from left to right with decreasing feed flow rate. The kinetic of RNH-CH120 is found to be slow. Consequently, decreasing flow rate is needed to increase the contact time of Cu(II) with chelating groups and consequently to increase the sorption capacity of RNH-CH120.

Elution steps were done using the same conditions in other column studies. Breakthrough and elution curves of RNH-CH120 resin are given in Figures 3.37 and 3.38, respectively.

Table 3.9 Column data of RNH-CH120 with different feed flow rates (from 10 mg Cu(II)/L)

	RNH-CH120		
	SV 5 h^{-1}	***SV 10 h^{-1}***	***SV 15 h^{-1}***
Break. Point (BV)	98	91	38
Breakthrough Capacity (mg Cu/mL-resin)	0.96	0.88	0.37
Total BV	296	297	297
Total Capacity (mg Cu/mL-resin)	1.86	1.47	1.29
Column Utilization (%)	51.8	59.8	28.4
Elution Efficiency (%)	98.2	99.8	100.0

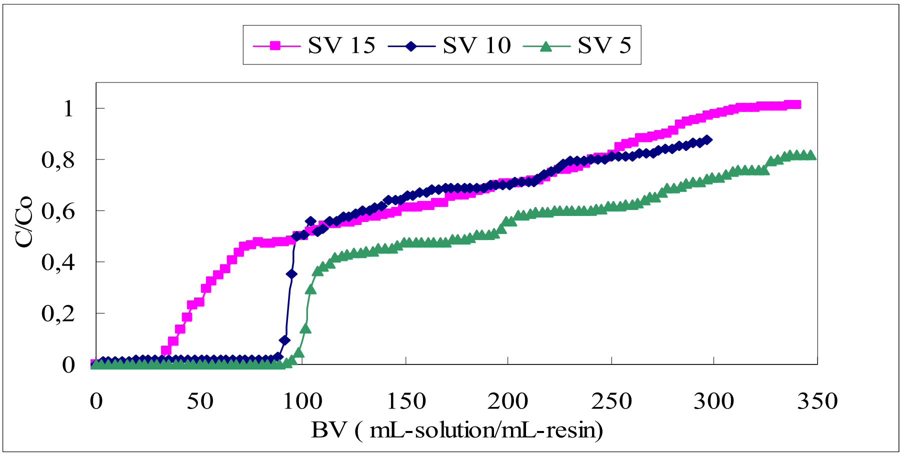

Figure 3.37 Breakthrough curves of Cu(II) by RNH-CH120 as a function of SV

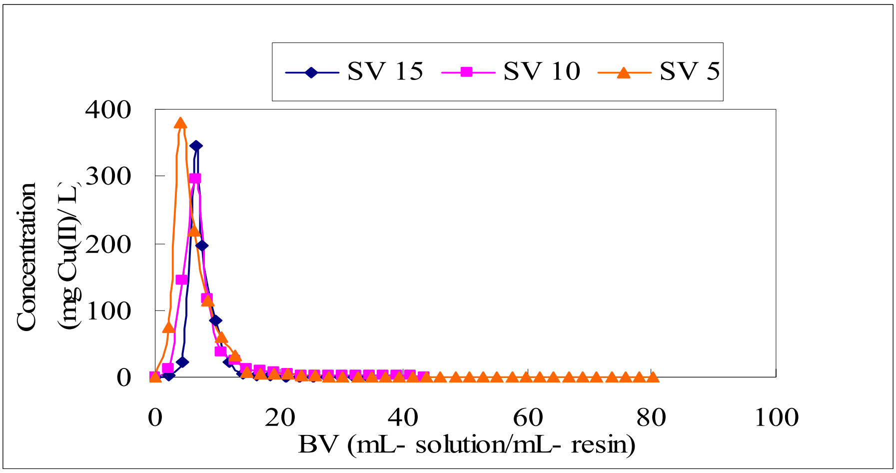

Figure 3.38 Elution curves of Cu(II) by RNH-CH120

3.3 IR Analysis

IR spectrophotometry was used to characterize original and used RNH-CH120 and Purolite C-160H resins. According to Figure 3.39, a small peak at nearly 1480-1500 cm^{-1} was observed for used RNH-CH120 following the sorption-washing-elution steps. This shows that, functional groups (amidoxime groups) could be hydrolyzed to some extent to give carboxylate groups. On the other hand, there was almost no change in the IR spectrum of used Purolite C-160H resin comparing with original one (Figure 3.40). This shows that Purolite C-160H has better chemical stability than RNH-CH120 after treatment with 1 M HCl during elution step.

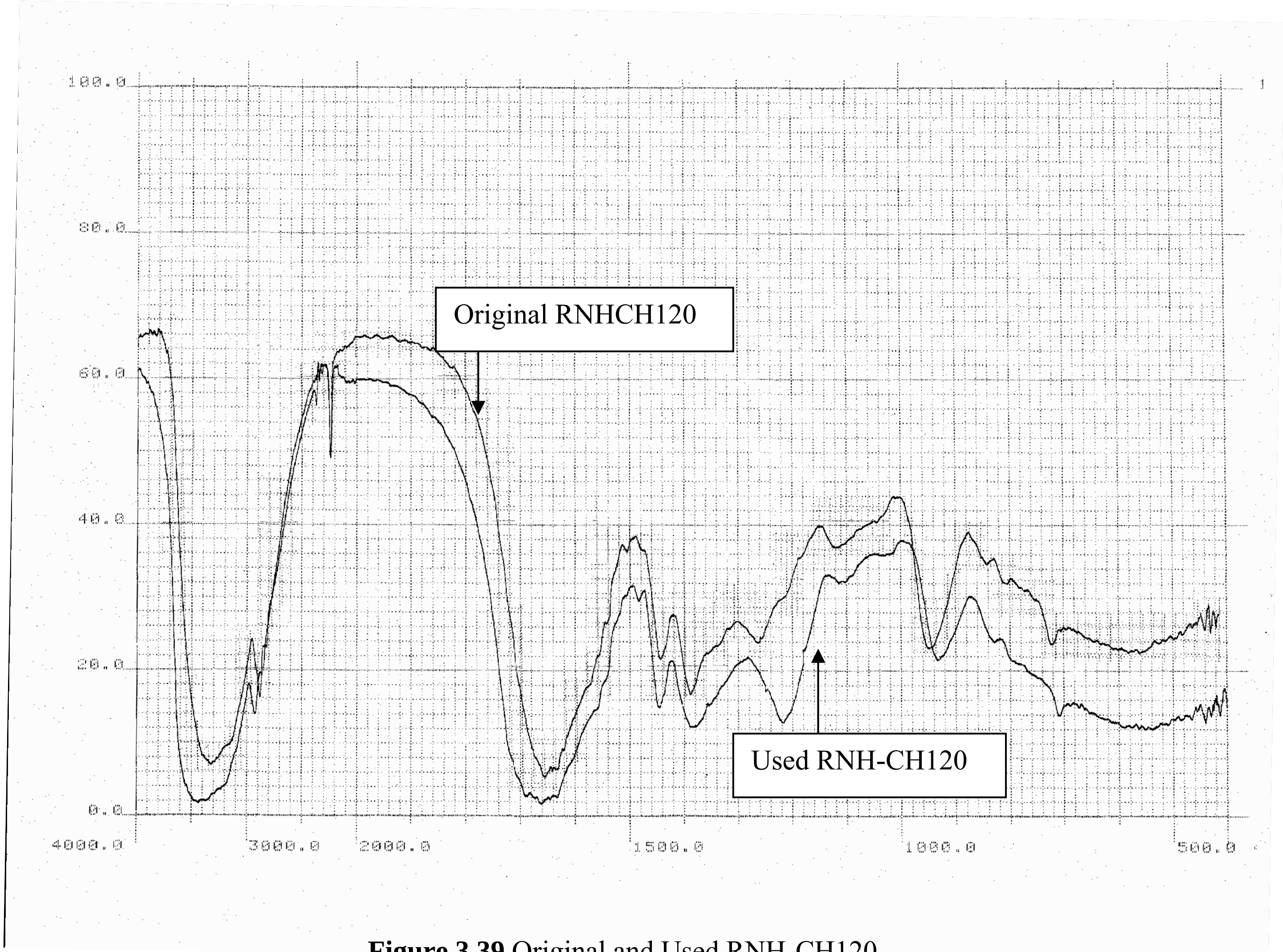

Figure 3.39 Original and Used RNH-CH120

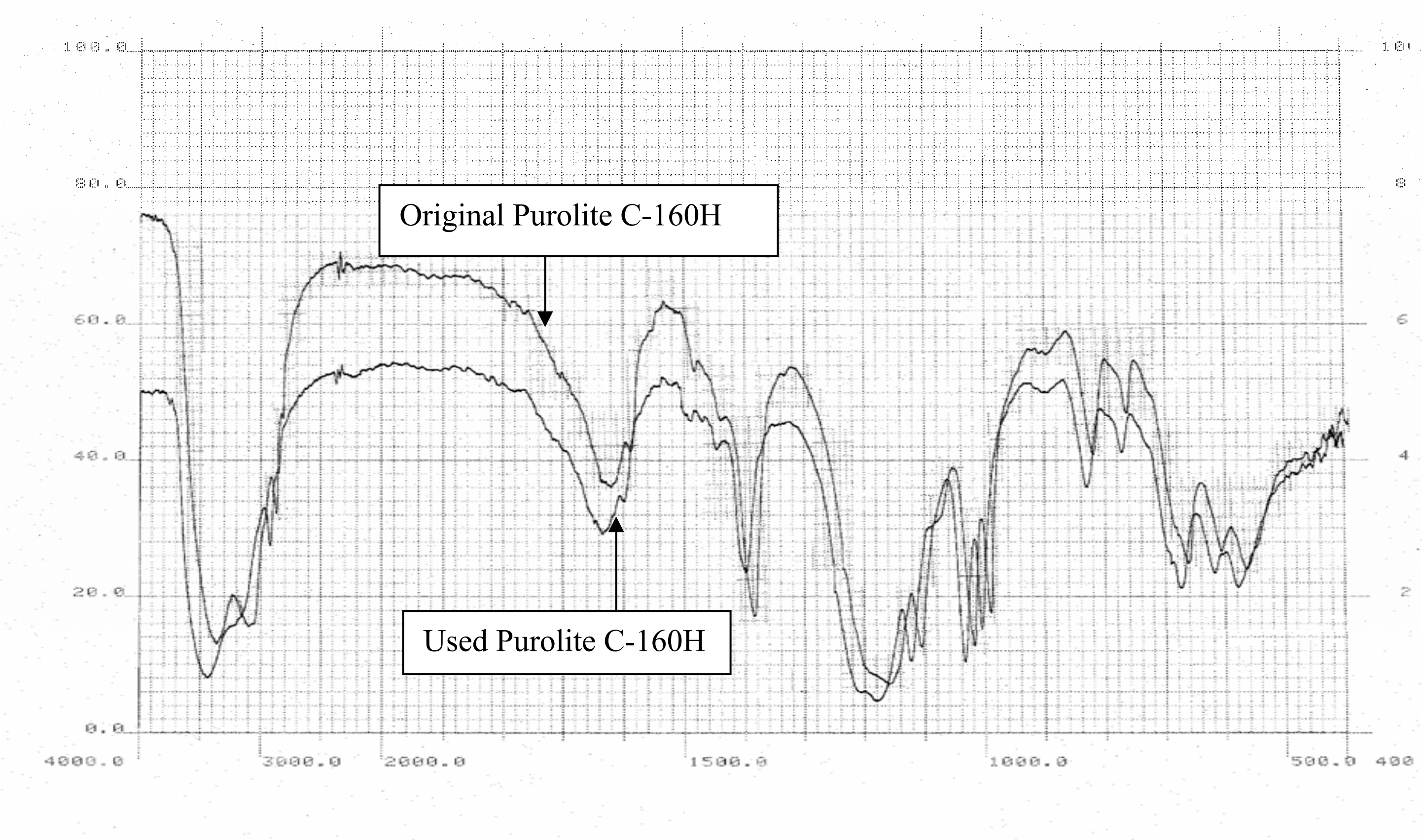

Figure 3.40 Original and Used Purolite C-160H

4.0 CONCLUSIONS

In this study, the macroporous chelating resins; RCSP(II) containing methylene phosphonic groups (DVB: 10 mol%), commercially available ion exchange resins Purolite C-160H containing sulphonic groups (DVB: 10 mol%) and RNH-CH120 containing amidoxime groups (DVB: 5 mol %) were used for heavy metal removal from aqueous solutions by batch and column methods. In batch studies, the effect of pH and resin amount on removal of Cu(II), Cr(III) and Cd(II) ions from aqueous solutions were investigated.

Metal ion sorption of chelating resins was studied by measuring pH dependency of distribution ratios of various metal ions (Cu(II), Cd(II), Cr(III)) between these resins and aqueous solutions containing 10^{-4} M metal ions. The percent removal of Cr(III) and Cu(II) reached a plateau with about 100% of removal at pH 2 and at pH 3 by RCSP(II) resin respectively. Purolite C-160H resin showed a higher sorption performance to Cu(II) than Cr(III). The percent removals of reached a plateau with about 80% of removal at pH 6, 100% of removal at pH 6, 100% of removal at pH 7 for Cr(III), Cu(II) and Cd(II) respectively by RNH-CH120.

The optimum resin amounts of Purolite C-160H and RNH-CH120 resins were determined for removal of Cu(II) from solution containing 100 mg Cu(II)/L (pH 3.5). The obtained results were used for the kinetic studies. Optimum resin amounts found are 3.0 g resin/500 mL for RNH-CH120 and 0.5 g resin/500 mL for Purolite C-160H.

The equilibrium half-time for Cu(II) removal were determined 9 min. and 185 min. with Purolite C-160H and RNH-CH120 resins, respectively when 100 mg Cu(II)/L solution was used. The kinetic data used for Infinite Solution Volume and Unreacted Core Kinetic Models and the rate controlling steps were found. For both resins the rate controlling step was found to be particle diffusion.

In column studies, the resin performances of two different kinds of resins on removal of copper were compared. The breakthrough capacity of Purolite C-160H was greater than RNH-CH120 for Cu(II). The Cu(II) on the resins was quantitatively eluted with 1 M HCl.

In the second part of column studies, the effects of concentration and feed flow rate were investigated for the removal of Cu(II) by RNH-CH120 resin. The column performances were compared with different Cu(II) concentrations (10, 30, 50 mg Cu(II)/L) at the same flow rate. The initial Cu(II) concentration influenced the breakthrough and total capacities of resin although the shift in breakthrough point was not so great with the change in Cu(II) concentration.

The effect of feed flow rate on column-mode removal of Cu(II) by RNH-CH120 was also studied. The decrease in feed flow rate influence the copper removal by RNH-CH120 greatly. If the flow rate is small, the breakthrough point shifted to right more.

IR spectrophotometry was used to characterize the original and used RNH-CH120 and Purolite C-160H resins. A peak at nearly 1480-1500 cm^{-1} was observed for used RNH-CH120. This shows that amidoxime groups could be hydrolyzed in the presence of 1 M HCl to give carboxylate groups. On the other hand, there was almost no change in the IR spectrum of used Purolite C-160H resin, showing the higher chemical stability of this resin than RNH-CH120.

5.0 APPENDIX

Batch-mode Studies:

The batch-mode studies data performed with RCSP(II), Purolite C-160H and RNH-CH120 are summarized in Tables 5.1 – 5.3.

Table 5.1 Effect of pH on Removal of heavy metals by RCSP(II) (Figures 3.1- 3.3)

pH_i	Cr^{3+}		Cu^{2+}	
	pH_{eq}	% Removal	pH_{eq}	% Removal
0.5	0.5	9.93	0.51	0.29
1	1.01	25.68	1.06	0.83
1.5	1.90	98.12	1.56	27.44
2	2.055	99.29	2.05	74.66
2.5	2.58	99.83	2.52	94.76
3	2.95	99.56	2.99	99.54
3.5	3.21	99.53	3.32	100
4	3.435	99.90	3.46	100
4.5	3.5	99.63	3.52	100
5	3.595	100	3.78	100

Table 5.2 Effect of pH on Removal of heavy metals by Purolite C-160H (Figures 3.7- 3.8)

pH_i	Cr^{3+}		Cu^{2+}	
	pH_{eq}	% Removal	pH_{eq}	% Removal
0.5	1.18	83.39	0.63	40.88
1	1.29	97.18	0.80	81.46
1.5	1.50	91.11	1.06	98.44
2	1.79	98.03	1.39	99.86
2.5	2.17	95.02	1.73	99.93
3	2.59	92.29	2.10	99.93
3.5	2.83	91.16	2.69	100
4	3.04	91.88	3.13	99.84
4.5	3.15	96.78	3.16	99.84
5	3.23	95.95	3.15	99.54

Table 5.3 Effect of pH on Removal of heavy metals by RNH-CH120

(Figures 3.10- 3.12- 3.14)

pH_i	**Cr^{3+}**		**Cu^{2+}**		**Cd^{2+}**	
	pH_{eq}	**% Removal**	**pH_{eq}**	**% Removal**	**pH_{eq}**	**% Removal**
0.5	0.82	12.29	0.62	6.03	0.51	0
1	0.97	23.45	1.05	18.81	0.96	0
1.5	1.77	22.21	1.70	52.35	1.47	0
2	2.35	35.06	2.27	77.81	2.14	0
2.5	2.88	22.40	3.15	87.48	3	0
3	4.13	24.57	3.85	87.82	4.35	0.32
3.5	5.23	48.32	4.70	94.97	5.73	50.82
4	5.97	80.75	5.75	99.93	6.81	96.04
4.5	6.51	83.33	5.92	99.68	6.75	92.96
5	6.47	84.13	5.91	97.67	7.18	99.87

Kinetic Studies:

The data of kinetic studies in batch-mode tests performed with RCSP(II), Purolite C-160H and RNH-CH120 are summarized in Tables 5.4– 5.5.

Table 5.4 Results of kinetic studies for Purolite C-160H (Figures 3.23-3.28)

t (min)	**C (mg/L)**	**C/Co**	**X**	**-ln(1-X)**	**-ln(1-X^2)**	**1-(1-X)$^{1/3}$**	**3-3(1-X)$^{2/3}$-2X**
0	105.6	1.000	0	0	0	0	0
5	56.5	0.535	0.469	0.633	0.248	0.190	0.094
10	51.9	0.491	0.513	0.720	0.305	0.213	0.117
15	43.2	0.409	0.596	0.907	0.439	0.261	0.168
20	38.3	0.362	0.643	1.031	0.534	0.290	0.204
30	27.4	0.259	0.747	1.376	0.818	0.368	0.306
45	17.4	0.164	0.843	1.852	1.241	0.460	0.441
60	10.3	0.097	0.911	2.420	1.772	0.553	0.580

Table 5.5 Results of kinetic studies for RNH-CH120 (Figure 3.23-3.28)

t (min)	**C (mg/L)**	**C/Co**	**X**	**-ln(1-X)**	**-ln(1-X^2)**	**1-(1-X)$^{1/3}$**	**3-3(1-X)$^{2/3}$-2X**
0	95.6	1.000	0	0	0	0	0.000
5	93.3	0.975	0.027	0.027	0.001	0.009	0.000
10	88.1	0.921	0.089	0.093	0.008	0.030	0.002
15	83.0	0.868	0.150	0.162	0.022	0.052	0.008
20	82.7	0.865	0.153	0.166	0.024	0.054	0.008
30	76.3	0.798	0.230	0.261	0.054	0.083	0.019
45	70.6	0.738	0.297	0.353	0.092	0.111	0.034
60	66.4	0.694	0.348	0.427	0.129	0.132	0.048
90	60.6	0.633	0.417	0.539	0.191	0.164	0.072
120	55.1	0.576	0.482	0.659	0.265	0.197	0.101

Column Studies:

The data of column-mode tests are summarized in Tables 5.6-5.21.

Table 5.6 Results of sorption studies for RNH-CH120 (Figure 3.29)

Frac. No	**BV**	**C/Co**	**Sorbed Amount (mg)**	**Frac. No**	**BV**	**C/Co**	**Sorbed Amount (mg)**
0	0	0	0	34	110.937	0.934	3.71268
1	3.183	0.001	0.31707	35	114.209	0.965	3.72380
2	6.260	0.002	0.62319	36	117.533	0.948	3.74076
3	9.442	0.047	0.92554	37	120.857	0.934	3.76237
4	12.653	0.114	1.20908	38	124.198	0.965	3.77373
5	15.879	0.172	1.47517	39	127.519	0.889	3.81025
6	19.110	0.215	1.72789	40	130.854	0.955	3.82492
7	22.393	0.258	1.97051	41	134.178	0.973	3.83357
8	25.680	0.311	2.19595	42	137.489	0.969	3.84350
9	28.962	0.354	2.40730	43	140.781	0.974	3.85173
10	32.223	0.400	2.60231	44	144.087	0.979	3.85834
11	35.488	0.488	2.76882	45	147.390	0.968	3.86858
12	38.778	0.555	2.91460	46	150.690	0.962	3.88079
13	42.071	0.632	3.03512	47	153.983	0.971	3.89001
14	45.336	0.692	3.13535	48	157.296	0.972	3.89896
15	48.531	0.752	3.21426	49	160.604	0.993	3.90094
16	51.790	0.797	3.28011	50	170.456	0.981	3.90916
17	55.074	0.830	3.33559	51	173.747	0.995	3.91048
18	58.376	0.854	3.38348	52	177.040	0.986	3.91476
19	61.682	0.909	3.41323	53	180.358	1.009	3.91476
20	64.986	0.884	3.45123	54	183.622	0.996	3.91574
21	68.292	0.913	3.47966	55	186.933	1.002	3.91574
22	71.595	0.925	3.50410	56	190.196	1.006	3.91574
23	74.851	0.953	3.51908	57	193.461	1.015	3.91574
24	78.096	0.961	3.53141	58	196.708	1.021	3.91574
25	81.362	0.966	3.54219	59	200.026	1.026	3.91574
26	84.638	0.968	3.55234	60	203.327	1.013	3.91574
27	87.911	0.965	3.56347	61	206.642	1.032	3.91574
28	91.114	0.951	3.57884	62	209.969	1.037	3.91574
29	94.412	0.940	3.59830	63	213.326	1.015	3.91574
30	97.721	0.925	3.62279	64	216.677	1.053	3.91574
31	101.030	0.952	3.63834	65	220.022	1.055	3.91574
32	104.347	0.908	3.66853	66	223.368	1.041	3.91574
33	107.643	0.930	3.69126				

Table 5.7 Results of elution studies for RNH-CH120 (Figure 3.32)

Frac. No	Con (mg/L)	Tot.BV	Tot. eluted amount (mg)	Frac. No	Con (mg/L)	Tot.BV	Tot. eluted amount (mg)
0	0	0	0	16	0.2	34.247	3.8744
1	72.5	2.143	0.1554	17	0.2	36.530	3.8749
2	948.8	4.339	2.2383	18	0.3	38.819	3.8756
3	517.5	6.528	3.3712	19	0.1	41.118	3.8758
4	95.0	7.619	3.4749	20	0.2	43.417	3.8763
5	57.2	9.833	3.6015	21	0.3	45.717	3.8769
6	44.3	12.032	3.6989	22	0.1	48.014	3.8772
7	32.8	14.254	3.7718	23	0.2	50.314	3.8776
8	22.0	16.479	3.8208	24	0.2	52.600	3.8781
9	14.4	18.705	3.8528	25	0.2	54.879	3.8786
10	5.2	20.933	3.8644	26	0.2	57.134	3.8790
11	1.9	23.163	3.8687	27	0.3	59.410	3.8797
12	1.0	25.379	3.8709	28	0.3	61.684	3.8804
13	0.7	27.599	3.8724	29	0.3	63.930	3.8810
14	0.4	29.828	3.8733	30	0.2	66.216	3.8815
15	0.3	32.035	3.8740				

Table 5.8 Results of sorption studies for Purolite C-160H (Figure 3.30)

Frac. No	BV	C/Co	Sorbed Amount (mg)	Frac. No	BV	C/Co	Sorbed Amount (mg)
0	0	0	0	15	114.518	0	11.41204
1	3.020	0.005	0.29960	16	117.551	0	11.71444
2	6.045	0.007	0.59914	17	120.783	0	12.03667
3	9.075	0.004	0.90000	18	123.893	0	12.34677
4	12.114	0.001	1.20263	19	126.922	0	12.64871
5	15.153	0	1.50564	20	130.208	0	12.97634
6	18.207	0	1.81018	21	133.378	0	13.29240
7	21.256	0.001	2.11382	22	136.502	0	13.60383
8	24.536	0	2.44088	23	139.615	0	13.91421
9	27.591	0	2.74545	24	142.747	0	14.22649
10	30.684	0	3.05381	25	146.550	0	14.60565
11	33.809	0	3.36530	26	150.762	0	15.02552
12	36.849	0	3.66846	27	153.901	0	15.33853
13	39.808	0	3.96342	28	157.057	0.002	15.65252
14	42.774	0	4.25915	29	160.195	0.006	15.96350

Table 5.8 Continued

Frac. No	C/Co	BV	Sorbed Amount (mg)	Frac. No	C/Co	BV	Sorbed Amount (mg)
30	0.006	163.341	16.27533	63	1.059	266.315	23.7809
31	0.009	166.485	16.58593	64	1.046	269.387	23.7809
32	0.008	169.609	16.89484	65	1.042	272.305	23.7809
33	0.008	172.732	17.20371	66	1.029	275.427	23.7809
34	0.007	176.086	17.53577	67	1.014	278.671	23.7809
35	0.008	179.194	17.84318	68	0.983	281.893	23.7861
36	0.010	182.302	18.14990	69	0.965	284.899	23.7963
37	0.013	185.406	18.45535	70	0.912	288.214	23.8251
38	0.015	188.503	18.75950	71	0.940	291.117	23.8422
39	0.017	191.616	19.06456	72	0.931	294.170	23.8630
40	0.021	194.726	19.36808	73	0.948	297.392	23.8794
41	0.027	197.823	19.66851	74	0.943	300.416	23.8964
42	0.031	200.923	19.96801	75	0.942	303.920	23.9163
43	0.039	204.027	20.26537	76	0.946	306.809	23.9317
44	0.048	207.132	20.56000	77	0.944	309.972	23.9491
45	0.058	210.231	20.85099	78	0.951	312.745	23.9624
46	0.068	213.334	21.13927	79	0.969	315.111	23.9695
47	0.082	216.342	21.41445	80	0.967	318.162	23.9792
48	0.099	219.467	21.69516	81	0.956	321.341	23.9929
49	0.126	222.571	21.96546	82	0.969	324.553	24.0025
50	0.152	225.692	22.22921	83	0.970	327.582	24.0113
51	0.168	228.781	22.48526	84	0.964	331.316	24.0244
52	0.217	231.870	22.72622	85	0.980	334.213	24.0299
53	0.281	235.261	22.96900	86	0.962	337.082	24.0405
54	0.349	238.061	23.15075	87	0.963	340.141	24.0515
55	0.406	241.174	23.33504	88	0.985	343.193	24.0558
56	0.493	244.275	23.49164	89	0.962	346.530	24.0681
57	0.595	247.456	23.61981	90	0.976	349.700	24.0754
58	0.729	250.601	23.70473	91	1.001	352.844	24.0754
59	0.844	253.828	23.75475	92	0.977	356.021	24.0824
60	0.919	256.708	23.77779	93	0.991	359.040	24.0848
61	0.989	259.860	23.78094	94	0.985	362.162	24.0892
62	1.034	262.996	23.78094	95	0.986	372.184	24.0933

Table 5.9 Results of elution studies for Purolite C-160H (Figure 3.33)

Frac. No	Con (mg/L)	Tot.BV	Tot. eluted amount (mg)	Frac. No	Con (mg/L)	Tot.BV	Tot. eluted amount (mg)
0	0	0	0	16	64.5	38.751	22.8819
1	1125	2.272	2.5566	17	51.2	41.203	23.0075
2	2350	4.549	7.9064	18	42.1	43.655	23.1107
3	1970	6.936	12.6086	19	34.1	46.109	23.1944
4	1027	9.387	15.1271	20	28.1	48.568	23.2635
5	657	11.832	16.7346	21	24.0	51.031	23.3226
6	488	14.277	17.9279	22	19.6	53.327	23.3676
7	380	16.723	18.8573	23	16.5	55.627	23.4055
8	325	19.173	19.6536	24	14.7	57.914	23.4392
9	305	21.623	20.4010	25	10.3	60.193	23.4626
10	255	24.072	21.0255	26	7.5	62.448	23.4795
11	201	26.518	21.5171	27	6.3	64.724	23.4939
12	170	28.968	21.9336	28	5.5	66.998	23.5064
13	138	31.425	22.2726	29	4.6	69.243	23.5167
14	100	33.869	22.5190	30	4.0	71.530	23.5259
15	84	36.306	22.7242				

Table 5.10 Results of sorption studies for RNH-CH120 (Figure 3.35)

Frac. No	C/Co	BV	Sorbed Amount (mg)	Frac. No	C/Co	BV	Sorbed Amount (mg)
0	0	0	0	17	0.351	51.774	2.31415
1	0.008	2.977	0.14614	18	0.392	54.848	2.40512
2	0.008	6.035	0.29384	19	0.435	57.922	2.48967
3	0.010	9.084	0.44077	20	0.457	61.007	2.57110
4	0.010	12.148	0.58849	21	0.486	64.092	2.64823
5	0.014	15.196	0.73477	22	0.509	67.177	2.72196
6	0.014	18.163	0.87721	23	0.517	70.257	2.79433
7	0.014	21.201	1.02300	24	0.521	73.338	2.86613
8	0.014	24.256	1.16968	25	0.558	76.414	2.93225
9	0.016	27.309	1.31589	26	0.577	79.496	2.99576
10	0.016	30.371	1.46256	27	0.589	82.586	3.05756
11	0.024	33.438	1.60824	28	0.605	85.679	3.11693
12	0.030	36.494	1.75251	29	0.624	88.778	3.17365
13	0.125	39.549	1.88262	30	0.642	91.883	3.22767
14	0.195	42.609	2.00257	31	0.663	94.986	3.27856
15	0.254	45.650	2.11299	32	0.673	98.088	3.32789
16	0.299	48.707	2.21720	33	0.679	101.195	3.37636

Table 5.10 Continued

Frac. No	C/Co	BV	Sorbed Amount (mg)	Frac. No	C/Co	BV	Sorbed Amount (mg)
34	0.685	104.303	3.42391	72	0.885	222.897	4.6586
35	0.694	107.409	3.47019	73	0.885	226.017	4.6754
36	0.696	110.520	3.51623	74	0.889	229.132	4.6916
37	0.706	113.630	3.56070	75	0.891	232.245	4.7075
38	0.708	116.745	3.60494	76	0.891	235.361	4.7234
39	0.708	119.864	3.64923	77	0.893	238.476	4.7390
40	0.714	122.992	3.69270	78	0.902	241.586	4.7533
41	0.714	126.127	3.73628	79	0.902	244.702	4.7676
42	0.718	129.258	3.77917	80	0.902	247.839	4.7820
43	0.722	132.408	3.82170	81	0.904	250.968	4.7961
44	0.724	135.557	3.86390	82	0.904	254.110	4.8103
45	0.724	138.700	3.90602	83	0.912	257.259	4.8232
46	0.724	141.851	3.94824	84	0.912	260.389	4.8360
47	0.728	144.997	3.98977	85	0.914	263.522	4.8485
48	0.735	148.134	4.03024	86	0.919	266.668	4.8605
49	0.747	151.282	4.06895	87	0.925	269.799	4.8714
50	0.757	154.431	4.10611	88	0.936	272.943	4.8809
51	0.759	157.584	4.14300	89	0.936	276.080	4.8903
52	0.763	160.740	4.17929	90	0.940	279.206	4.8990
53	0.770	163.891	4.21459	91	0.942	282.334	4.9075
54	0.778	167.037	4.24857	92	0.959	285.481	4.9135
55	0.778	170.193	4.28265	93	0.961	288.636	4.9191
56	0.780	173.335	4.31627	94	0.961	291.772	4.9248
57	0.792	176.476	4.34800	95	0.980	294.909	4.9276
58	0.794	179.560	4.37883	96	0.980	298.058	4.9304
59	0.829	182.657	4.40361	97	0.982	301.221	4.9330
60	0.840	185.752	4.42682	98	0.989	304.377	4.9346
61	0.853	188.842	4.44814	99	0.989	307.503	4.9361
62	0.857	191.945	4.46893	100	1.000	310.588	4.9361
63	0.861	195.037	4.48903	101	1.002	313.742	4.9361
64	0.861	198.100	4.50894	102	1.004	316.905	4.9361
65	0.863	201.196	4.52876	103	1.004	320.065	4.9361
66	0.863	204.287	4.54854	104	1.010	323.223	4.9361
67	0.863	207.374	4.56829	105	1.010	326.378	4.9361
68	0.868	210.466	4.58747	106	1.017	329.532	4.9361
69	0.872	213.565	4.60606	107	1.019	332.675	4.9361
70	0.876	216.658	4.62400	108	1.021	335.819	4.9361
71	0.878	219.770	4.64173	109	1.021	338.979	4.9361

Table 5.10 Continued

Frac. No	C/Co	BV	Sorbed Amount (mg)	Frac. No	C/Co	BV	Sorbed Amount (mg)
110	1.023	342.147	4.9361	114	1.027	354.779	4.9361
111	1.023	345.322	4.9361	115	1.027	357.949	4.9361
112	1.025	348.483	4.9361	116	1.027	361.108	4.9361
113	1.025	351.625	4.9361				

Table 5.11 Results of elution studies for RNH-CH120 (Figure 3.36)

Frac. No	Con (mg/L)	Tot.BV	Tot. eluted amount (mg)	Frac. No	Con (mg/L)	Tot.BV	Tot. eluted amount (mg)
0	0	0	0	16	1.3	35.048	4.8943
1	15	2.089	0.0313	17	1.2	37.307	4.8970
2	692	4.177	1.4772	18	1.0	39.571	4.8993
3	1472	6.269	4.5571	19	1.0	41.840	4.9015
4	112	8.371	4.7936	20	0.9	44.102	4.9036
5	21	10.357	4.8353	21	0.7	46.373	4.9052
6	6	12.595	4.8489	22	0.7	48.644	4.9067
7	2.8	14.838	4.8552	23	0.7	50.918	4.9083
8	2.7	17.085	4.8613	24	0.6	53.185	4.9097
9	2.4	19.335	4.8667	25	0.6	55.454	4.9111
10	2.2	21.583	4.8716	26	0.6	57.730	4.9124
11	2	23.821	4.8761	27	0.5	60.006	4.9136
12	1.9	26.073	4.8804	28	0.5	62.298	4.9147
13	1.8	28.325	4.8844	29	0.5	64.591	4.9159
14	1.7	30.572	4.8882	30	0.5	66.885	4.9170
15	1.4	32.805	4.8914	31	0.4	69.191	4.9179

Table 5.12 Results of sorption studies for RNH-CH120 (Figure 3.35)

Frac. No	C/Co	Tot.BV	Sorbed Amount (mg)	Frac. No	C/Co	Tot.BV	Sorbed Amount (mg)
0	0	0	0	38	0.509	117.765	2.89170
1	0.012	2.977	0.08820	39	0.544	120.965	2.93543
2	0.013	6.140	0.18176	40	0.544	124.169	2.97917
3	0.014	9.290	0.27484	41	0.596	127.374	3.01792
4	0.014	12.465	0.36866	42	0.604	130.583	3.05601
5	0.015	15.490	0.45796	43	0.617	133.791	3.09281
6	0.015	18.590	0.54946	44	0.629	136.984	3.12828
7	0.016	21.770	0.64330	45	0.632	140.068	3.16226
8	0.017	24.627	0.72753	46	0.645	143.203	3.19562
9	0.017	27.806	0.82117	47	0.669	146.347	3.22680
10	0.018	30.961	0.91411	48	0.679	149.495	3.25703
11	0.018	34.134	1.00754	49	0.681	152.646	3.28712
12	0.019	37.299	1.10062	50	0.684	155.799	3.31698
13	0.033	40.486	1.19298	51	0.694	158.951	3.34585
14	0.050	43.630	1.28253	52	0.718	162.086	3.37234
15	0.063	46.792	1.37137	53	0.738	165.228	3.39697
16	0.066	49.869	1.45756	54	0.753	168.363	3.42017
17	0.066	52.972	1.54447	55	0.753	171.478	3.44316
18	0.069	56.081	1.63121	56	0.777	174.623	3.46417
19	0.088	59.190	1.71624	57	0.794	177.760	3.48352
20	0.096	62.309	1.80075	58	0.805	180.888	3.50173
21	0.100	65.196	1.87863	59	0.811	183.645	3.51731
22	0.106	67.940	1.95220	60	0.813	186.783	3.53488
23	0.111	70.836	2.02938	61	0.818	189.947	3.55209
24	0.197	73.964	2.10465	62	0.821	193.112	3.56899
25	0.231	77.081	2.17647	63	0.826	196.208	3.58510
26	0.280	80.161	2.24289	64	0.837	199.354	3.60041
27	0.317	83.255	2.30620	65	0.844	202.472	3.61497
28	0.346	86.418	2.36822	66	0.848	205.625	3.62932
29	0.347	89.473	2.42804	67	0.849	208.792	3.64364
30	0.366	92.380	2.48328	68	0.862	211.961	3.65669
31	0.398	95.666	2.54259	69	0.873	215.137	3.66876
32	0.426	98.825	2.59689	70	0.874	218.307	3.68065
33	0.460	102.030	2.64874	71	0.885	221.483	3.69158
34	0.464	105.223	2.69999	72	0.893	224.661	3.70174
35	0.464	108.398	2.75096	73	0.897	227.829	3.71144
36	0.484	111.575	2.80006	74	0.899	230.973	3.72093
37	0.502	114.407	2.84230	75	0.900	234.113	3.73029

Table 5.12 Continued

Frac. No	C/Co	Tot.BV	Sorbed Amount (mg)	Frac. No	C/Co	Tot.BV	Sorbed Amount (mg)
76	0.939	237.305	3.73607	86	0.982	269.115	3.79048
77	0.909	240.493	3.74468	87	0.998	272.318	3.79057
78	0.911	243.662	3.75311	88	1.008	275.505	3.79057
79	0.917	246.790	3.76083	89	1.009	278.661	3.79057
80	0.919	249.934	3.76838	90	1.011	281.823	3.79057
81	0.937	253.113	3.77435	91	1.012	285.029	3.79057
82	0.940	256.309	3.78004	92	1.012	288.205	3.79057
83	0.958	259.507	3.78401	93	1.012	291.398	3.79057
84	0.968	262.705	3.78698	94	1.012	294.580	3.79057
85	0.980	265.909	3.78884				

Table 5.13 Results of elution studies for RNH-CH120

(Figure 3.36)

Frac. No	Con(mg/L)	Tot.BV	Tot. eluted amount (mg)
0	0	0	0
1	13.7	2.026	0.02786
2	920.0	4.028	1.86942
3	496.8	6.181	2.93933
4	205.2	8.282	3.37035
5	111.2	10.400	3.60606
6	42.2	12.508	3.69518
7	22.0	14.615	3.74153
8	9.5	16.719	3.76153
9	4.2	18.824	3.77050
10	2.5	20.927	3.77589
11	1.7	23.037	3.77949
12	1.3	25.151	3.78222
13	1.1	27.265	3.78459
14	0.9	29.379	3.78655
15	0.8	31.227	3.78818
16	0.8	33.169	3.78983

Table 5.14 Results of sorption studies for RNH-CH120 (Figure 3.35)

Frac. No	C/Co	Tot.BV	Sorbed Amount (mg)	Frac. No	C/Co	Tot.BV	Sorbed Amount (mg)
0	0	0	0	37	0.548	117.010	0.82114
1	0.001	3.075	0.03023	38	0.551	120.229	0.83533
2	0.001	6.189	0.06083	39	0.552	123.453	0.84952
3	0.001	9.482	0.09321	40	0.557	126.678	0.86355
4	0.001	12.611	0.12397	41	0.570	129.910	0.87722
5	0.001	15.746	0.15479	42	0.575	133.143	0.89073
6	0.001	18.887	0.18565	43	0.579	136.386	0.90416
7	0.001	22.032	0.21658	44	0.583	139.609	0.91737
8	0.001	25.183	0.24755	45	0.590	142.806	0.93026
9	0.002	28.336	0.27851	46	0.594	146.027	0.94311
10	0.003	31.488	0.30944	47	0.609	149.274	0.95558
11	0.053	34.636	0.33874	48	0.611	152.531	0.96802
12	0.086	37.786	0.36706	49	0.613	155.793	0.98041
13	0.137	40.935	0.39380	50	0.618	159.051	0.99263
14	0.180	44.065	0.41902	51	0.619	162.319	1.00486
15	0.226	47.150	0.44250	52	0.627	165.582	1.01683
16	0.241	50.264	0.46573	53	0.627	168.847	1.02881
17	0.293	53.404	0.48755	54	0.653	172.104	1.03992
18	0.322	56.559	0.50860	55	0.656	175.342	1.05086
19	0.349	59.731	0.52890	56	0.658	178.592	1.06178
20	0.368	62.909	0.54863	57	0.664	181.875	1.07262
21	0.403	66.094	0.56733	58	0.676	185.159	1.08306
22	0.435	69.287	0.58505	59	0.682	188.442	1.09330
23	0.460	72.474	0.60197	60	0.685	191.727	1.10345
24	0.466	75.643	0.61861	61	0.700	195.020	1.11317
25	0.475	78.772	0.6347	62	0.703	198.399	1.12304
26	0.470	81.916	0.6511	63	0.704	201.687	1.13260
27	0.472	85.094	0.66763	64	0.707	204.981	1.14209
28	0.474	88.291	0.68416	65	0.709	208.246	1.15143
29	0.475	91.489	0.70066	66	0.718	211.528	1.16052
30	0.484	94.687	0.71687	67	0.715	214.818	1.16973
31	0.498	97.890	0.73267	68	0.730	218.107	1.17845
32	0.498	101.097	0.74847	69	0.747	221.397	1.18661
33	0.519	104.299	0.76362	70	0.756	224.699	1.19453
34	0.521	107.486	0.77863	71	0.758	227.989	1.20236
35	0.542	110.643	0.79284	72	0.767	231.282	1.20990
36	0.547	113.804	0.80691	73	0.771	234.558	1.21727

Table 5.14 Continued

Frac. No	C/Co	Tot.BV	Sorbed Amount (mg)	Frac. No	C/Co	Tot.BV	Sorbed Amount (mg)
74	0.783	237.821	1.22422	90	0.953	290.372	1.28897
75	0.798	241.100	1.23072	91	0.957	293.651	1.29035
76	0.804	244.393	1.23704	92	0.970	296.944	1.29131
77	0.807	247.687	1.24326	93	0.975	300.238	1.29210
78	0.815	250.967	1.24923	94	0.982	303.519	1.29265
79	0.847	254.257	1.25417	95	0.985	306.808	1.29311
80	0.858	257.532	1.25872	96	0.995	310.084	1.29324
81	0.866	260.797	1.26300	97	0.997	313.386	1.29331
82	0.881	264.080	1.26684	98	1.001	316.642	1.29331
83	0.883	267.369	1.27062	99	1.002	319.887	1.29331
84	0.887	270.658	1.27427	100	1.003	323.154	1.29331
85	0.895	273.949	1.27766	101	1.004	326.429	1.29331
86	0.901	277.250	1.28086	102	1.006	329.703	1.29331
87	0.910	280.541	1.28376	103	1.007	332.905	1.29331
88	0.935	283.833	1.28583	104	1.009	336.203	1.29331
89	0.949	287.109	1.28747	105	1.011	339.512	1.29331

Table 5.15 Results of elution studies for RNH-CH120 (Figure 3.36)

Frac. No	Con(mg/L)	Tot.BV	Tot. eluted amount (mg)
0	0	0	0
1	3.5	2.143	0.00750
2	21.2	4.339	0.05415
3	345.0	6.528	0.80946
4	196.5	7.619	1.02390
5	84.6	9.833	1.21119
6	22.5	12.032	1.26062
7	5.8	14.254	1.27356
8	2.8	16.479	1.27996
9	1.4	18.705	1.28319
10	0.9	20.933	1.28535
11	0.7	23.163	1.28709
12	0.6	25.379	1.28855
13	0.5	27.599	1.28984
14	0.5	29.828	1.29100
15	0.4	32.035	1.29206
16	0.4	34.247	1.29306

Table 5.16 Results of sorption studies for RNH-CH120 (Figure 3.37)

Frac. No	C/Co	Tot.BV	Sorbed Amount (mg)	Frac. No	C/Co	Tot.BV	Sorbed Amount (mg)
0	0	0	0	40	0.424	119.094	1.09833
1	0	2.913	0.02866	41	0.429	122.084	1.11510
2	0	5.864	0.05770	42	0.434	125.106	1.13191
3	0	8.838	0.08696	43	0.436	128.119	1.14860
4	0	11.815	0.11626	44	0.441	131.116	1.16508
5	0	14.789	0.14552	45	0.443	134.127	1.18158
6	0	17.773	0.17489	46	0.450	137.115	1.19775
7	0	20.766	0.20434	47	0.453	140.142	1.21403
8	0	23.718	0.23338	48	0.454	143.169	1.23028
9	0	26.673	0.26247	49	0.466	146.195	1.24617
10	0	29.682	0.29207	50	0.474	149.218	1.26180
11	0	32.704	0.32180	51	0.475	152.231	1.27735
12	0	35.623	0.35053	52	0.476	155.255	1.29292
13	0	38.575	0.37958	53	0.476	158.130	1.30773
14	0	41.524	0.40860	54	0.477	161.053	1.32275
15	0	44.440	0.43729	55	0.478	163.979	1.33776
16	0	47.382	0.46624	56	0.478	166.936	1.35293
17	0	50.302	0.49498	57	0.478	169.897	1.36812
18	0.001	53.285	0.52429	58	0.486	172.790	1.38273
19	0.001	56.264	0.55358	59	0.486	175.686	1.39736
20	0.001	59.269	0.58311	60	0.486	178.586	1.41200
21	0.001	62.278	0.61270	61	0.493	181.484	1.42643
22	0.001	65.288	0.64229	62	0.505	184.376	1.44052
23	0.001	68.309	0.67198	63	0.506	187.252	1.45450
24	0.001	71.328	0.70166	64	0.507	190.162	1.46861
25	0.001	74.345	0.73131	65	0.510	193.060	1.48258
26	0.001	77.367	0.76102	66	0.527	195.993	1.49622
27	0.002	80.165	0.78849	67	0.556	198.903	1.50890
28	0.002	83.197	0.81827	68	0.558	201.818	1.52155
29	0.002	86.240	0.84816	69	0.581	204.739	1.53359
30	0.002	89.281	0.87801	70	0.584	207.662	1.54554
31	0.003	92.327	0.90790	71	0.586	210.583	1.55743
32	0.015	95.197	0.93571	72	0.591	213.502	1.56917
33	0.044	98.177	0.96372	73	0.594	216.410	1.58077
34	0.141	101.162	0.98894	74	0.596	219.330	1.59236
35	0.295	104.162	1.00974	75	0.597	222.256	1.60395
36	0.366	107.129	1.02822	76	0.597	225.188	1.61556
37	0.380	110.123	1.04648	77	0.599	228.120	1.62711
38	0.394	113.096	1.06420	78	0.599	231.049	1.63865
39	0.418	116.093	1.08134	79	0.601	233.986	1.65016

Table 5.16 Continued

Frac. No	C/Co	Tot.BV	Sorbed Amount (mg)	Frac. No	C/Co	Tot.BV	Sorbed Amount (mg)
80	0.602	236.844	1.66134	99	0.714	292.858	1.85365
81	0.602	239.701	1.67251	100	0.725	296.009	1.86216
82	0.605	242.540	1.68353	101	0.727	299.162	1.87061
83	0.605	245.381	1.69455	102	0.731	302.314	1.87893
84	0.614	248.255	1.70544	103	0.741	305.461	1.88693
85	0.614	251.141	1.71638	104	0.753	308.612	1.89458
86	0.617	254.039	1.72727	105	0.757	311.761	1.90211
87	0.620	256.948	1.73813	106	0.758	314.891	1.90956
88	0.622	259.852	1.74890	107	0.760	317.976	1.91684
89	0.630	262.759	1.75948	108	0.761	321.090	1.92416
90	0.639	265.669	1.76981	109	0.761	324.230	1.93154
91	0.650	268.590	1.77986	110	0.792	327.385	1.93797
92	0.654	271.509	1.78979	111	0.802	330.557	1.94413
93	0.668	274.429	1.79931	112	0.814	333.734	1.94994
94	0.686	277.361	1.80834	113	0.815	336.920	1.95574
95	0.690	280.308	1.81732	114	0.815	340.112	1.96155
96	0.696	283.437	1.82668	115	0.816	343.300	1.96732
97	0.703	286.572	1.83583	116	0.816	346.469	1.97305
98	0.709	289.712	1.84481				

Table 5.17 Results of elution studies for RNH-CH120 (Figure 3.38)

Frac. No	Con(mg/L)	Tot.BV	Tot. eluted amount (mg)	Frac. No	Con(mg/L)	Tot.BV	Tot. eluted amount (mg)
0	0	0	0	16	0.42	34.837	1.92828
1	75.0	2.055	0.15412	17	0.38	37.106	1.92914
2	379.0	4.180	0.95980	18	0.35	39.375	1.92993
3	218.0	6.321	1.42645	19	0.33	41.635	1.93068
4	113.5	8.460	1.66921	20	0.33	43.854	1.93141
5	60.0	10.610	1.79823	21	0.26	46.068	1.93199
6	32.0	12.769	1.86730	22	0.25	48.325	1.93255
7	6.4	14.928	1.88130	23	0.21	50.578	1.93302
8	6.0	17.085	1.89424	24	0.19	52.859	1.93346
9	5.2	19.250	1.90550	25	0.19	55.127	1.93389
10	3.7	21.409	1.91355	26	0.18	57.425	1.93430
11	2.4	23.617	1.91885	27	0.18	59.669	1.93471
12	1.6	25.846	1.92248	28	0.16	61.926	1.93507
13	1.0	28.086	1.92492	29	0.16	64.232	1.93544
14	0.5	30.344	1.92623	30	0.15	66.517	1.93578
15	0.4	32.598	1.92734	31	0.15	68.833	1.93613

Table 5.17 Continued

Frac. No	Con(mg/L)	Tot.BV	Tot. eluted amount(mg)
32	0.14	71.159	1.93645
33	0.14	73.449	1.93677
34	0.14	75.745	1.93709
35	0.10	78.059	1.93733
36	0.10	80.343	1.93755

Table 5.18 Results of sorption studies for RNH-CH120 (Figure 3.37)

Frac. No	C/Co	Tot.BV	Sorbed Amount (mg)	Frac. No	C/Co	Tot.BV	Sorbed Amount (mg)
0	0	0	0	30	0.35	94.484	0.89945
1	0.01	3.154	0.03072	31	0.49	97.643	0.91506
2	0.01	6.256	0.06094	32	0.50	100.804	0.93036
3	0.01	9.367	0.09123	33	0.55	103.960	0.94406
4	0.01	12.592	0.12264	34	0.51	107.121	0.95904
5	0.01	15.732	0.15323	35	0.52	110.275	0.97368
6	0.02	18.974	0.18448	36	0.55	113.428	0.98736
7	0.02	22.373	0.21725	37	0.55	116.580	1.00104
8	0.02	25.468	0.24708	38	0.57	119.736	1.01410
9	0.02	28.671	0.27796	39	0.57	122.884	1.02714
10	0.02	31.820	0.30831	40	0.58	126.042	1.03990
11	0.02	35.023	0.33920	41	0.59	129.196	1.05232
12	0.02	38.192	0.36974	42	0.59	132.353	1.06476
13	0.02	41.341	0.40010	43	0.60	135.500	1.07685
14	0.02	44.510	0.43065	44	0.62	138.546	1.08824
15	0.02	47.875	0.46308	45	0.64	141.695	1.09938
16	0.02	51.017	0.49338	46	0.64	144.832	1.11049
17	0.02	54.080	0.52290	47	0.64	147.879	1.12127
18	0.02	57.125	0.55226	48	0.66	150.944	1.13151
19	0.02	60.177	0.58168	49	0.66	154.013	1.14176
20	0.02	63.220	0.61101	50	0.67	157.077	1.15169
21	0.02	66.254	0.64027	51	0.67	160.149	1.16164
22	0.02	69.371	0.67031	52	0.68	163.224	1.17130
23	0.02	72.485	0.70032	53	0.68	166.288	1.18092
24	0.02	75.609	0.73044	54	0.69	169.343	1.19021
25	0.02	78.742	0.76065	55	0.69	172.412	1.19954
26	0.02	81.886	0.79096	56	0.69	175.499	1.20892
27	0.02	85.029	0.82125	57	0.69	178.596	1.21834
28	0.03	88.178	0.85129	58	0.69	181.701	1.22778
29	0.09	91.325	0.87943	59	0.69	184.797	1.23719

Table 5.18 Continued

Frac. No	C/Co	Tot.BV	Sorbed Amount (mg)	Frac. No	C/Co	Tot.BV	Sorbed Amount (mg)
60	0.69	187.90	1.24663	78	0.80	243.10	1.38490
61	0.70	191.01	1.25576	79	0.80	246.45	1.39139
62	0.70	194.11	1.26489	80	0.81	249.81	1.39756
63	0.70	197.22	1.27404	81	0.81	253.16	1.40373
64	0.70	200.33	1.28317	82	0.81	256.51	1.40990
65	0.71	203.46	1.29206	83	0.81	259.83	1.41601
66	0.71	206.59	1.30096	84	0.82	263.17	1.42182
67	0.71	209.72	1.30984	85	0.82	266.53	1.42766
68	0.71	212.17	1.31680	86	0.82	269.87	1.43347
69	0.72	214.41	1.32293	87	0.83	273.19	1.43891
70	0.74	217.54	1.33090	88	0.84	276.54	1.44407
71	0.75	220.69	1.33858	89	0.84	279.88	1.44923
72	0.76	223.83	1.34593	90	0.85	283.23	1.45404
73	0.78	226.99	1.35269	91	0.85	286.57	1.45885
74	0.79	230.13	1.35909	92	0.86	289.91	1.46332
75	0.79	233.28	1.36552	93	0.86	293.25	1.46780
76	0.79	236.44	1.37196	94	0.87	296.57	1.47192
77	0.80	239.79	1.37846				

Table 5.19 Results of elution studies for RNH-CH120 (Figure 3.38)

Frac. No	Con(mg/L)	Tot.BV	Tot. eluted amount (mg)
0	0	0	0
1	12.5	2.098	0.02623
2	145.0	4.301	0.34562
3	295.0	6.454	0.98090
4	116.0	8.579	1.22734
5	37.5	10.645	1.30482
6	25.0	12.737	1.35713
7	12.5	14.905	1.38423
8	10.2	17.078	1.40639
9	6.8	19.257	1.42121
10	4.6	21.442	1.43126
11	3.2	23.621	1.43823
12	2.3	25.808	1.44326
13	1.8	27.995	1.44720
14	1.7	30.184	1.45092
15	1.5	32.373	1.45420
16	1.5	34.587	1.45752
17	1.4	36.785	1.46060
18	1.3	39.008	1.46349
19	1.3	41.232	1.46638
20	1.2	43.459	1.46906

Table 5.20 Results of sorption studies for RNH-CH120 (Figure 3.37)

Frac. No	C/Co	Tot.BV	Sorbed Amount (mg)	Frac. No	C/Co	Tot.BV	Sorbed Amount (mg)
0	0	0	0	40	0.557	126.678	0.86355
1	0.001	3.075	0.03023	41	0.570	129.910	0.87722
2	0.001	6.189	0.06083	42	0.575	133.143	0.89073
3	0.001	9.482	0.09321	43	0.579	136.386	0.90416
4	0.001	12.611	0.12397	44	0.583	139.609	0.91737
5	0.001	15.746	0.15479	45	0.590	142.806	0.93026
6	0.001	18.887	0.18565	46	0.594	146.027	0.94311
7	0.001	22.032	0.21658	47	0.609	149.274	0.95558
8	0.001	25.183	0.24755	48	0.611	152.531	0.96802
9	0.002	28.336	0.27851	49	0.613	155.793	0.98041
10	0.003	31.488	0.30944	50	0.618	159.051	0.99263
11	0.053	34.636	0.33874	51	0.619	162.319	1.00486
12	0.086	37.786	0.36706	52	0.627	165.582	1.01683
13	0.137	40.935	0.39380	53	0.627	168.847	1.02881
14	0.180	44.065	0.41902	54	0.653	172.104	1.03992
15	0.226	47.150	0.44250	55	0.656	175.342	1.05086
16	0.241	50.264	0.46573	56	0.658	178.592	1.06178
17	0.293	53.404	0.48755	57	0.664	181.875	1.07262
18	0.322	56.559	0.50860	58	0.676	185.159	1.08306
19	0.349	59.731	0.52890	59	0.682	188.442	1.09330
20	0.368	62.909	0.54863	60	0.685	191.727	1.10345
21	0.403	66.094	0.56733	61	0.700	195.020	1.11317
22	0.435	69.287	0.58505	62	0.703	198.399	1.12304
23	0.460	72.474	0.60197	63	0.704	201.687	1.13260
24	0.466	75.643	0.61861	64	0.707	204.981	1.14209
25	0.475	78.772	0.63475	65	0.709	208.246	1.15143
26	0.470	81.916	0.65113	66	0.718	211.528	1.16052
27	0.472	85.094	0.66763	67	0.715	214.818	1.16973
28	0.474	88.291	0.68416	68	0.730	218.107	1.17845
29	0.475	91.489	0.70066	69	0.747	221.397	1.18661
30	0.484	94.687	0.71687	70	0.756	224.699	1.19453
31	0.498	97.890	0.73267	71	0.758	227.989	1.20236
32	0.498	101.097	0.74847	72	0.767	231.282	1.20990
33	0.519	104.299	0.76362	73	0.771	234.558	1.21727
34	0.521	107.486	0.77863	74	0.783	237.821	1.22422
35	0.542	110.643	0.79284	75	0.798	241.100	1.23072
36	0.547	113.804	0.80691	76	0.804	244.393	1.23704
37	0.548	117.010	0.82114	77	0.807	247.687	1.24326
38	0.551	120.229	0.83533	78	0.815	250.967	1.24923
39	0.552	123.453	0.84952	79	0.847	254.257	1.25417

Table 5.20 Continued

Frac. No	C/Co	Tot.BV	Sorbed Amount (mg)	Frac. No	C/Co	Tot.BV	Sorbed Amount (mg)
80	0.858	257.532	1.25872	93	0.975	300.238	1.29210
81	0.866	260.797	1.26300	94	0.982	303.519	1.29265
82	0.881	264.080	1.26684	95	0.985	306.808	1.29311
83	0.883	267.369	1.27062	96	0.995	310.084	1.29324
84	0.887	270.658	1.27427	97	0.997	313.386	1.29331
85	0.895	273.949	1.27766	98	1.001	316.642	1.29331
86	0.901	277.250	1.28086	99	1.002	319.887	1.29331
87	0.910	280.541	1.28376	100	1.003	323.154	1.29331
88	0.935	283.833	1.28583	101	1.004	326.429	1.29331
89	0.949	287.109	1.28747	102	1.006	329.703	1.29331
90	0.953	290.372	1.28897	103	1.007	332.905	1.29331
91	0.957	293.651	1.29035	104	1.009	336.203	1.29331
92	0.970	296.944	1.29131	105	1.011	339.512	1.29331

Table 5.21 Results of elution studies for RNH-CH120 (Figure 3.38)

Frac. No	Con(mg/L)	Tot.BV	Tot. eluted amount (mg)
0	0	0	0
1	3.5	2.143	0.00750
2	21.2	4.339	0.05415
3	345.0	6.528	0.80946
4	196.5	7.619	1.02390
5	84.6	9.833	1.21119
6	22.4	12.032	1.26062
7	5.8	14.254	1.27356
8	2.8	16.479	1.27996
9	1.4	18.705	1.28319
10	0.9	20.933	1.28535
11	0.7	23.163	1.28709
12	0.6	25.379	1.28855
13	0.5	27.599	1.28984
14	0.5	29.828	1.29100
15	0.4	32.035	1.29206
16	0.4	34.247	1.29306

6.0 REFERENCES

1. **Alexandratos, S.D. and Crick, D.W.,** 1996, Uptake of metal ions by new chelating ion exchange resins, Ind. Eng. Chem. Res., 35: 635.

2. **Agency for Toxic Substances and Disease Registry (ATSDR),** 2000, Toxicological Profile for chromium, GA: U.S. Department of Health and Human Services, Atlanta, (Subcontract No. ATSDR-205-1999-00024).

3. **Some metals and metallic compounds**, 1980, IARC Monographs on the Evaluation of the Carcinogenic Risk of Chemicals to Humans, Lyon, International Agency for Research on Cancer, Vol. 23.

4. **Langard, S.,** 1990, One hundred years of chromium and cancer; a review of the epidemiological evidence and selected case reports, American journal of industrial medicine, 17: 189–215.

5. **Health assessment document for chromium**, 1984, United States Environmental Protection Agency, Research Triangle Park, NC, (Final report No. EPA600/ 8-83-014F).

6. **WHO**, 2003, Chromium in drinking-water Background document for preparation of WHO Guidelines for drinking-water quality, Geneva, World Health Organization ,(WHO/SDE/WSH/03.04/4).

7. **ATSDR**, 2002, Toxicological profile for copper (draft for public comment), US Department of Health and Human Services, Public Health Service, Atlanta, GA.

6.0 REFERENCES (Continued)

8. Barceloux, D.G., 1999, Copper- Clinical Toxicology, 37(2):217–230.

9. Lenntech Water treatment & air purification Holding B.V., The Netherlands.

10. ATSDR, 2002, Toxicological profile for cadmium (draft for public comment), US Department of Health and Human Services, Public Health Service, Atlanta.

11. Calvert, J.B., Retrieved April 5, 2005, Mercury: The lore of mercury, especially its uses in science and engineering.

12. Kolev, S.T. and Bates, N., Mercury (UK PID). National Poisons Information Service: Medical Toxicology Unit (London Centre).

13. Lieser, K.H., 1979, New ion exchangers, preparation, properties and application, Pure Appl. Chem., 51:1503.

14. Cortina, J.L., Meinhardt, E., Roijals, O. and Marti, **V.**, 1998, Modification and preparation of polymeric adsorbents for precious-metal extraction in hydrometallurgical processes, React. Funct. Polym., 36:149.

15. Rabelo, D. and Coutinho, **F.M.B.,** 1994, Porous structure formation and swelling properties of estyrene-divinylnenzene copolymers, Eur. Polym., 30 (6): 675.

6.0 REFERENCES (continued)

16. Shumickler, G., in: Frank, H., Bikales, N.M., Overberg, C.G. and Menges G.(Eds.), 1985, Encyclopedia of Polymer Science and Engineering, Chelate-Forming Polymers, Vol. 3, J. Wiley and Sons, New York, p. 363.

17. Kun, K.A. and Kunin, R., 1968, Macroreticular resins. III. Formation of macroreticular styrene-divinylbenzene copolymers, J. Polym. Sci., 6 (Part A-1):2689.

18. Reevillon, A., Guyot, A., Yuan, Q. and Prato, P., 1989, Macroporous gel-type styrene-divinylbenzene materials, React. Polym., 10-11.

19. Muraviev, D., 1998, Solvent extraction and ion exchange, Reactive and Functional Polymers, 16: 381-457.

20. Ekinci, H., 1996, Removal of heavy metal ions from aqueous solutions by polymeric resins and activated carbons prepared from agricultural wastes, MSc Project, Ege University.

21. Kunin, R., 1960, Elements of Ion Exchange, Reinhold Publishing Corporation, New York.

22. Zagarodni, A., 1997, Seminar Notes, Ege University Chemical Engineering Department, İzmir.

23. Bolto, B. A. and Pawlowski, L., 1987, Wastewater Treatment by Ion exchange, McGraw-Hill Publishing, London, 57-62 pp.

6.0 REFERENCES (continued)

24. Helfferich, F., 1962, Ion Exchange, Dover Publications, Inc., New York.

25. Desilva, J., 1999, Essentials of Ion Exchange, 25th W.Q.A. Annual Conference.

26. Marinsky, A., 1966, Ion Exchange, Marcel Dekker, Inc., New York, V: 1

27. Harland, C.E., 1994, Ion Exchange: Theory and Practise, The Permutit Company Limited, UK.

28. Samuelson, O., 1963, Ion Exchange Separations in Analytical Chemistry, Engineering Chemistry, Chalmers University of Technical, Sweden, John Wiley & Sons.

29. Colella, M.B., Siggia, S. and Barnes, R.M., 1980,Preparation of polyacryloamidoxime chelating cloth for the extraction of heavy metals from water, Anal. Chem., 52:967.

30. Kabay, N., Hayashi, T., Jyo, A. and Egawa, H., 1994, Amidoxime resins based on poly(acrylonitrile-co-vinylidene chloride-co-divinylbenzene) and their behavior in uptake of uranium from seawater, J.Appl.Polym.Sci., 54: 333-338.

31. Nakayama, M., Uemura, K., Nonaka, T. and Egawa, H., 1988, Chelating Sorbents in Inorganic Chemical Analysis, J. Appl. Polym. Sci., 36:1617.

6.0 REFERENCES (continued)

32. Vernon, F., 1982, Chelating ion exchangers - The Synthesis and uses of poly(hydroxanic acid) resins, Pure Appl. Chem., 54 (II):2151.

33. Arshady, R. and Ledwith, A., 1983, Suspension polymerisation and its application to the preparation of polymer supports, React. Polym., 1:159.

34. Fetscher, C. A., Hills, S., Lipowski, S. A. and Livingston, N. J., 1967, Process for conversion of amidoxime polymers to polyhydroxamic acids using aqueous hydrochloric acid solutions, Patente Americana, 3:345-344.

35. Hirotsu, T., Katoh, S., Sugasaka, K., Takai, N., Seno, M. and Itagaki, T., 1988, Effect of water content of hydrophilic amidoxime polymer on adsorption rate of uranium from seawater, J. Appl. Polym. Sci., 36:1741.

36. Kocacık, N., 1998, Experimental and Computational Study on the removal of Uranium and Cadmium from Phosphoric acid solution by Ion Exchange process, MSc Thesis, Ege University, 87 pp.

37. Vermeulen, T., Hiester, N.K, 1952, Saturation performance of ion exchange and adsorption columns, Chemical Engineering Progress, 48:505-516.

38. Levenspiel, O., 1962, Chemical Reaction Engineering, New York, John Wiley and Sons.

6.0 REFERENCES (continued)

39. Liberti, L., Petruzelli, D., Hellferich, L., Millar, J. R. and Passino, R., 1987, Instationary shrinking-core models for heterogeneous ionic reactions, Reactive Polymers, 1:1-13.